Polyomavirus Interactions with Host Cell Surface Receptors Mediate Important Steps in Virus Infection: From Signaling to Pathogenesis

By Samantha D. O'Hara
BS Biochemistry, Florida State University, 2011

A thesis submitted to the
Faculty of the Graduate School
in partial fulfillment of the requirements
for the degree Doctor of Philosophy

Department of Molecular, Cellular, and Developmental Biology
2016

This thesis entitled:

Polyomavirus Interactions with Host Cell Surface Receptors Mediate Important Steps in Virus Infection: From Signaling to Pathogenesis

written by Samantha D. O'Hara

has been approved for the Department of Molecular, Cellular, and Developmental Biology

---

Gia Voeltz, Ph.D.

Robert Garcea, M.D.

Date:_____

The final copy of this thesis has been examined by the signatories, and we find that both the content and the form meet acceptable presentation standards of scholarly work in the above mentioned discipline.

O'Hara, Samantha D. (Ph.D. Molecular, Cellular and Developmental Biology)

Polyomavirus Interactions with Host Cell Surface Receptors Mediate Important Steps in Virus Infection: From Signaling to Pathogenesis

Thesis Directed by Robert L. Garcea

Abstract

Virus binding to the cell surface triggers an array of host responses important for infection. Gangliosides are the cell surface receptors for Polyomavirus (PyV) infection. Specificity is determined by recognition of carbohydrate moieties on the ganglioside by the major viral capsid protein VP1 and alterations in ganglioside binding cause dramatic changes in virus tropism and pathogenesis. Knockout mice lacking complex gangliosides are completely resistant to Mouse Polyomavirus (MuPyV) infection. Fibroblasts (MEFs) from these mice are likewise resistant to infection, and supplementation with specific gangliosides: GD1a, GT1b, and GT1a rescues infection. MuPyV also binds a protein receptor α4-integrin and loss of integrin binding results in a 60% decrease in infection. In the absence of these receptors MuPyV binds and enter cells, thus how glycan receptors mediate infectious entry is unclear. Using mutant viruses and cell lines we determined that gangliosides and α4-integrin receptors mediate MuPyV activation of specific host signaling pathways. Using small molecule inhibitors, we identified that the PI3K and FAK/SRC pathways were required for MuPyV infection. The PI3K pathway was required for MuPyV endocytosis, while the FAK/SRC pathway enabled trafficking of MuPyV along microtubules. Thus, MuPyV interactions with specific cell surface receptors facilitate activation of signaling pathways required for virus entry and trafficking. Understanding how different viruses manipulate cell-signaling pathways though interactions with host receptors could lead to the identification of new therapeutic targets for viral infection.

Dedication

This thesis is dedicated to my family. My parents, Don and JoBee O'Hara, who have always supported me in my ambitions no matter how far away from home they may take me. My brother, Ryan O'Hara, who thinks I am much smarter than I am. To my husband, Dr. Tim Read, whose optimism and love for science has been a constant source of inspiration. Lastly, I dedicate this thesis to Lucy, who has been my faithful writing companion and friend.

Acknowledgments

I would like to thank my advisor, Dr. Robert Garcea for his constant faith and patience not only in the development of my project, but also with my development as a scientist. I would like to thank Dr. Kim Erickson for always gladly offering her expertise and providing valuable advice on science and life. I would like to thank Natalie Meirnez for her helpful nature, for organizing and funding unforgettable cookie h, and making sure we never went hungry at group meeting. I would like to thank past and present graduate students, Dr. Katie Heiser and Doug Peters, for their h of scientific advice and whom without their comradery and friendship this accomplishment would not be possible. I am forever indebted to the National Institute of Health and the National Institute of Allergy and Infectious Diseases for funding of my predoctoral fellowship (F31-AI-115920) and the National Institute of General Medical Science for the Signaling and Cell Cycle Regulation training grant (T32-GM08759). I would like to thank collaborators, Dr. Thilo Stehle, Dr. Thomas Benjamin, and Dr. Tom Perkins for the chance to contribute to their projects. Lastly, I would like to thank current and past members of my thesis committee for their support and mentorship, Dr. Leslie Leinwand, Dr. Robbin Dowell, Dr. Natalie Ahn, Dr. Gia Voeltz, and Dr. Sara Sawyer.

Contents

Tables

Figures

Chapter 1: Introduction

1.1 Polyomavirus Life Cycle

Polyomaviruses are non-enveloped dsDNA viruses that infect a variety of hosts, ranging from birds to humans. The root “poly” was first given to the *Polyomaviridae* (PyV) family due to their ability to give rise to a diverse array of tumors in different tissue types (Gross 1953). Today this name continues to adequately describe polyomaviruses in terms of their ability to bind multiple cell-surface receptors and enter cells though multiple endocytic routes.

Polyomaviruses bind to sialic acid-containing glycosphingolipids, termed gangliosides (Tsai et al. 2003; Low et al. 2006; Erickson et al. 2009). Many ganglioside receptors have been identified as receptors for polyomaviruses (reviewed in chapter 2). Polyomaviruses bind to gangliosides tough interactions with a shallow surface pocket on the virus coat (Stehle et al. 1994; Stehle & Harrison 1996). The virus capsid is approximately 50 nM in size and is composed of the 72-pentamers of the major coat protein VP1, with minor internal capsid proteins VP2 and VP3 making contacts with the dsDNA genome. The VP1 capsid contains 360 possible sialic acid binding sites, allowing for multivalent binding to ganglioside receptors. This multivalent binding leads to a high avidity association between the plasmid membrane and the virus capsid, causing wrapping of the plasma membrane around the virus capsid and tubular projections into the cytoplasm (Ewers et al. 2010).

This plasma membrane wrapping of virus is thought to induce virus entry; however, the cellular proteins required for Polyomavirus entry are not well understood

and are both species and cell type specific (Pho et al. 2000; Damm et al. 2005; Gilbert & Benjamin 2000). A human polyomavirus, JCPyV, is unique in that it enters cells though clatrhin-mediated endocytosis, while the known entry pathways of many other species of PyV are clatin-independent (Pho et al. 2000). Caveolin-mediated endocytosis has been reported to be required for SV40 infection in some cell types (Damm et al. 2005; Anderson et al. 1996). Murine polyomavirus infectious-internalization is clatin, caveolin, and dynamin independent; however, cholesterol depletion blocks virus infection (Gilbert et al. 2000; Gilbert et al. 2003). Thus, murine polyomavirus (MuPyV) is considered to undergo “lipid-mediated endocytosis” (Ewers et al. 2011). MuPyV enters cells though multiple endocytic routes, even in the absence of infection, making the subset of virus undergoing productive endocytosis difficult to identify (You & O’Hara et al. 2015).

While a detailed knowledge of MuPyV endocytosis is lacking, there are hallmarks of MuPyV infection that have been observed. During internalization, MuPyV induces transient disorganization of cellular actin fibers followed by trafficking of virus-containing-endosomes along microtubules to the lumen of the endoplasmic reticulum (ER) (Figure 1.1) (Zila et al. 2014; Gilbert et al. 2003). Depolymerization of microtubules with small molecule inhibitors blocks MuPyV infection, while depolymerization of actin fibers increases virus infection (Figure 1.2) (Gilbert et al. 2004). How MuPyV induces actin breakdown and microtubule-mediated trafficking to the ER is not understood.

Only minor populations of virus are observed in Rab5 early endosomes, with a slightly higher percentage associating with EEA1 positive early endosomes (Liebl et al. 2006). Dominant negative mutants of Rab5 decrease MuPyV infection by approximately

50%, suggesting this pathway is involved in productive virus trafficking (Qian et al. 2009). Virus is subsequently detected in late (Rab7) and recycling (Rab11) endosomes; however, dominant negative mutants of Rab7 decrease infection by less than 30% making the importance of these endosomes unclear (Liebl et al. 2006; Qian et al. 2009; Mannová & Forstová 2003). Inhibition of endosome acidification also inhibits MuPyV infection, supporting maturation of endosomes as important for virus trafficking (Liebl et al. 2006). Thus, the productive pathway of infection for MuPyV is considered to be the subpopulation of virus trafficked to Rab7 positive “endolysosomes” where gangliosides mediate endolysosomal escape of the virus to the ER (Qian et al. 2009).

While it is clear that gangliosides are required for proper virus trafficking, the cellular proteins that interact with gangliosides to mediate this trafficking remain unknown. Retrograde transport is not a factor in MuPyV trafficking to the ER, as MuPyV is not observed in the golgi apparatus and its trafficking to the ER is independent of COP1 (Mannová & Forstová 2003). Once the virus has been trafficked to the ER, the virus coat is degraded though ER-associated degradation pathways (ERAD), leading to viral genome release to the cytosol (Lilley et al. 2006; Schelhaas et al. 2007; Goodwin et al. 2011). VP2 is myristoylated on its N-terminus and can penetrate the ER membrane. It has been suggested that VP2 penetration may be important for ER escape along with other ER resident proteins. Once reaching the cytosol, the viral genome must be trafficked to the nucleus for DNA replication and expression of early gene products (Figure 1.1). The minor capsid proteins VP2 and VP3 may facilitate genome transport to the nucleus as they are bound to the viral genome and contain a nuclear localization signal (NLS). The NLS of VP2/3 can be bound by nuclear transport

proteins, α/β importins (Bennett et al. 2015). Importin binding to the minor capsid proteins may facilitate transport of the viral genome though the nuclear pore complex. Once the genome has reached the nucleus the host cell RNA polymerase II will bind and express the early genes, termed the T-ags. The T-ags then prepare the cell for DNA replication.

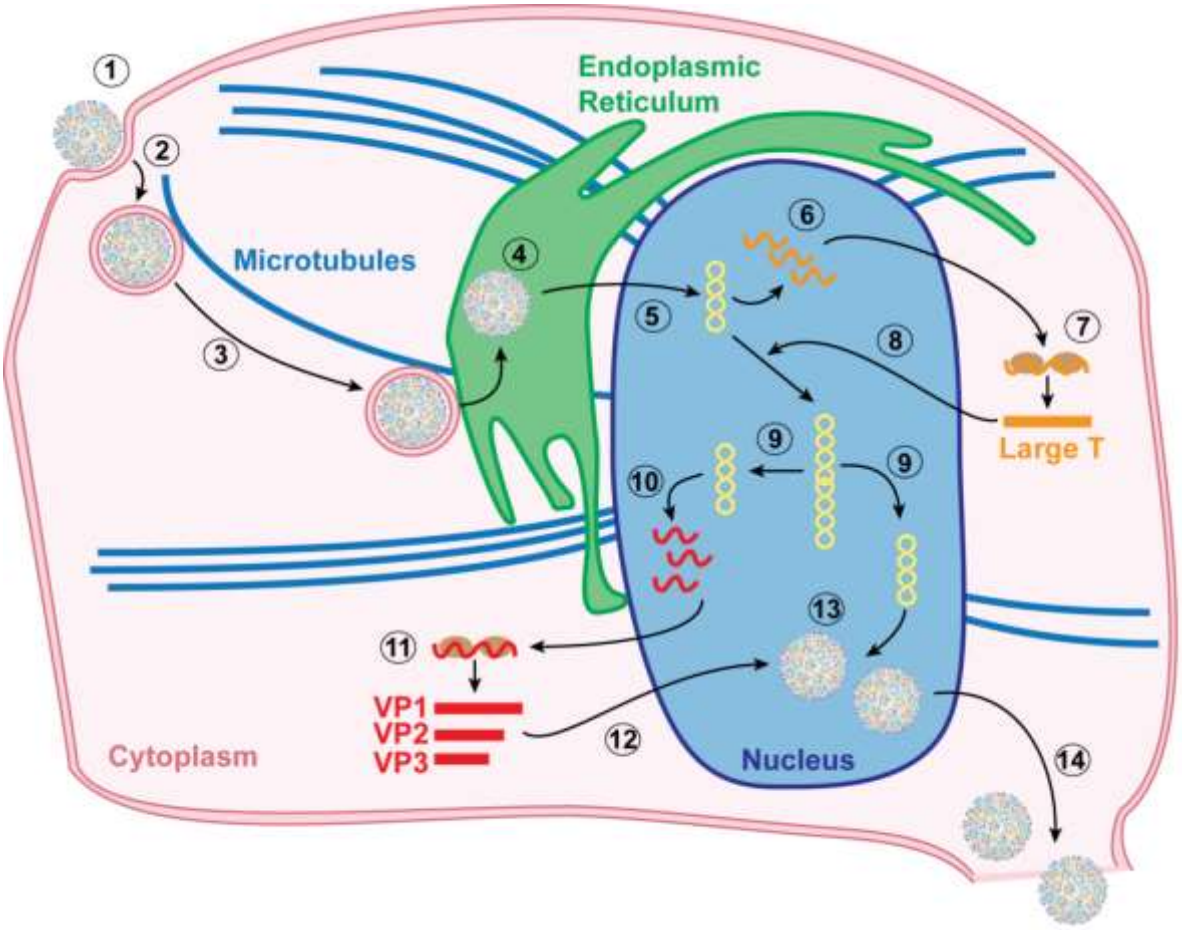

Figure 1.1: Murine Polyomavirus Life Cycle. Virus binds to glycan receptors on the cell surface (1), followed by endocytosis (2) and trafficking along microtubules (3) to the endoplasmic reticulum (ER). Once in the ER, the virus coat breaks down leading to release of the viral dsDNA genome (4). The genome is trafficked to the nucleus (5) where the host RNA polymerase begins to transcribe the early proteins, the T-ags (6). After translation (7), large T-ag re-enters the nucleus (8), binds the viral genome, and induces viral DNA replication (9) as well as expression of the late genes (10), the viral capsid proteins VP1/2/3. After translation (11) the viral coat proteins re-enter the nucleus (12) and combine with newly replicated viral genomes to form new viral progeny (13). Eventually, the nucleus will fill with new viral particles leading to cell lysis and virus release (14).

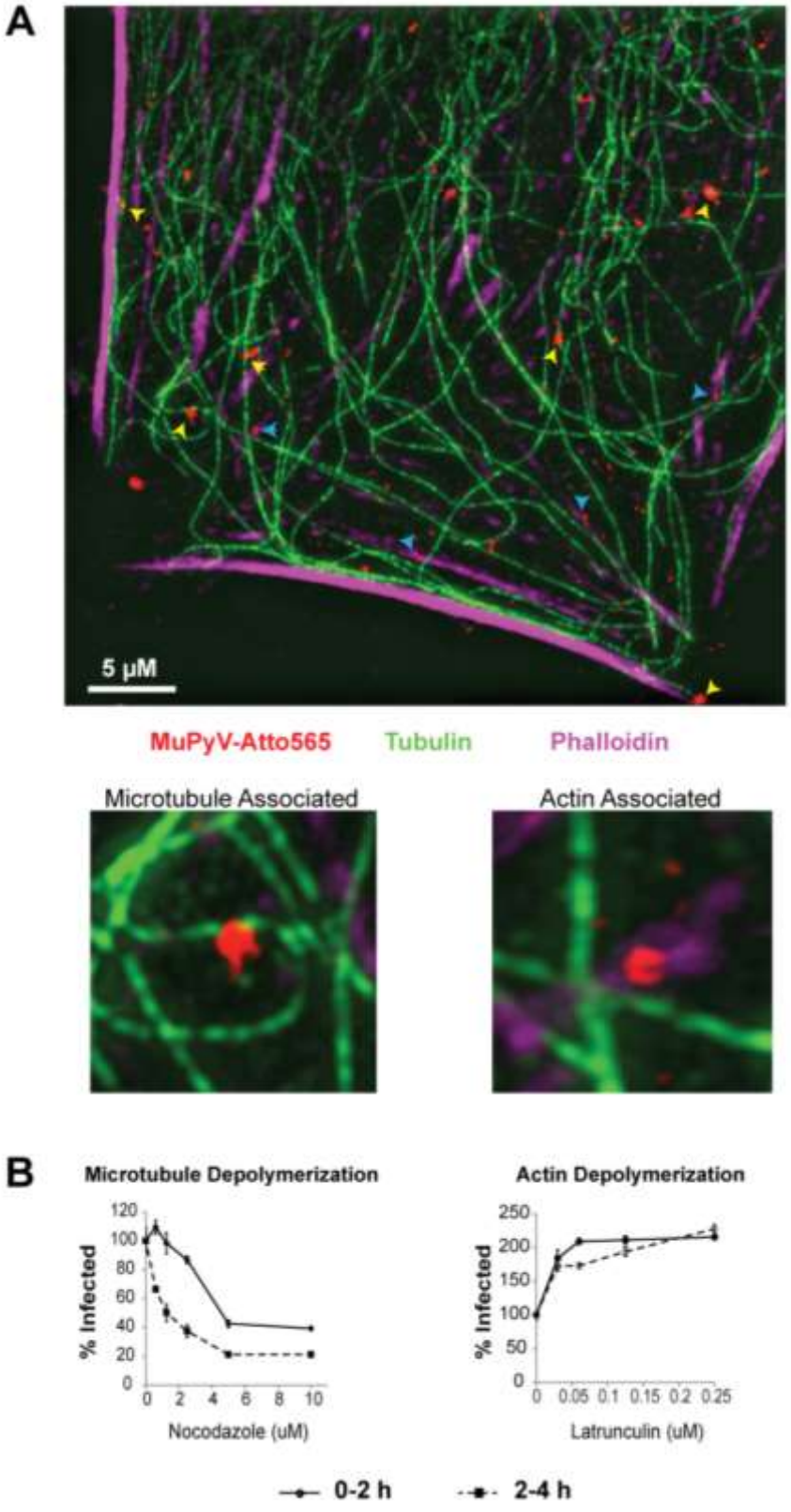

Figure 1.2: MuPyV Trafficking Along Microtubules. (A) Structured Illumination Microscopy (SIM) image 1 h post infection. Shown are virus (red), microtubules (green), and actin filaments (magenta). Virus particles can be found trafficking along microtubules (yellow arrows) as well as virus associated with actin filaments (blue arrows). Enlarged examples of each are shown below. **(B)** Microtubule depolymerization with nocodazole either during virus entry (0-2 h), or post virus entry (2-4 h), blocks infection. Actin depolymerization with latrunculin either during virus entry (0-2 h), or post virus entry (2-4 h), increases virus infection.

1.2 Polyomavirus Genome

The Murine Polyomavirus dsDNA genome is small; approximately 5kB, coding for only 6 gene products: 3 early genes, termed T-ags, and 3 late genes, the viral capsid proteins. Polyomaviruses are completely dependent on host transcription, translation, and replication machinery for production of new viral progeny. The early genes, the T-ags, are expressed as early as 16 h after infection.

The T-ags are viral “oncoproteins” and are alternatively spliced products of the early region (Figure 1.3). The tee early protein products are termed Large, Middle, and Small T-Ags. The early region is transcribed in the opposite direction of the late region, with their transcription start sites adjacent to the origin of replication. The late region codes for the tee viral capsid proteins VP1, VP2, and VP3. Large T-ag is the power house of viral infection and tough interactions with host proteins it induces viral DNA replication, as well as expression of the late genes. Large T-ag primes the cell for DNA replication by binding to retinoblastoma protein (Rb) and inducing the cell to enter S-phase. Large T-ag also activates DNA damage repair proteins (DDR) essential for proper genome replication and packaging (Heiser et al. 2016). Middle T-ag is a membrane protein that is necessary for MuPyV’s transformation of cells and tumorigenesis (Cheng et al. 2009). Middle T-ag binds and activates SRC family kinases and phosphositide-3-kinase (PI3K) (Cheng et al. 2009). Middle and small T-ags alter the phosphorylation state of cellular signaling proteins by inhibiting protein phosphatase 2A (PP2A), leading to activation of many mitogenic signaling pathways such as MAPK and AKT (Meili et al. 1998). Together, the T-ags alter the cellular environment to promote

viral DNA replication and protein expression, leading to efficient production of viral progeny and eventual cell lysis and progeny release (Figure 1.1).

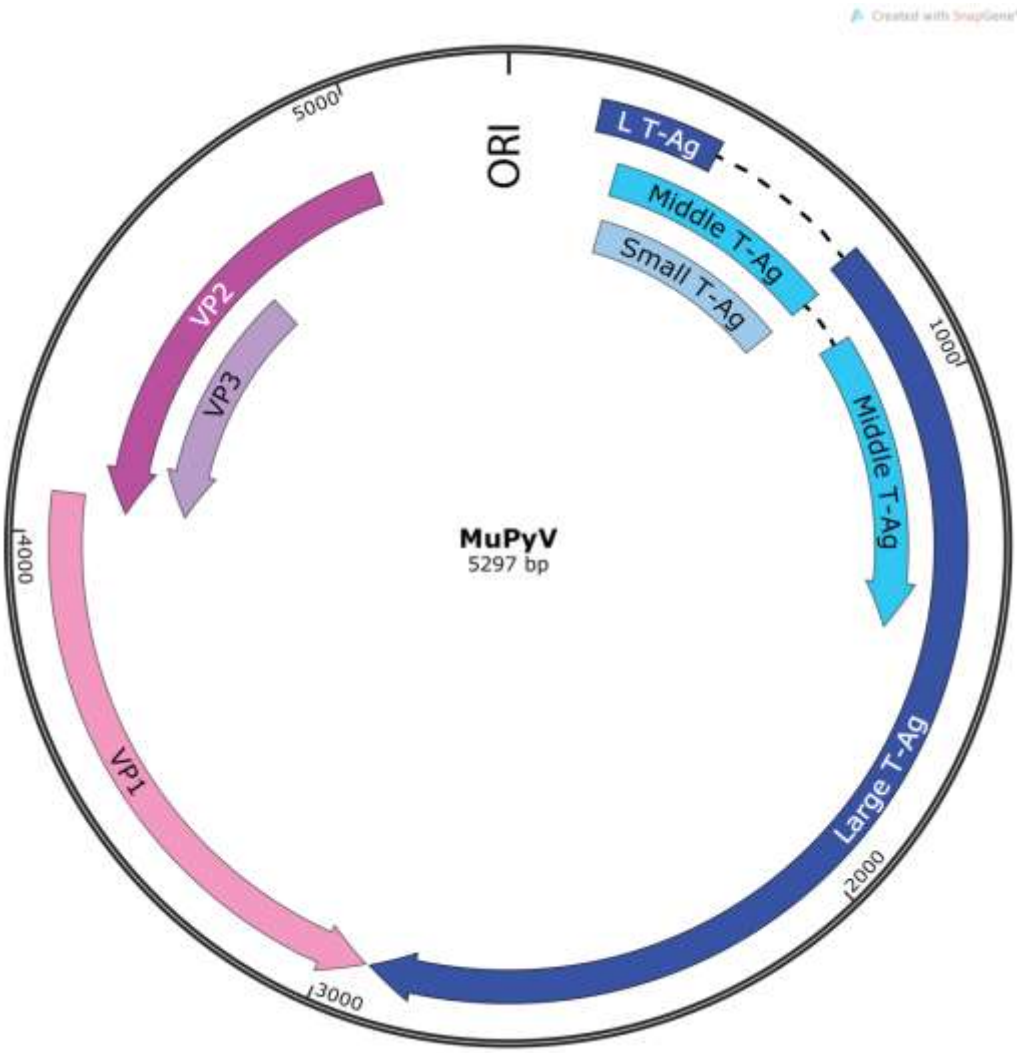

Figure 1.3: Murine Polyomavirus Genome. The MuPyV genome codes for 6 gene products. Shown in blue are the early genes, the T-ags, which are important for viral DNA replication and for expression of the late genes. The late genes are the virus capsid proteins: the major capsid protein VP1, and two minor capsid proteins, VP2 and VP3.

Chapter 2: Glycan Receptors of The *Polyomaviridae*: Structure, Function, and Pathogenesis

2.1 Introduction: Polyomaviruses (PyVs) are small, non-enveloped, dsDNA viruses with capsids comprised of 72 VP1 pentamers, termed capsomeres (Figure 2.1). Gangliosides are sialylated oligosaccharides (glycans) with lipid tails that function as the primary cell surface receptors for many polyomaviruses (Taube et al. 2010). Each capsomere has five low affinity glycan binding sites, facilitating multivalent binding of receptors and subsequent high avidity interactions that are critical for PyV cell entry and targeting to endocytic pathways (Ewers et al. 2010; Szklarczyk et al. 2013) . Cell surface binding is the first determinant of infection, thus subtle changes in VP1-glycan interactions can result in dramatic changes in PyV tropism and pathogenesis. Candidate glycan receptors have been identified for mouse (MuPyV), simian virus 40 (SV40), JC (JCPyV), BK (BKPyV), Merkel Cell (MCPyV), and simian B-Lymphotropic (LPyV) polyomaviruses. We will discuss recent findings concerning the identification of PyV glycan receptors and how glycan specificity affects PyV pathogenesis.

2.2 Structures of VP1 pentamer-glycan complexes. The first structure of intact mouse polyomavirus (MPyV) particles in complex with the oligosaccharide Neu5Ac-(α2,3)-Gal(β1,4)-Glc (3'sialyllactose, 3SL) showed the outer surface loops of VP1 binding to sialic acid (Neu5Ac) in a shallow pocket, resulting in five possible binding sites per pentamer (Figure 2.1) (Stehle et al. 1994). Subsequently, higher resolution was obtained by first crystallizing assembly-incompetent MuPyV VP1 pentamers, then soaking the crystals with specific glycans, and solving the resulting structure in complex with 3SL and a branched disialylated glycan (Disialyllacto-N-tetraose, DSLNT) (Stehle &

Harrison 1996). In this manner, the structures of glycan-VP1 pentamer complexes now have been determined for SV40, JCPyV, BKPyV, MCPyV, LPyV and HPyV9 (Neu et al. 2008; Neu et al. 2010; Neu, Allen, et al. 2013; Neu et al. 2012; Neu, Khan, et al. 2013; Khan et al. 2014).

Although the location of the sialic acid (Neu5Ac) binding site on VP1 is generally conserved across polyomaviruses, each PyV uses a unique set of residues to interact with oligosaccharides, resulting in distinctive orientations of the sugar within the binding pocket (Figure 2.2). The structure of SV40 VP1 has been determined with the oligosaccharide portion of GM1 (Neu et al. 2008). Binding occurs in a highly specific manner, with VP1 residues contacting both branches of GM1, Gal-(β1,3)-GalNAc-(β1,4) and (α2,3)-Neu5Ac (Neu et al. 2008). The structure of JCPyV VP1 has been solved with the pentasacharide lactoseries tetrasaccharide c (LSTc), containing the terminal Neu5Ac-(α2,6)-Gal(β1,4)-GlcNAc motif (Neu et al. 2010). Although JCPyV binds the terminal Neu5Ac in a similar orientation and with similar contacts as seen in SV40, JCPyV VP1 makes additional unique contacts to other residues in LSTc that confer remarkable specificity for the observed interaction. Furthermore, JCPyV VP1 undergoes a structural rearrangement upon binding to its ligand, in contrast to all other PyV VP1 structures solved to date (Neu et al. 2010). This rearrangement accommodates the unique L-shape adopted by the LSTc ligand.

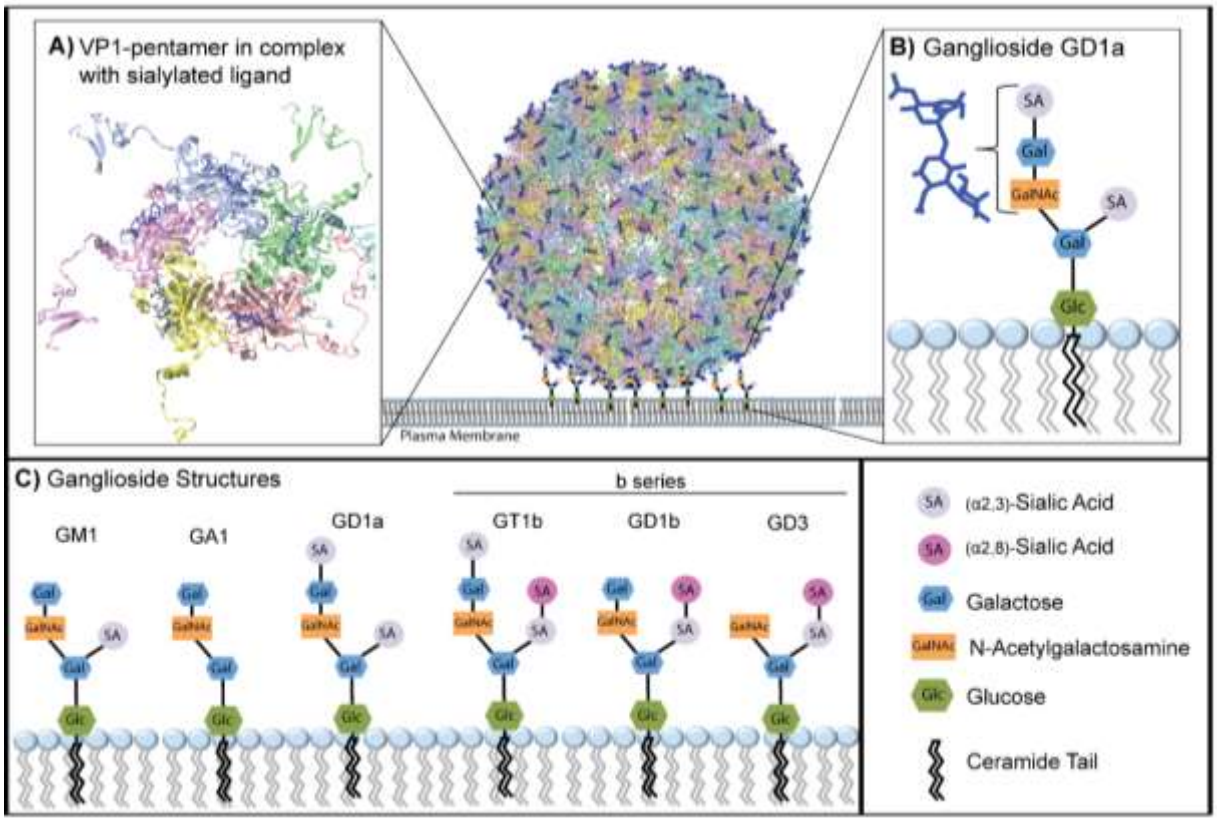

Figure 2.1 Mouse polyomavirus (MPyV) ganglioside binding. Schematic of the mouse polyomavirus (MPyV) capsid in complex with the Neu5Ac-(α2,3)-Gal(β1,3)-GalNAc-(α2,6)-Neu5Ac ligand (DSLNT) [27]. The capsid is composed of 72 VP1-pentamers, each with a ligand-binding site, which results in 360 possible binding sites per capsid. **(A)** A VP1-pentamer with ligand occupying each of the five available binding sites. **(B)** The terminal portion of the bound glycan, NeuNAc-(α2,3)-Gal-(β1,3)-GalNAc, is also present in gangliosides GD1a and GT1b, which are thought to function as MPyV receptors. Gangliosides are anchored in the outer plasma membrane by a ceramide tail allowing them to move laterally across the plasma membrane. Gangliosides are abundant on the cell surface, facilitating multivalent binding of receptors by a virus capsid. **(C)** Structures of common ganglioside receptors; many have been identified as possible polyomavirus receptors. Figure adapted from (O'Hara et al. 2014)

The structures of MCPyV and BKPyV pentamers have been determined with glycans of b-series gangliosides (Figure 2.1). BKPyV pentamers bind the glycan portion of GD3, which contains a Neu5Ac-(α2,8)-Neu5Ac-(α2,3)-Gal motif (Neu, Allen, et al. 2013). BKPyV binds the terminal, α2,8-linked sialic acid of GD3 in the same orientation seen for SV40 and JCPyV, but specificity for this glycan is achieved by additional contacts to the second sialic acid of GD3 (Neu, Allen, et al. 2013). Thus, while SV40, JCPyV and BKPyV all engage terminal Neu5Ac in a conserved manner, they nevertheless are each highly specific for tee different linkages (α2,3, α2,6 and α2,8-linked Neu5Ac, respectively). The structure of MCPyV VP1 has been determined in complex with several oligosaccharides containing a terminal Neu5Ac-(α2,3)-Gal motif, indicating that MCPyV may bind a range of different glycan receptors bearing this disaccharide sequence (Neu et al. 2012). Interestingly, MCPyV binds Neu5Ac in an orientation and with contacts that are different from those seen in the SV40, JCPyV and BKPyV complexes or the MPyV structures, Figure 2.2 (O'Hara et al. 2014).

The simian LPyV VP1 structure has been determined in complex with 3SL, and exhibits the most profoundly altered binding interaction (Neu, Khan, et al. 2013). Instead of the shallow binding pocket seen in other PyVs, LPyV binds the sugar motif in a deep and slender pocket, likely increasing LPyV VP1 affinity for this glycan. The structure of HPyV9 VP1 shows that this virus binds 3SL and related ligands essentially as seen in LPyV, with some differences in the specificity for modified sialic acids (Khan et al. 2014).

2.3 Glycan arrays and flotation assays. Two biochemical methods have been used to assay VP1 glycan-binding *in vitro*. First, glycan microarrays have been used to

screen VP1 pentamers against a diverse pool of sialylated oligosaccharides, and have identified or confirmed binding motifs for SV40, BKPyV, JCPyV, and LPyV (Table 2.1). Although glycan arrays allow screening of diverse sugar motifs, spacing of oligosaccharides in the array format may affect multivalent ligand binding. The linker connecting the glycans to the arrays is also a variable, and may affect signals by modulating the accessibility and mobility of a particular glycan sequence (Oyelaran & Gildersleeve 2009). Arrays also may identify high affinity ligands that are not functional for virus entry *in vivo,* but could be motifs of pseudo-receptors (Qian et al. 2010).

In addition to receptor identification, glycan arrays recently have been used to study interspecies differences in sialic acid binding between human polyomavirus BKPyV and SV40. Humans lack the enzyme CMP-N-acetylneuraminic acid hydroxylase, which hydroxylates the Neu5Ac methyl group to generate N-glycolyl neuraminic acid (Neu5Gc). Thus, Neu5Ac is the most prevalent human sialic acid, while other mammals possess both Neu5Ac and Neu5Gc (Varki 2001). Simian LPyV and the related human HPyV9 can engage glycans terminating in either Neu5Ac or Neu5Gc, with subtle differences in specificity for each virus (Khan et al. 2014). Likewise, SV40 binds preferentially to simian Neu5Gc-GM1. A point mutation in the BKPyV VP1 binding pocket can retarget BKPyV from the disialylated receptor GD1b, to the monosialylated receptor GM1. Unlike SV40, retargeted BKPyV exclusively engages Neu5Ac-GM1 and not Neu5Gc-GM1 (Neu, Allen, et al. 2013). These data suggest that each virus has adapted to bind the most prevalent sialic acid in their host and could indicate a possible challenge to host jumping of PyV from non-human to human host**.**

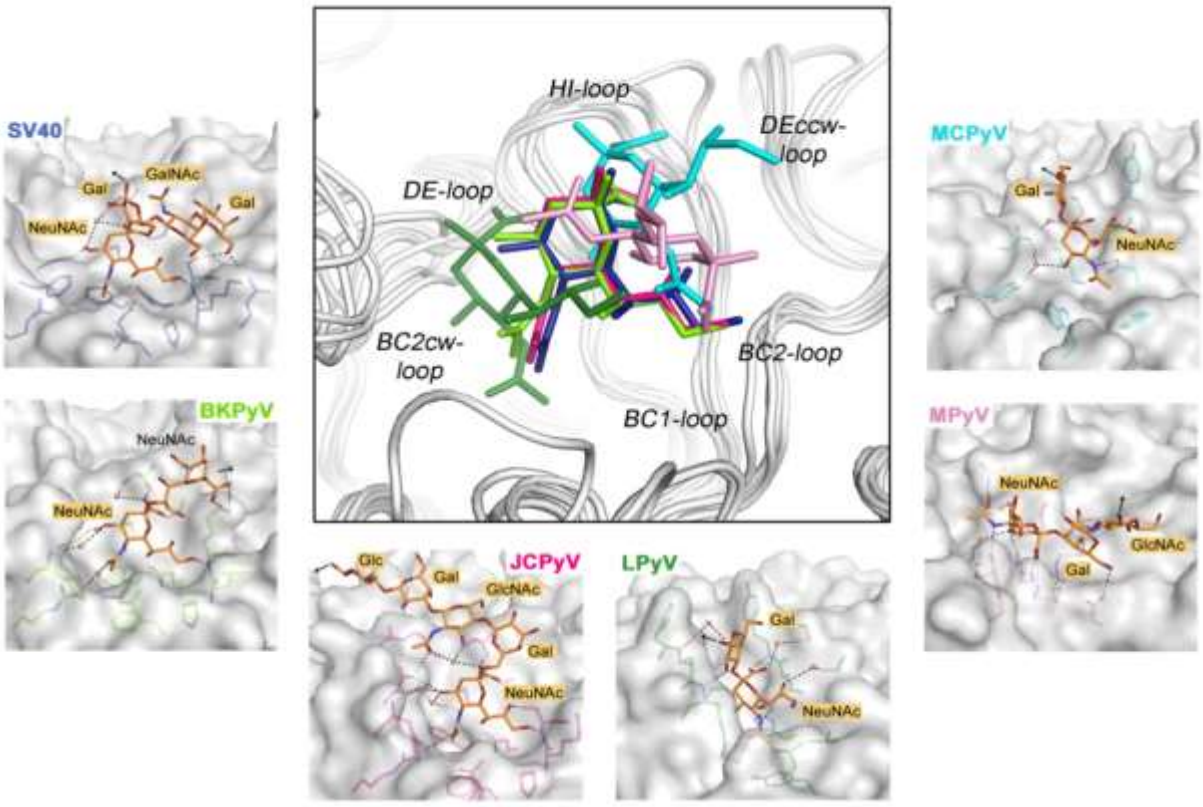

Figure 2.2 Comparison of polyomavirus VP1 structures in complex with siaylated glycans. The central panel shows a superposition of the six terminal sialic acid (Neu5Ac) residues seen in the VP1 structures of SV40 bound to GM1, BKPyV bound to GD3, JCPyV bound to LSTc, LPyV bound to 3SL, MPyV bound to DSLNT and MCPyV bound to 3SL [6-10, 28]. The loops surrounding the binding sites are labeled. Labels cw and ccw denote loops contributed by clockwise and counterclockwise VP1 monomer neighbors, respectively, of the shown VP1 monomer. The superposition highlights a conserved location of the Neu5Ac binding site, with distinct interaction networks within or adjacent to the core binding sites. Surrounding panels show similar views of interactions seen in the binding sites of each of the six viruses, using the same color scheme. The VP1 proteins are shown in a semitransparent surface representation, with glycans and contacting protein represented with sticks. Hydrogen bonds and salt bridges between glycans and proteins are indicated with black dashed lines. Figure adapted from (O'Hara et al. 2014).

In flotation assays, virions, virus-like-particles (VLPs), or VP1 pentamers are incubated with plasma membrane preparations, and then subjected to sucrose gradient sedimentation. When bound, VP1 floats with the membrane fraction, but pellets in the absence of binding. Flotation assays permit testing of gangliosides for binding by mixing specific gangliosides with artificial membranes prior to incubation with the viral ligand. Flotation assays have validated GD1a and GT1b as receptors for MPyV and GM1 as the receptor for SV40 (Tsai et al. 2003). Flotation assays have also demonstrated that BKPyV binds GD1b and GT1b, and MCPyV binds GT1b (Low et al. 2006; Erickson et al. 2009). Although flotation assays do not necessarily indicate *in vivo* function they allow ligand-receptor movement within the membranes, facilitating multivalent binding and avidity effects. Flotation assays showed that BKPyV could bind GT1b and GD1b and crystallization showed BKPyV binding to GD3. However, glycan arrays conducted with BKPyV showed a high signal exclusively for GD1b, with low signals for both GD3 and GT1b (Table 1) (Neu, Allen, et al. 2013). *Such inconsistencies make functional testing of receptors essential, as discussed below.*

2.4 Ganglioside supplementation assays. Although both structural and *in vitro* binding data have identified glycans bound by different polyomaviruses, functional assays testing whether specific gangliosides are required for infection have been limited. Ganglioside supplementation is a useful assay in which gangliosides are incorporated into the plasma membrane of cells by exogenous addition. This assay tests whether specific gangliosides can restore or enhance infection of ganglioside-deficient cells. Many deficient cell lines have been used: 1) hamster ovary Lec2 cells

that lack a sialic acid transporter and have no sialylated glycans, 2) murine GM95 cells that have a nonfunctional ceramide glucosyltransferase, and 3) ganglioside-deficient C6 rat glioma cells (Schowalter et al. 2011; Tsai et al. 2003; Ewers et al. 2010). While supplementation assays allow functional testing of a particular ganglioside; these assays are often performed at ganglioside concentrations greater than physiological, and results may vary depending on the cell line used since multiple additional genetic changes are likely present.

Supplementation of C6 rat glioma cells with GD1a increased MuPyV infection and GM1 addition increased SV40 infection. These results are consistent with the complex structures of MuPyV and SV40, glycan array data, and flotation data, strongly supporting that these are the relevant receptors for MuPyV and SV40 infection (Table 2.1) (Tsai et al. 2003; Qian et al. 2010). However, results for other viruses are not as consistent as those for MuPyV and SV40. The development of virus-based reporter vectors, pseudoviruses (PsV), allows “infection” to be measured in a variety of cellular backgrounds based on transduction of a reporter plasmid. For example, GT1b supplementation rescued transduction of Lec2 cells by BK PsVs and enhanced transduction of poorly permissive GM95 cells (Schowalter et al. 2011; Pastrana et al. 2013). Additionally, GT1b and GD1b supplementation rescued infection of human prostate carcinoma cells (Low et al. 2006). These data suggest that GT1b and GD1b may be relevant receptors for BKPyV *in vivo*, although GT1b gave a negligible signal for BKPyV binding in the glycan array (Table 2.1).

BKPyV persists in the proximal renal tubule and MCPyV infects the skin. MCPyV and BKPyV both bind b-series gangliosides although they have distinct tissue tropisms

(Figure 2.1). Interestingly, MCPyV has been shown to bind glycosaminoglycans (GAGs) prior to binding of a sialylated entry factor, possibly indicating a difference in the entry pathways of PyVs that infect epithelial *versus* mesenchymal cell types (Schowalter et al. 2011). MC PsVs and BK PsVs are both unable to transduce Lec2 cells. GT1b supplementation of Lec2 cells restored BK PsV transduction but did not restore MC PsV transduction, while transient expression of the Lec2 sialic acid transporter exclusively restored MC PsV transduction without rescuing BK PsV transduction (Schowalter et al. 2011). These data indicate differences in cell surface interactions for these viruses, independent of their ability to bind similar glycans *in vitro*. This data also suggests that co-receptors may play distinct roles in the entry process of different PyVs, and indeed possible co-receptors have been identified for other polyomaviruses (Table2.1).

Table 2.1 Receptors Identified for PyVs

	Ligands Crystrallized with VP1	Receptors Identified in Glycan Arrays	Receptors Identified in Flotation Assays	Receptors Identified in Supplementation Assays	Possible Co-Receptors
MPyV	**3SL** (Neu5Ac-(α2,3)-Gal-(β1,4)-Glc) **DSLNT** (Neu5Ac-(α2,3)-Gal-(β1,3)-GlcNAc-(α 2,6)-Neu5Ac)	–	**GD1a, GT1b**	**GD1a**	**α4β1-Integrin**
SV40	**GM1** (Gal-(β1,3)-GalNAc-(β1,4)-[Neu5Ac-(α2,3)]-Gal-(β1,4)-Glc)	**GM1**	**GM1**	**GM1**	**MHC Class 1**
BKPyV	**GD3** (Neu5Ac-(α2,8)-Neu5Ac-(α2,3)-Gal-(β 1,4)-Glc)	**GD1b**	**GT1b, GD1b**	**GD3, GD2, GD1b, GT1b**	–
MCPyV	**GD1a** (Neu5Ac-(α2,3)-Gal-(β1,3)-GalNAc) **3SLN** (Neu5Ac-(α2,3)-Gal-(β1,4)-GlcNAc) **DSL** (Neu5Ac-(α2,8)-Neu5Ac-(α2,3)-Gal-(β 1,4)-Glc)	–	**GT1b**	–	**Glycosaminoglycans**
JCPyV	**LSTc** (Neu5Ac-(α2,6)-Gal-(β1,4)-GlcNAc-(β 1,3)-Gal-(β1,4)-Glc)	**LSTc** ****GT1b, GD1b, GD2**	–	–	**Serotonin Receptor 5HT2A**
LPyV	**3SL** (Neu5Ac-(α2,3)-Gal-(β1,4)-Glc) **3SLN** (Neu5Ac-(α2,3)-Gal-(β1,4)-GlcNAc)	**3SL, 3SLN** **PI-1** (Neu5Ac-(α2,3)-[NAc-(α 2,6)]-Gal-(β1,4)-GalNAc) **PI-2** (Neu5Ac-(α2,3)-[NBz-(α 2,6)]-Gal-(β1,4)-GalNAc)	–	–	–

**Identified by Enzyme Linked Immunosorbent Assay (ELISA)

2.5 *In vivo* pathogenesis related to glycan recognition. Mouse polyomavirus (MuPyV) is the best example of glycan binding influencing *in vivo* tissue tropism and pathogenesis. Tee strains of MuPyV have been well-studied: small plaque (RA), large plaque tumorigenic (PTA), and large plaque virulent (LID). These viruses differ in only one or two amino acid residues in the sialic acid binding pockets of VP1, but these point mutations result in marked differences in virulence and tropism. The prototypic RA strain binds to α2,3-linked sialic acid sequences Neu5Ac-a2,3-Gal (3SL and DSLNT), which are present in GD1a and GT1b (Figure 2.1) (Stehle & Harrison 1996; Buch et al. 2015). The RA strain infects the kidney, with limited spread in the animal. PTA has a single amino acid substitution in VP1 relative to RA, G91E, which is thought to allow binding to linear Neu5Ac-a2,3-Gal sequences, but interfere with binding of sequences that carry a branching Neu5Ac (e.g. in DSLNT). PTA has increased tissue tropism and can cause tumors in mice. LID has an additional amino acid substitution to PTA in VP1, V296A, which is predicted to further decrease the affinity of the VP1 binding pocket by removing a contact. LID spreads rapidly, killing animals within a few weeks. The inability of large plaque strains to recognize branched receptors may allow the virus to avoid multiple binding events and spread readily thoughout the animal (Bauer et al. 1995; Carroll et al. 2007).

No animal models exist for JCPyV infection, but information from immunosuppressed humans suggests that glycan recognition may influence *in vivo* spread. JCPyV typically establishes a persistent, asymptomatic infection in the urinary tract. In immunosuppressed individuals, JCPyV can spread to the central nervous system (CNS) causing a lytic infection of oligodendrocytes resulting in progressive

multifocal leukoencephalopathy (PML). Sequences of JCPyV isolated from the urine, blood, and cerebrospinal fluid (CSF) have identified VP1 variants exclusively in CSF isolates (Gorelik et al. 2011). These CSF VP1 variants display altered glycan-binding interactions, including loss of binding to sialyated glycans and increased binding to a nonsialylated ganglioside, GA1 (Figure 2.1). VLPs from these variants also show decreased binding to kidney tubular epithelial cells, while binding human glial cells at levels equal to or greater than wild-type VLPs (Gorelik et al. 2011). Thus it has been suggested that the CSF VP1 variants are generated during persistent infection, and that these variants are able to spread in the absence of immunologic surveillance. However, in contrast to cell binding results, CSF VP1 mutant PsVs were unable to transduce any of several glial cell lines tested, suggesting that the VP1 variants are noninfectious (Maginnis et al. 2013). Whether VP1 mutations play a functional role in the progression of JCPyV infection to PML remains unclear.

There appear to be multiple serotypes of BKPyV attributable to changes in VP1, and neutralizing antibodies against one serotype do not necessarily confer protection from another (Pastrana et al. 2012). Variations in the VP1 outer surface loops of BKPyV serotypes may provide escape from recognition by neutralizing antibodies against other serotypes, and may also affect receptor binding. For example, GT1b-supplemented GM95 cells were tested with five different serotypes of BK PsVs. Four of the PsV serotypes responded to GT1b supplementation by increasing transduction 6-300 fold; however, one serotype was unresponsive to GT1b and highly transduced GM95 cells in the absence of any gangliosides (Pastrana et al. 2013). The variations in VP1 of BKPyV

serotypes may therefore alter glycan binding, and have implications for serotype specific differences in pathogenesis.

2.6 Conclusions: Sialylated oligosaccharides are important polyomavirus receptors, but often the specific glycan linkage required for infection has been difficult to confirm. Discrepancies between assays may indicate that there is promiscuity in ligand binding or that some ligands are used as "decoys" rather than coupled to cell entry. Although many ganglioside receptors have been identified, gangliosides are likely not the only ligand for PyV infection, as both integrins and GAGs also have been implicated for some PyVs (Table 1) (Schowalter et al. 2011; Breau et al. 1992; Elphick et al. 2004; Caruso et al. 2007; Caruso et al. 2003). Moreover, some viruses such as JCPyV bind to glycans that are clearly not gangliosides. Nonetheless, *in vivo* data from MPyV suggests that alterations in VP1 glycan-binding dramatically alter tissue tropism and pathogenesis, and these results likely portend a similar significance for glycan-interactions of other members of the *Polyomaviridae* family.

Chapter 3: Ganglioside and Non-Ganglioside Mediated Host Responses to Polyomavirus Infection

The following results and discussion sections were adapted from “Ganglioside and non-ganglioside mediated host responses to the Mouse Polyomavirus infection.” Our collaborator, Thomas Benjamin at Harvard Medical School carried out the initial infections in these animals.

3.1 Introduction

The *Polyomaviridae* comprise an expanding family of viruses of human, non-human primate and rodent origin as well as several avian species (DeCaprio et al. 2013). These small non-enveloped icosahedral DNA viruses are similar in their structural and genetic organization. Studies in cell culture with several members of the group have demonstrated that gangliosides serve as necessary receptors for infection. Initial studies showed mouse polyomavirus (MuPyV) binding to specific gangliosides in the plasma membrane leads to internalization and transport via endolysosomes to the endoplasmic reticulum (Tsai et al. 2003; Liebl et al. 2006). There the virus is thought to undergo partial disassembly followed by translocation to the cytosol and nuclear entry. Steps of virus disassembly leading to export from the endoplasmic reticulum are partially understood (Qian et al. 2009; Qian et al. 2010; Lilley et al. 2006; Gilbert et al. 2006; Horvath et al. 2010; Walczak et al. 2014).

Gangliosides are sialic acid containing glycosphingolipids that are ubiquitously expressed on all cells. Gangliosides are anchored in the outer leaflet of the plasma membrane by a ceramide tail with their sialylated oligosaccharide portion (glycan)

facing extracellularly. Binding specificity among the polyomaviruses is based on recognition of the glycan by the major viral capsid protein VP1. High-resolution structural and biochemical studies have revealed details of how recognition of sialic acids in various linkages occurs with different polyomaviruses (O'Hara et al. 2014; Stehle et al. 1994; Neu et al. 2012; Neu et al. 2011; Neu, Allen, et al. 2013; Buch et al. 2015). MuPyV binds to oligosaccharides carrying terminal sialic acids in specific linkages found in several gangliosides (Buch et al. 2015). Studies with different strains of MuPyV have shown how differences in glycan recognition can have dramatically altered tropism and pathogenesis. MuPyV has also been shown to bind to the $\alpha 4\beta 1$ integrin. Mutagenesis of the integrin binding site on VP1 decreases infectivity by 50% and alters virus tropism *in vivo*, suggesting that $\alpha 4\beta 1$ may serve as a 'co-receptor' mediating a post-attachment step of infection (Caruso et al. 2003; Caruso et al. 2007).

The outcome of infection by MuPyV depends on the genetic background of both virus and host. Inbred strains of mice have been used to identify host determinants that underlie susceptibility or resistance to the virus. Strains of MuPyV differing widely in pathogenicity owe their differences to polymorphisms in VP1 that allow the virus to discriminate among different oligosaccharides or that affect avidity of binding to sialic acid (Dubensky et al. 1991; Bauer et al. 1995; Freund et al. 1991). High-resolution structural studies of complexes between recombinant VP1s of several MuPyV strains and various glycans have extended and refined our understanding of receptor interactions (Buch et al. 2015). Here we utilize mice with knockouts in ganglioside biosynthetic pathways to investigate the importance of

specific gangliosides for infection and to determine whether gangliosides are essential for other host-responses such as mitogenic gene induction and innate immunity.

3.2 Materials and Methods

MuPyV virus strains. The PTA and RA strains have been described (CD – AJP, 1987; RF, GM Dubensky 1991; Freund, AC 1991; CD,RF 1987). PTA is a standard large plaque 'high tumor' strain that binds straight chain oligosaccharides with terminal α 2,3-linked sialic acid. RA is a standard small plaque 'low tumor' strain that binds branched as well as straight chain sialic acids (Bolen et al. 1985). LID is a virulent strain derived from PTA (Bolen et al. 1985). All strains were propagated in primary baby mouse kidney cells.

Infections of Cells from Ganglioside-deficient Mice and Immunofluorescence Assay for Large T Ag Expression. Fibroblast cultures (MEFs) were prepared from embryos of 18 to 19 days gestation and genotyped to generate B4 -/-, St8 -/- and B4St8 -/- mouse embryo fibroblast lines (MEFs). MEFs were maintained by serial passage in Dulbecco's Modified Eagle's medium with 10% fetal bovine serum and used for viral infections at passages between 2 and 5. Cells on coverslips were infected by MuPyV strains RA or PTA at various multiplicities of infection and fixed at 24 h post-infection with 4% neutral buffered paraformaldehyde (Electron Microscopy Sciences, Ft Washington, PA). Cells were permeabilized with 0.3% Triton X-100 in phosphate buffered saline (PBS) and stained with rat polyclonal anti-T antibody (Goldman & Benjamin 1975) and rhodamine-conjugated donkey anti-rat IgG.

Confocal Microscopy for Virus Entry. Wild type and B4St8 MEFs were seeded onto glass coverslips in Dulbecco's Modified Eagle's Medium supplemented with 10% fetal bovine serum (FBS). Cells were incubated overnight in serum free media prior to infection. Cells were then infected with RA. At indicated times post infection (30min, 3h) cells were washed in phosphate buffered saline (PBS) and fixed with 4% paraformaldehyde (PFA) at room temperature (RT) for 10 min. Cells were blocked in 10% FBS in PBS overnight at 4°C followed by staining for cell surface VP1 (I58 antibody/Alexa Flour secondary 546). Cells were then re-fixed with 4% PFA at RT for 10 min followed by permeabilization with 0.5% Triton X-100 for 15 min at RT. Cells were blocked in 10% FBS in PBS overnight at 4°C followed by staining for total VP1 (I58 antibody/Alexa Flour secondary 488). Confocal images were taken as a 5 step (.25 um) z-stack and slices were taken though the center of the cells. Each z-stack was aligned and compressed into a max intensity Z projection image for quantification of cell surface and total VP1 staining. Line scans were taken sampling the cell surface and cytoplasm of each cell to measure both cell surface and internalized virus as indicated by VP1 staining.

Immunofluorescence and Confocal Microscopy. Cells were seeded onto glass coverslips in Dulbecco's Modified Eagle's Medium supplemented with 10% fetal bovine serum (FBS). Cells were incubated overnight in serum free media prior to infection. For ganglioside-supplemented cells, serum free media containing the indicated concentration of gangliosides was used. Cells were then infected with RA (moi 5 to 10). At indicated times post infection cells were washed in phosphate buffered saline and fixed with 4% paraformaldehyde at RT. Cells were blocked in 10% FBS and then

stained for GD1a using the MAB5606 (Millipore). Cells were then permeabilized with 0.1% Triton X-100 and stained for T-ag (E1) and VP1 (I58). Samples were then incubated with Alexa Fluor labeled secondary antibodies. Cells were imaged on a Nikon A1R confocal microscope and infection was quantified for each sample as described below.

Image Analysis. Confocal images were taken as a 9 to13 step (.25 um) z-stack. Each z-stack was aligned and compressed into a max intensity Z projection image for quantification of T-ag staining. To quantify infection, T-ag staining was measured per each DAPI labeled nuclei. The DAPI channel on each image was thesholded and nuclei were counted using ImageJ (Analyze Particles). These particles were marked as "Regions of Interest" (ROI) and then the average pixel intensity of T-ag staining was measured for each nuclei (ROI). These were then binned into T-ag positive or T-ag negative nuclei to create % infected.

Flow Cytometry. Cells were dissociated from the plate with Versene solution (EDTA) for 10 min at RT. Resuspended cells were then washed in cold PBS followed by incubation with MuPyV (RA, moi 10) on ice. Samples were removed at indicated time points and temperatures, washed with cold PBS, and fixed with 0.5% paraformaldehyde (RT for 5 min), followed by staining for GD1a (MAB5606) and VP1 (I58). Cells were not permeabilized. Cell surface GD1a and virus levels were measured for >10,000 cells per sample by flow cytometry using a CyAn™ ADP Analyzer. Endocytosis of the virus particles was measured by decreased VP1 staining on the cell surface, when the VP1 antibody was no longer accessible to the virus. For picogreen experiments, MuPyV was incubated with picogreen dye at 1:200 dilution for 20 min at 45 degrees to allow the dye

to enter the virus capsid and intercalate with the viral genome. The picogreen labeled-MuPyV was then centrifuged though a 100 kDa Millipore filter to remove excess dye and washed with PBS. Cells were infected with picogreen-labeled MuPyV at 4°C, then shifted to 37°C for 30 min followed by fixation with 0.5% paraformaldehyde (RT for 5 min). Picogreen staining was measured for >10,000 cells per sample by flow cytometry using a CyAn™ ADP Analyzer. Virus accumulation can be measured by picogreen staining of cells, which indicates both virus bound to the cell surface as well as virus that has been endocytosed.

3.3 Results

3.3.1 Disruptions of Ganglioside Biosynthetic Pathways in Knockout Mice.

Previous studies have used ganglioside-deficient cell lines (*i.e.*, rat glioma C6 cells, R- mouse cells) to evaluate the importance of ganglioside receptors for MuPyV infection. These cell lines are often from a heterologous-host for MuPyV, and are not genetically defined. Thus, Tom Benjamin's laboratory generated ganglioside-deficient mice with known ganglioside composition to clearly identify the role of specific gangliosides in MuPyV infection (You & O'Hara et al. 2015). The B4 -/- mouse is blocked in a β1-4 GalNAc transferase (GM2/GD2 synthase) and is expected to lack the previously identified MuPyV ganglioside receptors, GD1a and GT1b, while maintaining expression of GM3 and GD3 (Figure 3.1A). The ganglioside composition was validated in B4 -/- mice by analyzing total acidic lipid fractions from kidneys, a major site of replication and tissue destruction by MuPyV. High performance thin layer chromatography of kidney lipid fractions from uninfected wild type and B4 -/- mice confirmed that only GD3 and its precursor GM3

are made in B4 -/- mice. B4 heterozygous (+/-) mice showed decreased levels of gangliosides compared to wild-type mice. I carried out immunofluorescence staining to confirm that B4 -/- mice lack a-series gangliosides such as GD1a. GD3 has been shown to bind pentamers of MuPyV VP1 in an *in vitro* screen, but its function as a receptor has not been evaluated. To determine the possible role of GD3 in MuPyV infection, St8 mice lacking α-2,8 sialyltransferase (GD3 synthase) were generated. St8 mice cannot synthesize b-series gangliosides, including GD3 and its derivatives, but retain a-series gangliosides, such as GD1a as verified by immunofluorescence staining with a GD1a antibody (Figure 3.1C). Thus, the B4St8 double -/- mouse is expected to synthesize only GM3, which was previously shown to be unable to bind or mediate infection by MuPyV. Protein glycosylation pathways are expected to be unaltered in these ganglioside-deficient mice.

Figure 3.1: (A) B4 and St8 knockouts in pathways of ganglioside biosynthesis. Gangliosides previously shown or shown here to function as MuPyV receptors are outlined. **(B) High performance TLC on acidic lipid fractions from kidneys of wild-type and B4 knockout mice.** Lane 1 – standards for GM1, GD1a, GD1b and GT1b; lane 2 – standards for GM1 and GD1a loaded at 50% volume of lane 1; lane 3 – B4 -/-; lane 4 - B4 +/-; lane 5 – B4 +/+; lane 6 – GM3 standard; lane 7 – GM2 standard; lane 8 – GD3 standard. Performed by Sherry Castle at the University of New Hampshire. **(C) St8 -/- MEFs retain a-series gangliosides.** GD1a staining of WT and St8 -/- MEFs show that both cell lines express GD1a**.** B4 -/- and B4St8 -/- MEFs do not express GD1a.

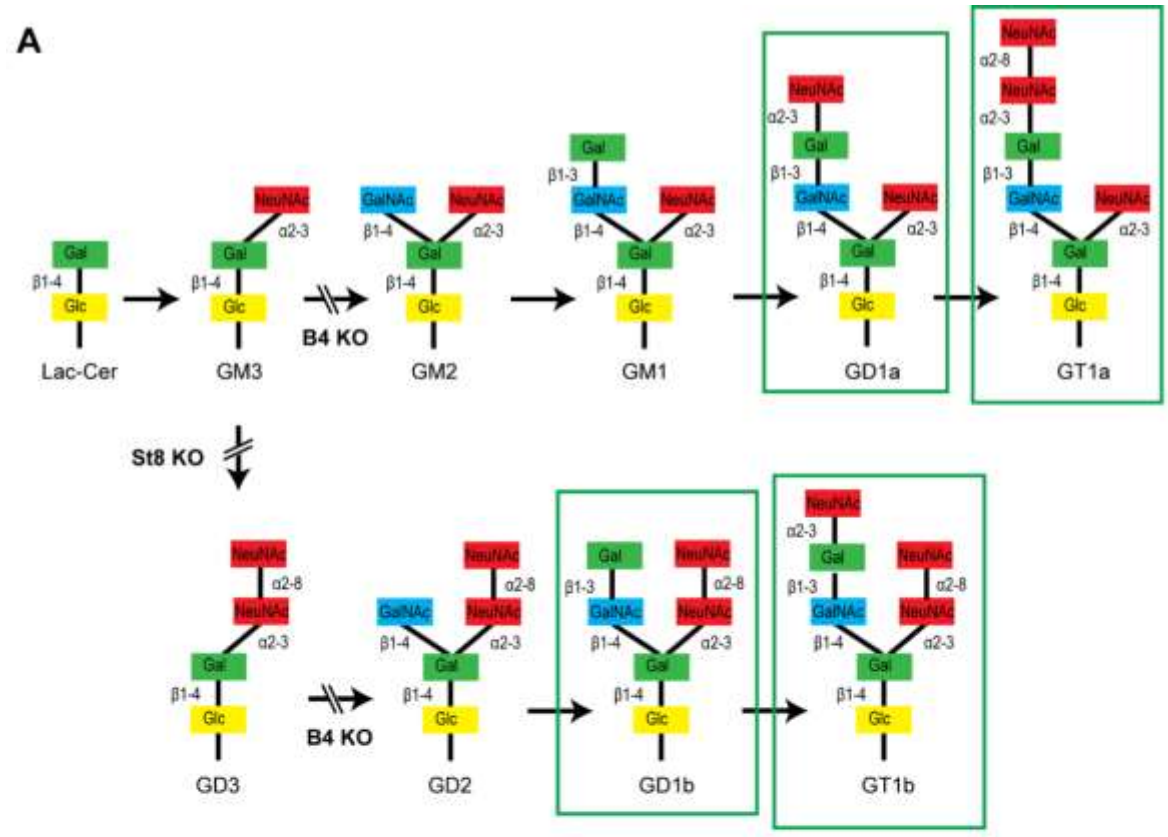
A
Lac-Cer
GM3
B4 KO
GM2
GM1
GD1a
GT1a
St8 KO
GD3
B4 KO
GD2
GD1b
GT1b

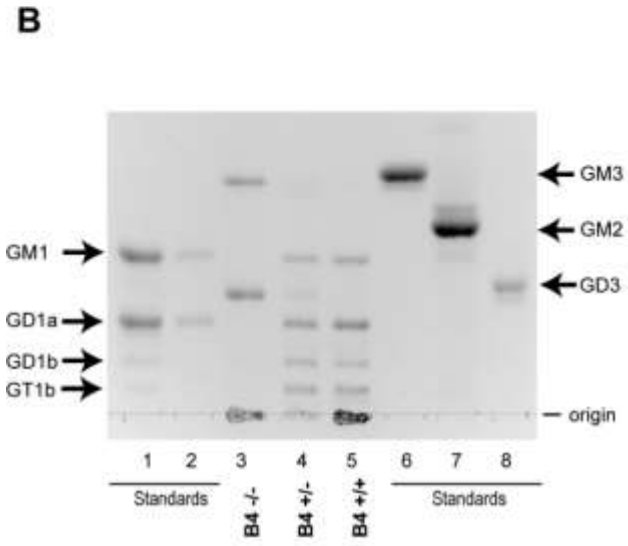
B
GM1
GD1a
GD1b
GT1b
GM3
GM2
GD3
origin
1 2 3 4 5 6 7 8
Standards
B4 -/-
B4 +/-
B4 +/+
Standards

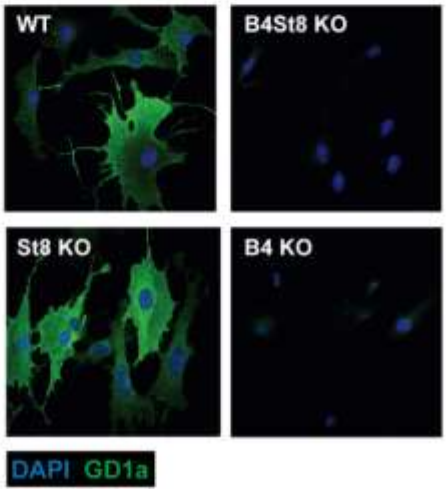
C
WT
B4St8 KO
St8 KO
B4 KO
DAPI GD1a

3.3.2 B4 -/- Mice Survive Infection by a Lethal Strain of MuPyV. The LID strain of MuPyV induces a rapidly lethal infection of newborn mice of most backgrounds. Mice typically succumb within a few weeks due to a widely disseminated infection with extensive destruction of the kidney and other vital tissues. LID owes its virulence to an amino acid substitution in the major capsid protein VP1 that is thought to reduce its hydrophobic interactions with the sialic acid ring. This lower avidity binding of virus to cells may facilitate release from cell debris and promotes virus spread. To establish the importance of gangliosides in mediating this infection, newborn mice from a cross of heterozygous B4 -/- mice were inoculated with LID in Tom Benjamin's laboratory. Mice were followed daily and death was used as an endpoint. Genotyping was carried out retrospectively, *i.e.,* at time of death or at the end of the experiment.

Wild-type mice (B4 +/+) all succumbed within 14 days, as expected. Homozygous knockout mice (B4 -/-) all survived and showed no overt signs of illness at 35 days post infection when the experiment was terminated. Heterozygous mice (B4 +/-) also succumbed, though with a delay compared to wild-type mice. A single copy of the GM2/GD2 synthase gene targeted in the B4 -/- mouse thus sufficed to confer susceptibility. The extended survival of B4 heterozygotes is consistent with a gene dosage effect, whereby overall levels of enzyme activity (*i.e.,* ganglioside synthesis) correlate inversely with mean survival time. Results with homozygous St8 -/- mice were also consistent with this view. These mice (St8 -/-) all succumbed, but like B4 +/-, survived longer than wild-type mice (Figure 3.2A). The St8 mice retain GD1a and other a-series gangliosides (Figure 3.1A, 3.1C)

indicating that these receptors are sufficient for lethal LID infection in the absence of GT1b and other b-series gangliosides. Thus, MuPyV infection is delayed by either decreased ganglioside diversity or decreased abundance of complex gangliosides. These results establish the importance of complex gangliosides lacking in the B4 -/- mouse for mediating infection, and confirm for the first time that specific gangliosides are required for virus infection *in vivo*. These results establish the importance of complex gangliosides lacking in the B4 -/- mouse for mediating infection by the LID strain of MuPyV. They confirm for the first time that specific gangliosides are required for virus infection *in vivo*.

3.3.3 GD3 Does Not Function as a Receptor in Mice Despite Binding VP1 *In Vitro*.

B4 -/- mice express only GD3 and GM3 and are not susceptible to lethal LID infection (Figure 3.2). GM3 was previously shown to be unable to bind virus based on a flotation assay using ganglioside-supplemented liposomes. However, GD3 has been identified in a glycan array screen as a strong binder of recombinant VP1 pentamers. A co-crystal structure of recombinant VP1 pentamers with the GD3 glycan has been determined (Buch et al. 2015). B4 -/- MEFs synthesize GD3 while B4St8 MEFs do not (Figure 3.1A). GD3 accumulates to high levels in kidneys of B4 -/- mice (Figure 3.1B, lane 3). Despite the high endogenous levels of GD3, B4 -/- mice are resistant to infection (Figure 3.2). We conclude that GD3 does not serve as an efficient functional receptor *in vivo* despite its ability to bind the viral capsid subunits *in vitro*.

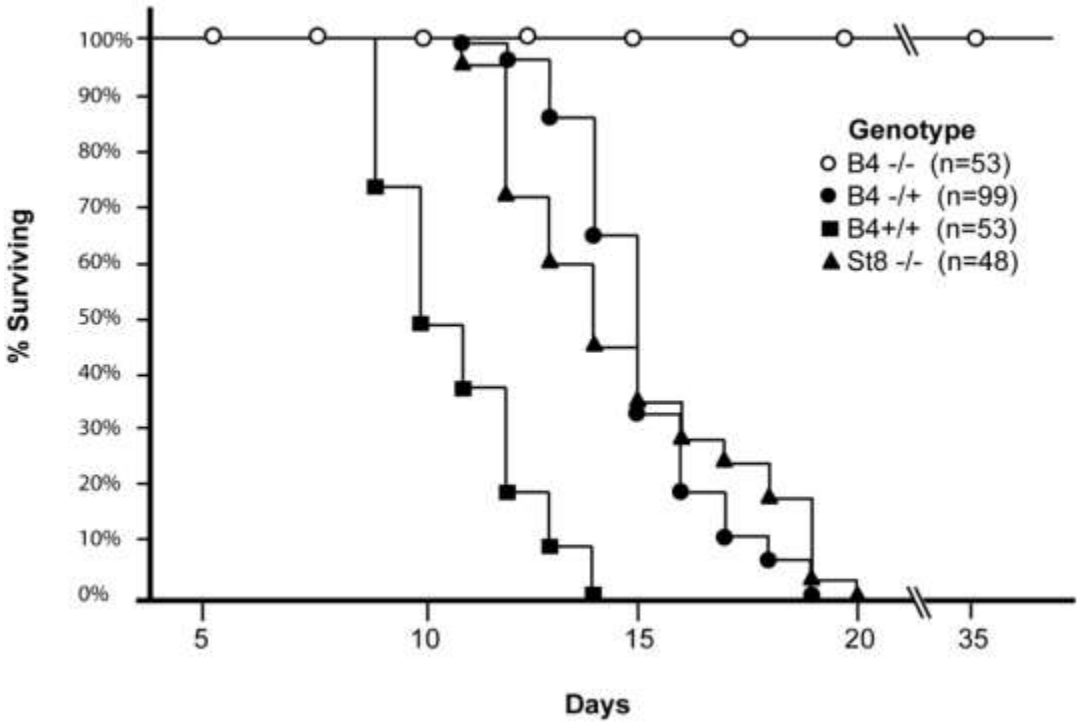

Figure 3.2: Characterization of St8 and B4 -/- mice. A. Kaplan-Meier survival curves for wild-type and ganglioside-knockout mice. Newborn mice were inoculated intraperitoneally with ~10^6 PFU of the LID strain of virus and followed using death as an endpoint. Figure adapted from (You & O'Hara et al. 2015)

3.3.4 Supplementation of GT1a and GD1b restores infection of B4St8 MEFs. Mouse embryo fibroblast cultures (MEFs) were established from wild-type and ganglioside-deficient mice. These cells were used to access the degree of resistance and the roles of specific gangliosides in mediating infection. B4St8 MEFs were completely resistant to infection (DMSO Figure 3.3). GD1a and GT1b have previously been shown to confer susceptibility to MuPyV infection when added to ganglioside-deficient rat and mouse cell lines (Gilbert et al. 2005; Tsai et al. 2003). We sought to extend these results using the B4St8 -/- cells, which are genetically defined and have known ganglioside composition (Figure 3.1). GD1a was used as a positive control, and GM1, the SV40 receptor, as a negative control to confirm previous results. We then tested the ability of additional gangliosides, GT1a and GD1b, to confer susceptibility using the RA strain of virus. GT1a had been suggested as a possible receptor based on co-crystallization with MuPyV VP1 further discussed in Chapter 4 (Buch et al. 2015). Cells were pre-incubated with 0.5 to 2.0 μM gangliosides in serum-free medium for 16 h, then infected and scored for T-ag expression 24 h post-infection. GT1a conferred infectibility slightly more efficiently than GD1a, a result consistent with *in vitro* affinity studies and GD1b conferred low levels of infectibility, much less efficiently than GT1a or GD1a (Figure 3.3A). The SV40 receptor GM1 did not confer any infection of B4St8 -/- cells.

3.3.6 Gangliosides are required for high levels of virus accumulation on the cell surface. The VP1 binding pocket of MuPyV is thought to accommodate both glycolipid (ganglioside) and glycoprotein binding. Thus, we investigated the dynamics and levels of cell surface binding of virus in the presence or absence of

ganglioside receptors. Wild-type, B4St8 -/-, and GD1a-supplemented B4St8 -/- MEFs were infected (RA MuPyV, 10 PFU/cell) at 4°C followed by fixation and staining for cell surface VP1 using a VP1 antibody. Virus binding to wild-type MEFs at 4°C was time dependent with two cell populations at 1 h post virus addition: a cell population with low virus accumulation ($<10^2$ VP1 staining) and a cell population with high virus accumulation ($>10^2$ VP1 staining) (Figure 3.3B). B4St8 -/- MEFs were also bound by virus in a time dependent manner; however, these cells displayed only low virus accumulation after 1 h at 4°C ($<10^2$ VP1 staining) (Figure 3.3B). Supplementation of B4St8 -/- MEFs with 5 µM GD1a prior to virus addition restored virus accumulation on the cell surface after 1 h at 4°C ($>10^2$ VP1 staining) (Figure 3.3B). These data indicate that although virus binds cells in the absence of ganglioside receptors, the dynamics of binding are changed. Gangliosides result in high levels of virus accumulation on the cell surface, whereas alternative interactions result in lower levels of overall virus binding.

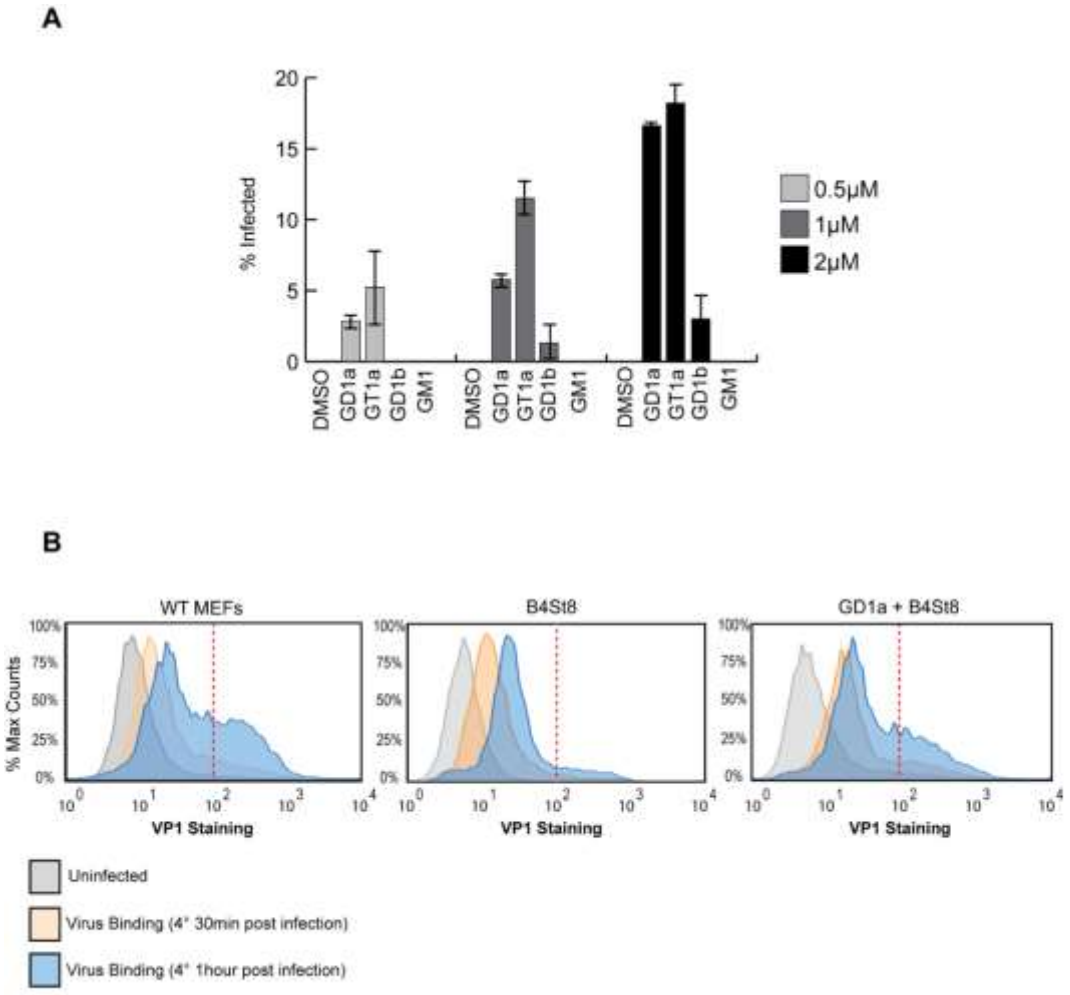

Figure 3.3: A. GT1a and GD1b restore Infectibility to B4St8 MEFs. GT1a, GD1a, and GD1b supplementation of B4St8 -/- MEFs rescued RA infection in a dose responsive manner (0.5 μM to 2 μM). GM1 supplementation did not rescue infection of B4St8 -/- MEFs. **B. Virus binding to wild-type, B4St8, and GD1a-supplemented B4St8 MEFs.** WT, B4St8, and GD1a-supplemented B4St8 -/- MEFs were assayed for MuPyV binding by flow cytometry. Cells were starved overnight in serum free media with or without 5μM GD1a. Cells were then infected with MuPyV (NG59RA, MOI 10) at 4°C. After 30 min at 4°C, bound virus was detected by VP1 staining. WT, B4St8, and GD1a-supplemented B4ST8 -/- MEFs had a 6 to 8 fold increase in VP1 staining compared to uninfected cells (shown in grey). GD1a-supplemented B4St8 -/- MEFs showed a similar VP1 binding pattern as WT MEFs and B4St8 -/- MEFs showed lower levels of VP1 accumulation on the cell surface. The x-axis is VP1 staining and the y-axis is normalized cell counts, each sample contained >10,000 cells.

3.3.6 Virus Endocytosis Occurs in Ganglioside-deficient Fibroblasts. Using the B4St8 ganglioside -/- MEFs we determined whether gangliosides are required for virus entry. Wild-type MEFs and B4St8 -/- MEFs were infected with MuPyV (RA, 50 PFU/cell) and then fixed at the indicated times post-infection (30 min, 3 h). At 30 min post-infection in wild-type MEFs a line scan analysis showed that MEFs exhibit similar staining for cell surface (shown in red) and total VP1 (shown in green), indicating minimal virus internalization at this early time (Figure 3.4B). Similar results were seen in B4St8 -/- MEFs at 30 min post infection (Figure 3.5B). At 3 h post-infection in wild-type MEFs a line scan analysis showed that MEFs had abundant intracellular VP1 staining (green only), indicating a large fraction of internalized virus (Figure 3.4C). B4St8 ganglioside -/- MEFs also displayed high levels of internalized virus as shown by line scan analysis (green only) (Figure 3.5C). These data demonstrate that gangliosides are not required for virus entry into MEFs, and virus can enter cells though non-ganglioside mediated pathways. Given the complete resistance of these B4St8 -/- cells to MuPyV infection (Figure 3.3A), it can be assumed that virus uptake *via* these alternative routes proceeds along a non-infectious or 'dead end' pathway. While the presence of glycoproteins such as $\alpha 4\beta 1$ integrin have been observed to enhance infection, gangliosides are required for virus uptake along infectious pathways.

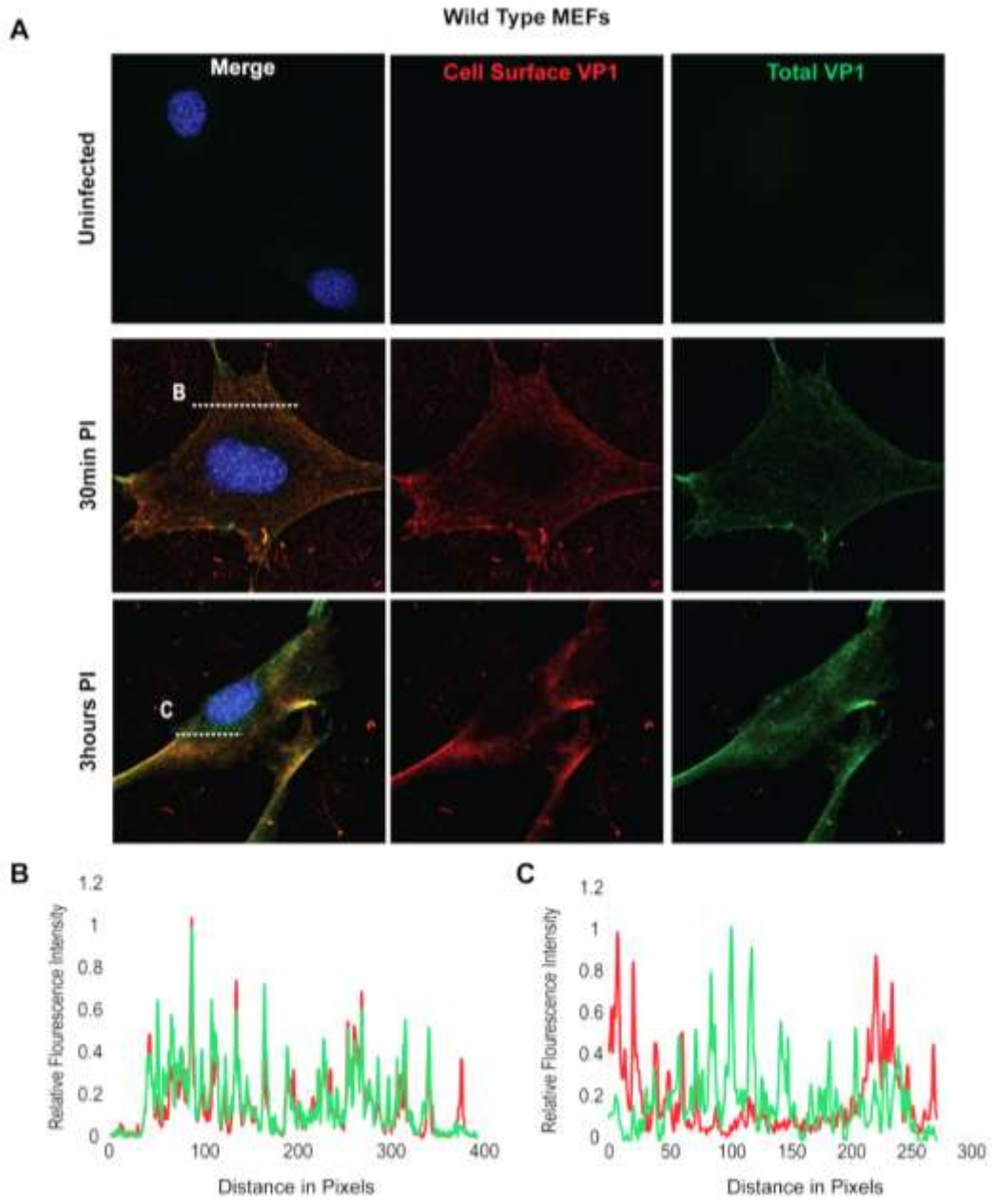

Figure 3.4: Virus Internalization in Wild-Type MEFs. Wild-type MEFs were infected with MuPyV and then fixed at the indicated times post infection (30 min, 3h). **(A)** Slides were stained for cell surface VP1 (red), and then permeabilized and stained for total VP1, showing both cell surface and intracellular VP1 (green). **(B)** At 30 min post-infection line scan analysis shows that MEFs exhibit similar staining for cell surface and total VP1, indicating minimal virus internalization. **(C)** At 3 h post-infection line scan analysis shows that MEFs exhibit abundant intracellular VP1 staining (green only), indicating internalized virus.

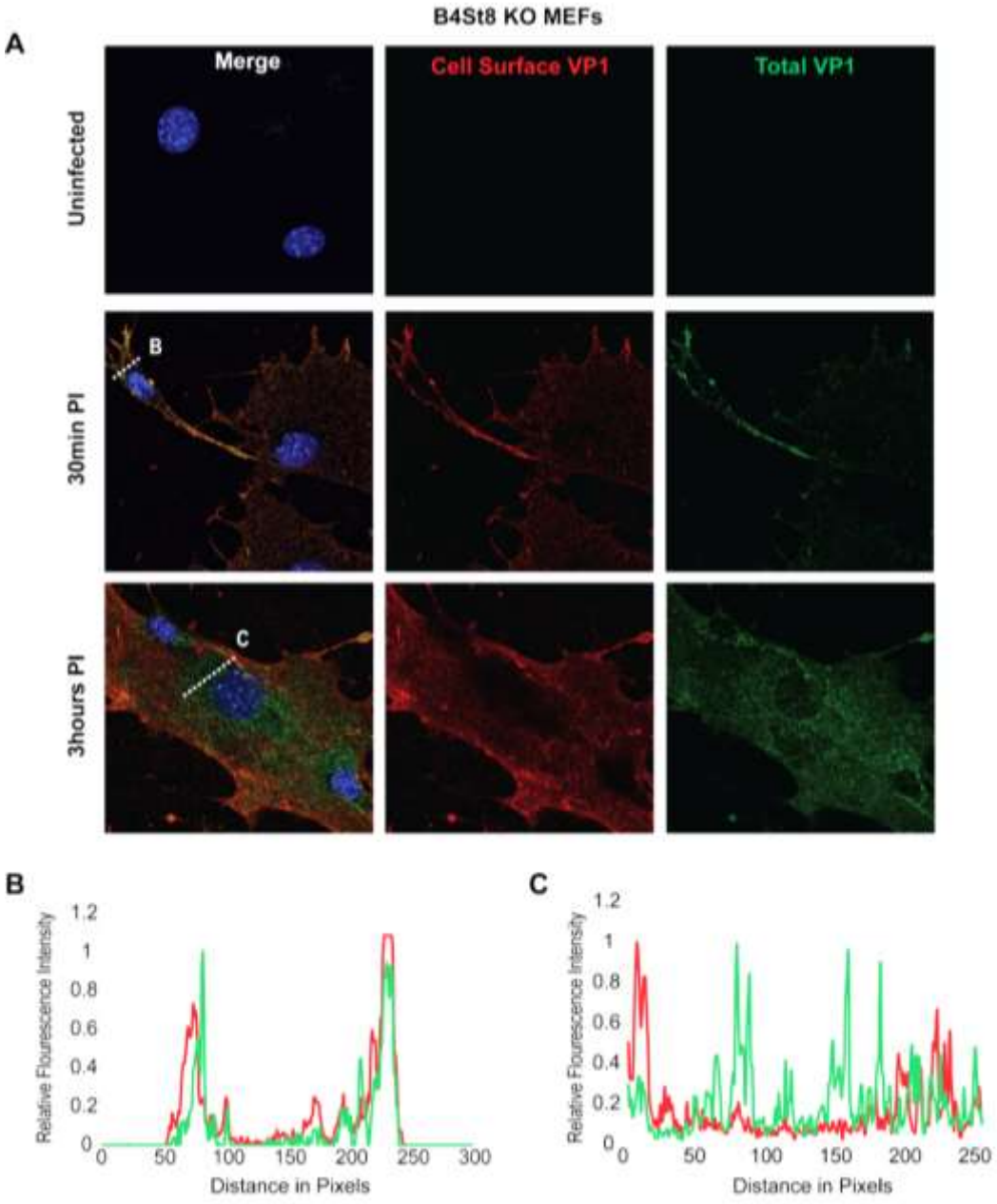

Figure 3.5: Virus Internalization in B4St8 -/- MEFs. B4St8 knock out MEFs were infected with MuPyV and then fixed at the indicated times post infection (30 min, 3 h). **(A)** Slides were stained for cell surface VP1 (red), and then permeabilized and stained for total VP1, showing both cell surface and intracellular VP1 (green). **(B)** At 30 min post-infection line scan analysis shows that B4St8 MEFs exhibit similar staining for cell surface and total VP1, indicating minimal virus internalization. **(C)** At 3 h post-infection line scan analysis shows that B4St8 -/- MEFs exhibit abundant intracellular VP1 staining (green only), indicating internalized virus.

3.4 Discussion

Ganglioside supplementation experiments in ganglioside-deficient rat and mouse cell lines have identified specific gangliosides (GD1a and GT1b) as MuPyV receptors; however, these findings had not previously been validated *in vivo* (Gilbert & Benjamin 2004; Tsai et al. 2003). Additionally, the role of gangliosides in other host-responses to MuPyV infection such as mitogenic gene induction and innate immunity has not been investigated. Tom Benjamin's lab generated mouse strains that are deficient (St8 -/-) and null (B4 -/-) for complex gangliosides to further characterize the specificity of ganglioside-mediated host responses to MuPyV *in vivo*. The St8 -/- mice are deficient in GD3 synthase and do not synthesize b-series gangliosides (GD1b and GT1b) but retain synthesis of the a-series gangliosides (GD1a and GT1a) (Figure 3.1 A and C). St8 -/- mice succumb to LID infection, indicating that a-series gangliosides are sufficient to mediate a lethal virus infection (Figure 3.2). The B4 -/- mouse lacks GM2/GD2 synthase, which is required for both a-series and b-series ganglioside synthesis (Figure 3.1 A and C). The finding that newborn B4 -/- mice are completely resistant to infection by the normally lethal LID strain of MuPyV provides clear evidence that gangliosides are required for infection (You & O'Hara et al. 2015). The LID strain was chosen to evaluate the role of gangliosides in the animal because of its rapid effects ending in death as a discrete endpoint. Because the knock-out strains were derived from tumor-resistant C57BL/6 mice the tumorigenicity of the PTA and RA strains cannot be evaluated for ganglioside dependence using these mice. However, because these strains of MuPyV, like LID, are unable to infect B4St8 -/- MEFs, it is expected that they would

be unable to infect ganglioside-deficient mice. Results using LID have shown for the first time that the GM2/GD2 synthase pathway is necessary and sufficient for MuPyV infection *in vivo*. This finding in the natural host is an important *in vivo* validation of earlier biochemical and cell culture results (Gilbert & Benjamin 2004; Gilbert et al. 2005). Additionally, these mice provide an excellent model to test the role of gangliosides in other host responses to MuPyV infection.

Early biochemical and *in vitro* experiments were extremely valuable in first identifying gangliosides as possible receptors for MuPyV based on ganglioside binding to VP1-pentamers, reviewed in Chapter 2. However, results presented here have shown that distinctions must be made between gangliosides that bind *in vitro* and those that serve as functional receptors *in vivo.* GD3 was identified in a screen of a glycan array as an effective binder of VP1-pentamers. The GD3 glycan also binds recombinant VP1 pentamers in crystallographic studies (Buch et al. 2015). This ganglioside however does not confer susceptibility to infection under normal conditions. The observation that B4 -/- mice have high levels of GD3 in the kidney (Figure 3.1B), yet are resistant to infection, is convincing evidence that this ganglioside is unable to mediate infection *in vivo* despite binding to VP1 *in vitro.* Discrepancies between results of biochemical binding and *in vivo* infection are important to recognize for a full evaluation of receptors from a functional standpoint.

Previous experiments have shown that GD1a or GT1b are sufficient for infection of ganglioside-deficient rat glioma cells (Gilbert et al. 2005). When fibroblasts from B4St8 ganglioside-deficient mice were pre-incubated with gangliosides GT1a or GD1b their infectibility was restored (Figure 3.3A). Because

B4St8 MEFs lack all complex gangliosides, these data show that supplementation with single gangliosides is sufficient for MuPyV infection.

Structural studies of the MuPyV capsid protein VP1 have revealed that VP1 binds sialic acid within a pre-formed sialic acid binding pocket on the virus surface (Stehle et al. 1994). These results suggest that MuPyV could potentially bind sialyated oligosaccharides on either glycoproteins or glycolipids (*i.e.,* gangliosides) though interactions with sialic acid. Thus, we evaluated MuPyV cell surface binding in the presence or absence of ganglioside receptors. We found that while virus binds to the cell surface of B4St8 -/- MEFs, it accumulates to lower levels than in wild-type MEFs or GD1a-supplemented B4St8 MEFs (Figure 3.3B). These results suggest that virus binding to gangliosides is required for high levels of virus accumulation on the cell surface, although the presence of glycoprotein or other interactions on ganglioside-deficient cells allows for some virus binding to the cell surface. Cell surface binding of virus is not necessarily indicative of virus entry. Therefore, we determined if virus enters cells in the absence of ganglioside receptors. We observed that MuPyV is internalized in the absence of gangliosides (Figure 3.5). Importantly, uptake of virus under these conditions does not lead to infection. Previous studies have shown that proteinase treatment of cells prior to MuPyV addition leads to slight increases in infection, suggesting that MuPyV-glycoprotein interactions inhibition MuPyV infection. This inhibition may be due to altered trafficking of MuPyV, whereby ganglioside receptors mediate transport of MuPyV to the ER along an infectious pathway while glycoproteins act as “decoy receptors” and lead to MuPyV degradation. Our results are consistent with the idea

that MuPyV-glycoprotein interactions lead to non-infectious pathways of entry. It is possible that glycoprotein interactions mediate other host responses to virus infection, such as mitogenic signaling, or the immune response. Alterations of these responses are not readily apparent in infection-based cell culture experiments.

It has previously been shown that ag-presenting cells from wild-type mice that mount effective adaptive anti-tumor responses respond to virus challenge at the innate level by secretion of the type 1 cytokine IL-12 (Velupillai et al. 2012). TLR-4 is required for the IL-12 response in these mice and mice lacking TLR-4 are suspectible to MuPyV tumor induction, likely due to a loss of IL-12 secretion. MuPyV is thought to bind to TLR-4 though sialic acid containing oligosacharride regions on the extracellular domains of TLR-4 (Velupillai et al. 2012). To confirm that sialic acid interactions are required for IL-12 induction Tom Benjamin's lab treated splenocytes with neuraminidase prior to challenge with virus. As expected, pretreatment with neuraminidase blocks the cytokine response to MuPyV in both wild-type, St8 -/-, and B4 -/- cells; however, neuraminidase treatment also abrogates MuPyV-ganglioside interactions and thus is not informative about the role of gangliosides in IL-12 induction (You & O'Hara et al. 2015). Tom Benjamin's lab sought to abolish MuPyV-TLR4 interactions while retaining ganglioside interactions, by treating with Peptide-*N*-Glycosidase (PNGase), which removes N-linked carbohydrate chains from glycoproteins, prior to virus challenge. They found inhibition of the IL-12 response by pretreatment with PNGase providing further support for TLR4 as a required receptor in the innate immune response to MuPyV and confirming that MuPyV-ganglioside interactions are not sufficient for IL-12

induction. Lastly, they wanted to determined whether gangliosides contribute positively or negatively to the innate immune response induced by virus binding. Splenocytes from B4 -/- mice display an increased IL-12 response compared to wild-type or St8 -/- splenocytes (You & O'Hara et al. 2015). These data indicate that gangliosides may dampen the cytokine response, possibly by competing for virus binding with the TLR4 glycoprotein receptor. This observation suggests that glycolipids and glycoprotein receptors act in an opposing manner in multiple ways, even at the level of the innate immune response.

Gangliosides contribute to a diverse array of physiological responses involved in viral infection. Results of experiments in ganglioside-deficient mice show that while gangliosides are essential as receptors for MuPyV infection, they are not essential for cell surface binding, cell entry, or innate immune responses of the host. Additionally, the antiviral immune response was heightened in ganglioside-deficient splenocytes, indicating that gangliosides somehow serve to dampen the antiviral cytokine response. These data establish that multiple types of receptors bearing sialic acid are utilized by the virus to mediate different aspects of virus-host interaction. These results could have implications for tissue tropism and immune response generated *in vivo* by other Polyomaviruses.

Chapter 4: Structural and Functional Analysis of Murine Polyomavirus Capsid Proteins Establish the Determinants of Ligand Recognition and Pathogenicity

4.1 Introduction:

Virus attachment to the cell surface is a major determinant of infection. Viruses bind to protein, lipid, and carbohydrate receptors on the cell surface. Virus tropism is dependent on host receptor expression as well as on the affinity of the virus-receptor interaction. Enveloped viruses often express proteins in their lipid coat that bind to cell surface receptors and lead to eventual membrane fusion with the host plasma or endosomal membrane. Non-enveloped viruses are dependent upon their protein capsid for cell surface binding and the capsid contains receptor binding sites embedded in its surfaceThe ganglioside binding pocket of VP1 is a shallow groove that binds sialic acid and attached sugars with millimolar affinity (Stehle et al. 1994; Stehle & Harrison 1997). Each VP1 monomer contains a ganglioside binding pocket, thus there are 360 possible ganglioside binding sites per capsid allowing for multivalent binding to receptors.

Mouse polyomavirus (MuPyV) infects the kidneys and other mesenchymal tissues of newborn mice (Dubensky et al. 1991). The gangliosides GD1a and GT1b are known to be infectious receptors for MuPyV (Gilbert & Benjamin 2004; Tsai et al. 2003). GD1a is an a-series ganglioside that contains terminal [α2-3]-linked sialic acids (Neu5Ac) on both the right and left hands of the sugar. GT1b is a b-series ganglioside that contains both the sialic acids in GD1a, with an additional [α2-8]-linked sialic acid sialic acid on the right hand of the sugar (Figure 3.1A). The sialic acid head groups as well as the linked galactose and N-acetyl galactosamine lie in the shallow binding pocket of the VP1 capsid (Figure 4.1). The affinity of a single VP1 monomer for GD1a is

extremely low, estimated to be 5mM (Stehle & Harrison 1997). However, due to the 360 possible binding sites per capsid, the avidity of ganglioside binding is very high, on the order of a covalent bond (Ewers & Helenius 2011).

MuPyV is an example of a virus whose infectivity and tropism can be dramatically changed by slight alterations in receptor binding. The MuPyV strains RA, PTA, and LID display extreme differences in tumorigenicity and tropism caused solely by single amino acid substitutions in the glycan binding pocket (Figure 4.1) (Bauer et al. 1995; Bauer et al. 1999; Bolen et al. 1985). RA MuPyV is the prototypic small plaque laboratory strain, which is asymptomatic and non-tumorigenic with limited spread toughout the organism. PTA MuPyV, a laboratory derived large plaque virus, contains a single point mutation in VP1 G91E, and infection of mice with PTA leads to tumors and altered tropism, with tissues of both mesenchymal and epithelial origin being infected. LID MuPyV is also a laboratory derived large plaque virus, and in addition to G91E contains an additional point mutation V296A (Bauer et al. 1995). LID is extremely virulent in mice and infects almost every tissue type leading to brain hemorrhaging and kidney failure. The ability of PTA and LID to form large plaques and spread toughout the organism has long been attributed to a possible decrease in ganglioside receptor binding either though altered affinity of interactions or exclusion from binding to certain ganglioside receptors. The substitutions at G91 and V296 reside in the ganglioside binding pocket, further suggesting altered glycan interactions in the virus strains.

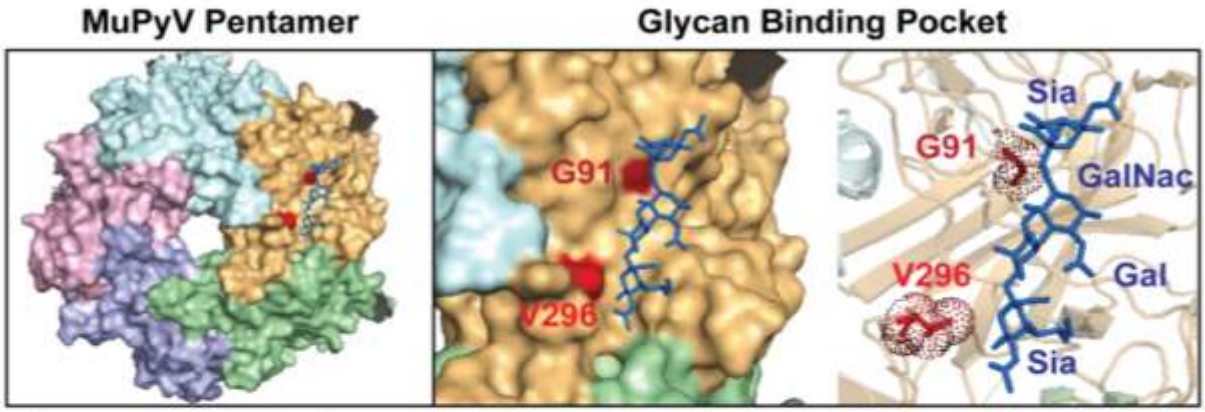

	RA	PTA	LID
Amino Acids	G91, V296	E91, V296	E91, A296
Pathogenicity	Asymptomatic. Infects tissues of mesenchymal origin.	Tumor Causing. Infects both epithelial and mesenchymal tissues.	Virulent. Lytic infection of all tissue types. Causes brain hemorrhages and kidney failure. Lethal.
Plaque Size	Small	Large	Large
Latency	Long	Short	Very Short

Figure 4.1: MuPyV Strains Have Single Amino Acid Substitutions in the VP1 glycan binding pocket. The MuPyV VP1 pentamer with the sites of the single amino acid mutations shown in red (G91 and V296). Sia = Sialic acid, Gal = galactose, GalNac = n-acteylglucosamine. Table shows amino acid substitutions and tropism information about the three MuPyV strains. MuPyV pentamer structure generated in PyMol (PDB 1SIE).

Modelling carried out by Dr. Michael Buch and colleagues in the Stehle lab suggested that a glutamate at position 91 could hinder PTA and LID MuPyV binding to gangliosides containing a [α2-6] linked sialic acid head group; whereas RA MuPyV may be able to bind to such receptors, effectivley limitting RAs spread thoughout the organism (Buch et al. 2015). To define the interactions of RA, PTA, and LID MuPyV strains with ganglioside receptors Dr. Buch and colleagues solved high-resolution structures of RA and PTA VP1 pentamers in complex with three ganglioside glycans that feature [α-2,3]-, [α-2,6]-, and [α-2,8]-linked sialic acids. Interestingly, Dr. Buch was unable to form crystals with the LID MuPyV in complex with ganglioside receptor fragments. Using crystallographic soaking experiments at different ligand concentrations Dr. Buch determined relative affinities of each virus-receptor combination (Buch et al. 2015). Additionally, during these experiments Dr. Buch identified a new oligosaccharide that bound to all three MuPyV strains at levels comparable to the oligosaccharide portions of confirmed gangliosides GD1a and GT1b. The newly identified oligosaccharide portions corresponded to the ganglioside GT1a, which is an a-series ganglioside, similar to GD1a, which contains an additional terminal [α2-8]-linked sialic acid on the left arm of the receptor. Binding of virus to a receptor does not necessarily indicate a receptor is an infectious receptor. Thus, in order to determine whether GT1a functions as an infectious receptor for MuPyV, or is a non-infectious pseudo-receptor, I carried out ganglioside supplementation experiments to determine if GT1a could restore MuPyV infection of ganglioside-deficient mouse embryonic fibroblast (gang -/- MEFs). Additionally, I compared infectivity of RA, PTA, and LID MuPyV after supplementation with multiple ganglioside family members to determine if the ganglioside usage of these

three virus strains were altered. This functional data was then combined with Dr. Buch's affinity experiments to determine whether there are differences in ganglioside binding between strains of MuPyV that might be linked to their altered tropism and pathogenesis.

4.2 Materials and Methods:

Ganglioside Supplementation and Quantification of MuPyV infection.

Wild-type and ganglioside -/- MEFs were seeded onto 96-well Costar 3906 imaging plates in Dulbecco's Modified Eagle's Medium supplemented with 10% fetal bovine serum (FBS). WT (B4+/+St8+/+) and ganglioside -/- MEFs (B4-/-St8-/-) were provided by Thomas Benjamin at Harvard Medical School. Gangliosides were purchased from Matreya LLC and resuspended in DMSO upon arrival, aliquoted, and stored at -20°C until use. Cells were incubated overnight in serum free media prior to infection. For ganglioside supplemented of ganglioside -/- MEFs, cells were starved in serum free media containing the indicated concentration of ganglioside. Gangliosides were then removed, and cells were washed with serum free media to remove any free ganglioside. Cells were then infected with NG59RA, PTA, and LID MuPyV (MOI ~10-30). At 24 h post infection cells were washed in phosphate buffered saline and fixed with 4% paraformaldehyde at room temperature for 10 min. Cells were then permeabilized with 0.1% Triton X-100, blocked in 10% FBS in PBS, and then stained for the viral protein, T-ag (E1). Samples were then incubated with Alexa Fluor labeled secondary antibodies (546). Plates were imaged with the Molecular Devices ImageXpress Micro XL High-Content Screener. To quantify infection, T-ag staining was measured per each DAPI labeled nuclei. For image analysis, the DAPI channel on each image was thesholded

and nuclei were counted using ImageJ (Analyze Particles). These particles were marked as “Regions of Interest” (ROI) and then the average pixel intensity of T-ag staining was measured for each nuclei (ROI). These were then binned into T-ag positive or T-ag negative nuclei to create % infected. The percent infected was calculated for each well (5 images were taken per well). These wells were quantified per sample and the average percent infected, standard error, and standard deviation were calculated for each sample.

Immunofluorescence Quantitation of VP1 staining.

Wild type and ganglioside -/- MEFs were seeded onto glass coverslips in Dulbecco's Modified Eagle's Medium supplemented with 10% fetal bovine serum (FBS). Cells were incubated overnight in serum free media prior to infection. For ganglioside supplementation, ganglioside -/- MEFs were starved in serum free media containing the indicated concentration of ganglioside. Gangliosides were then removed and cells were washed with serum free media to remove any free ganglioside. Cells were then infected with NG59RA. At indicated times post infection the cells were fixed with 4% paraformaldehyde at room temperature. Cells were blocked in 10% FBS in PBS and then stained for GD1a using mAb MAB5606 (Millipore). Cells were then permeabilized with 0.1% Triton X-100 and stained for the viral proteins, VP1 (I58 antibody) and T-ag (E1 antibody). Samples were washed and then incubated with Alexa Fluor labeled secondary antibodies (488, 546, 647). Slides were then mounted using DAPI prolong gold mounting media. Slides were imaged with a Nikon A1R confocal microscope. All images were taken as a 9 to 13 step (.25µm) z-stacks on a laser scanning confocal

microscope. Each z-stack was aligned and compressed into a max intensity Z projection image.

Virus Binding to Ganglioside Supplemented ganglioside -/- MEFs.

Wild type and ganglioside -/- MEFs were seeded onto a 24 well dish in Dulbecco's Modified Eagle's Medium supplemented with 10% fetal bovine serum (FBS). Cells were incubated overnight in serum free media prior to infection. For ganglioside supplemented ganglioside -/- MEFs, cells were starved in serum free media containing the indicated concentration of ganglioside. Gangliosides were then removed and cells were washed with serum free media to remove any free ganglioside. Cells were then infected with either NG59RA, PTA, or LID at an MOI ~10-30 (250µL/well). At 4h post infection 150 µL of virus supernatant was removed and placed into a microcentrifuge tube. This virus supernatant was then used to infect wild type MEFs seeded onto a 96 well plate (50 µL/well). The amount of free virus was then quantified as percent of infection of the 96-well reinfection plate. At 24 h post virus addition the plate was washed in PBS and fixed with 4% PFA at RT for 10 min. Cells were then permeabilized with 0.1% Triton X-100, blocked in 10% FBS in PBS, and then stained for the viral protein, T-ag (E1). Samples were then incubated with Alexa Fluor labeled secondary antibodies (546). Plates were imaged with the Molecular Devices ImageXpress Micro XL High-Content Screener. The percent infected was calculated for each well (5 images were taken per well) as indicated by T-ag positive nuclei. These wells were quantified per sample and the average percent infected, standard error, and standard deviation were calculated for each sample. For image analysis, the DAPI channel on each image

was thresholded and nuclei were counted using ImageJ (Analyze Particles). These particles were marked as “Regions of Interest” (ROI) and then the average pixel intensity of T-ag staining was measured for each nuclei (ROI). These were then binned into T-ag positive or T-ag negative nuclei to create % infected.

4.3 Results:

4.3.1 GT1a is an infectious receptor for all strains of MuPyV

We utilized a mouse embryo knock-out fibroblast cell line (ganglioside -/- MEFs) deficient in ganglioside synthesis that is completely resistant to MuPyV infection to test the ability of ganglioside receptors to rescue infection by different strains of MuPyV (You & O’Hara et al. 2015). Ganglioside -/- MEFs were supplemented with individual gangliosides followed by infection with RA, PTA, or LID MuPyV. The previously identified ganglioside receptors GD1a and GT1b rescued RA, PTA, and LID infection of ganglioside -/- MEFs in a dose-responsive manner (Figure 4.2). We also investigated if GT1a serves as an infectious receptor for MuPyV. We found that GT1a, a member of the ganglio-series synthesized from GD1a, also rescued RA, PTA, and LID infection in a dose responsive manner. Moreover, GT1a supplementation of ganglioside -/- MEFs conferred higher levels of RA, PTA, and LID MuPyV infection than the previously identified receptors GD1a and GT1b (Figure 4.2). Finally, we tested the ability of the gangliosides GD1b and GM1 to rescue MuPyV infection of ganglioside -/- MEFs. GD1b and GT1b supplementation has previously been shown to restore BKPyV infection of ganglioside deficient cells; however, GD1b restored little to no MuPyV infection of ganglioside -/- MEFs. GM1 supplementation has previously been shown to restore

infection by SV40; however, GM1 did not rescue MuPyV infection of ganglioside -/- MEFs. These data confirm that GT1a is an infectious receptor for all strains of MuPyV.

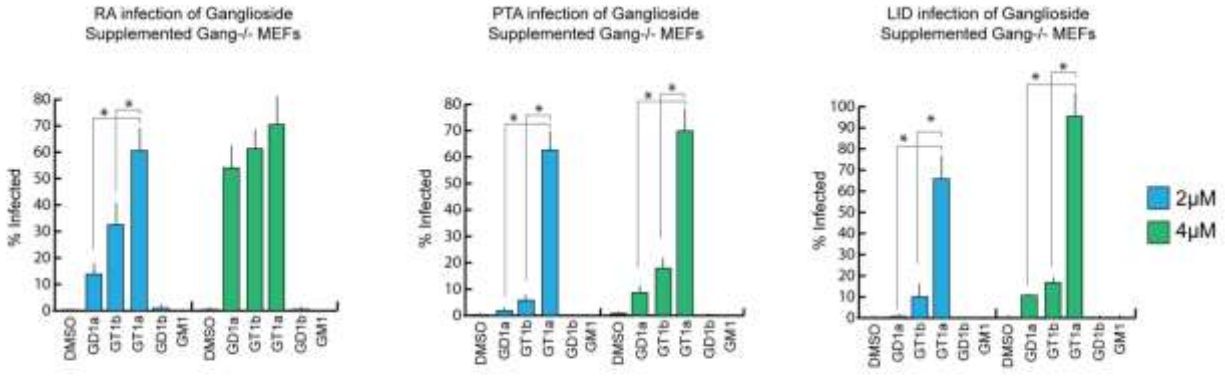

Infection P-Values

	RA		PTA		LID	
	2μM	4μM	2μM	4μM	2μM	4μM
GT1a/GD1a	0.0000	0.1203	0.0000	0.0000	0.0018	0.0026
GT1a/GT1b	0.0001	0.3808	0.0000	0.0000	0.0055	0.0044

Figure 4.2: GT1a, GT1b and GD1a supplementation rescues MuPyV infection of Gang-/- MEFs. Ganglioside knock-out (Gang-/-) MEFs were completely resistant to infection of all strains of MuPyV as shown by the absence of T-ag positive nuclei at 24 h post infection (DMSO control). GD1a, GT1b, and GT1a ganglioside supplementation of Gang-/- MEFs restored RA, PTA, and LID MuPyV infection, while GD1b and GM1 supplementation resulted in little to no infection by any virus strain. Infection levels were quantified at both 2 μM and 4 μM ganglioside supplementation (blue and green bars, respectively). Infection levels are normalized to MuPyV infection of WT MEFs, and error bars correspond to standard error.

4.3.2 Virus binding does not correlate with infection.

We also investigated whether MuPyV cell surface binding to infectious or non-infectious ganglioside receptors correlated MuPyV infection. To this end, we measured the levels of free (unbound) virus in each ganglioside supplemented sample at 4 h post infection. A higher ratio of free virus corresponds to less virus binding the cell surface. We were unable to detect significant differences in MuPyV cell surface binding to different ganglioside receptors or wild type MEFs, suggesting that cell surface binding alone does not determine infection (Figure 4.4). There was a slight correlation between RA MuPyV binding levels and infectivity as GD1a, GT1b, and GT1a show increased binding compared to GM1; however, it was not complete as GD1b does not serve as an infectious receptor and still decreased binding. It is perhaps unsurprising that we could not detect significant differences in MuPyV binding to ganglioside supplemented MEFs as MuPyV binds to ganglioside -/- MEFs in the absence of ganglioside supplementation (Figure 4.5) and the virus is also endocytosed in ganglioside -/- MEFs; however, did not lead to infection (discussed in Chapter 3). Virus binding to other receptors, such as α4-integrin may mediate binding in ganglioside -/- MEFs although this interaction was not sufficient for infection.

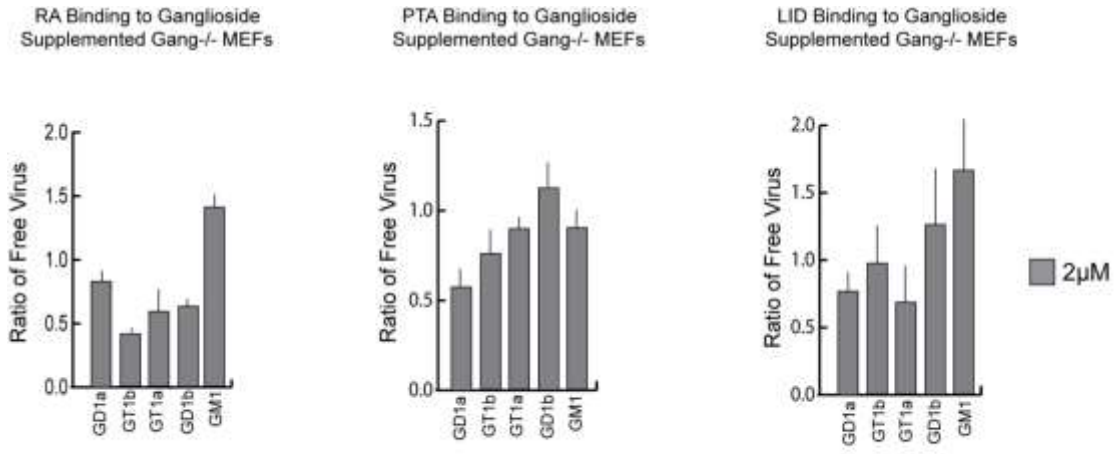

Figure 4.4: Binding levels of MuPyV strains to different ganglioside receptors. Gang-/- MEFs were supplemented with 2 μM GD1a, GT1b, GT1a, GD1b and GM1 followed by infection with RA, PTA, and LID MuPyV. At 4h post infection virus supernatant was removed and the amount of free virus was quantified for each sample by re-infection of WT MEFs. Virus bound to all cells at similar levels and there were no significant differences in virus binding to infectious *versus* non-infectious ganglioside receptors. Error bars are standard error and virus binding to WT MEFs is normalized to one.

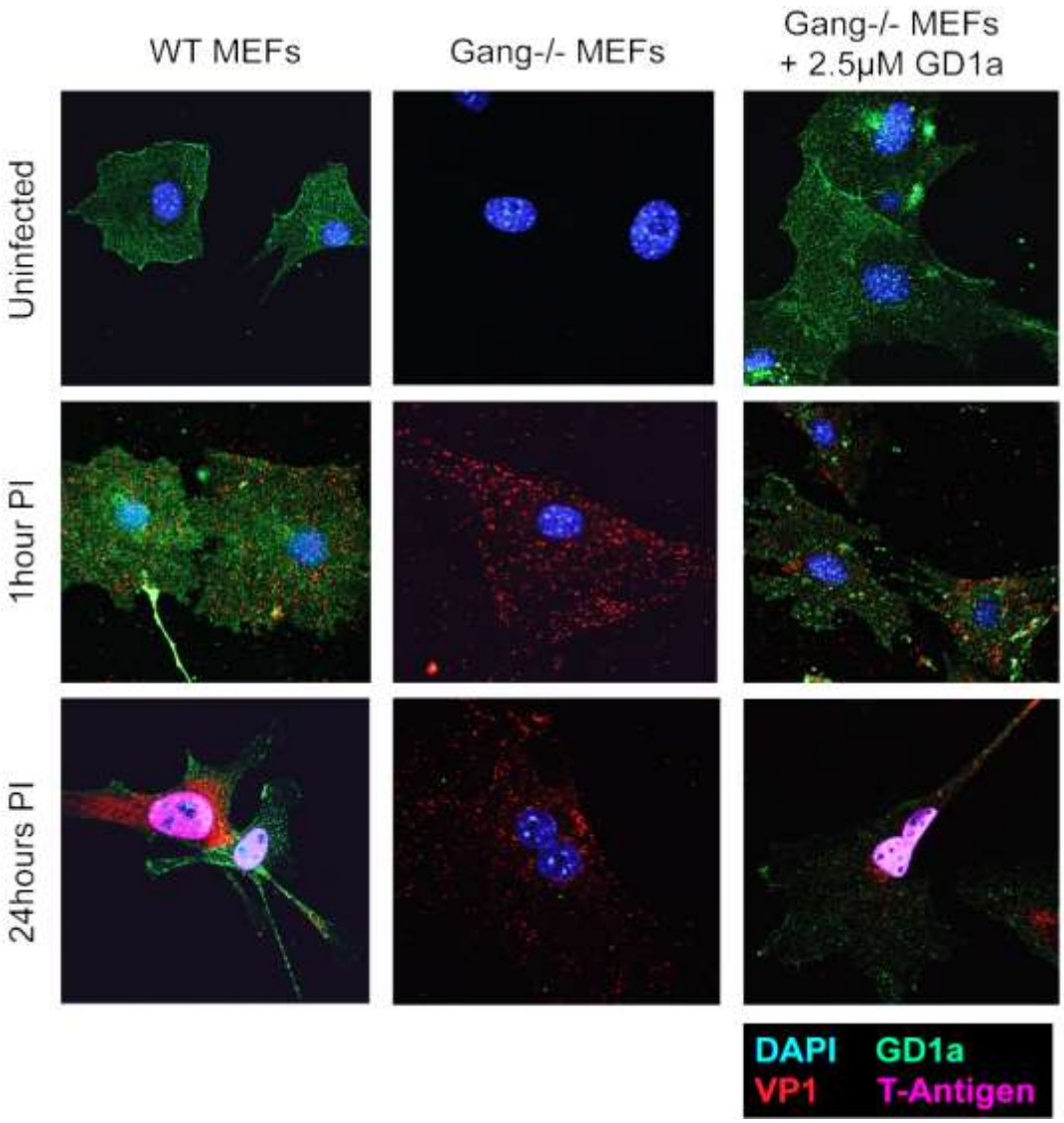

Figure 4.5: Virus binds the cell surface of ganglioside -/- MEFs. WT, gang-/- MEFs, and gang-/- MEFs supplemented with GD1a were infected with NG59RA MuPyV. The MuPyV ganglioside receptor GD1a can be detected on the WT MEFs and GD1a-supplemented gang-/- MEFs (green), but is absent in gang-/- MEFs. Virus binds WT, gang-/-, and GD1a-supplemented gang-/- MEFs as shown by VP1 staining (red) on the cell surface at 1hour post infection. At 24 h post infection, WT and GD1a-supplemented gang-/- MEFs show robust infection as indicated by nuclear T-ag staining (magenta).

4.4 Discussion

Receptor specificity is a major determinant of viral tissue tropism and virulence. Three strains of MuPyV that contain single amino acid mutations in their glycan binding pocket display drastically different tumorigenicity and spread *in vivo* (Bauer et al. 1995; Bolen et al. 1985). Although altered glycan binding is most likely the cause of these strain differences due to the location of these mutations in VP1, we were unable to confirm conclusive differences in the receptor affinity interactions of these viruses and this may be due to the already low affinity of RA MuPyV for GD1a, which is in the millimolar range. Slight differences in such a low affinity are difficult to measure, although even minor differences in affinity may have dramatic effects on avidity. Additionally, there may be other receptors *in vivo* that have yet to be uncovered and these may contribute to the altered virulence of these viruses.

Dr. Buch discovered a new sialic acid containing oligosaccharide sequence that bound to VP1 pentamers *in vitro,* and this oligosaccharide corresponded to the extracellular portion of the ganglioside GT1a. GT1a had not been previously characterized as a receptor for MuPyV, but shares similar structural aspects to verified receptors GD1a and GT1b. Dr. Buch was able to obtain the crystal structure of VP1 in complex with GT1a with RA and PTA strains of MuPyV (Figure 4.4). The E91 mutation causes steric hindrance with the GalNac (N-acteylglucosamine) of GT1a; however, the [α2-8]- and [α2-6]-linked sialic acid head groups binds in the binding pocket suggesting that the ganglioside may serve as a MuPyV receptor for both strains. Interestingly, Dr. Buch was unable to obtain crystals with LID MuPyV and GT1a, perhaps due to lowered affinity for the receptor caused by the A296 substitution, even though they were still able

to obtain binding data *via* crystal soaking experiments. I demonstrated that GT1a is an infectious receptor for all strains of MuPyV using ganglioside supplementation in ganglioside deficient cells followed by infection with RA, PTA, and LID MuPyV. Surprisingly, GT1a conferred higher levels of infection than the validated receptors GD1a and GT1b for all tee strains of MuPyV. Dr. Buch's crystal soaking experiments also showed VP1 to have the highest affinity for GT1a, further confirming GT1a as an infectious receptor for MuPyV.

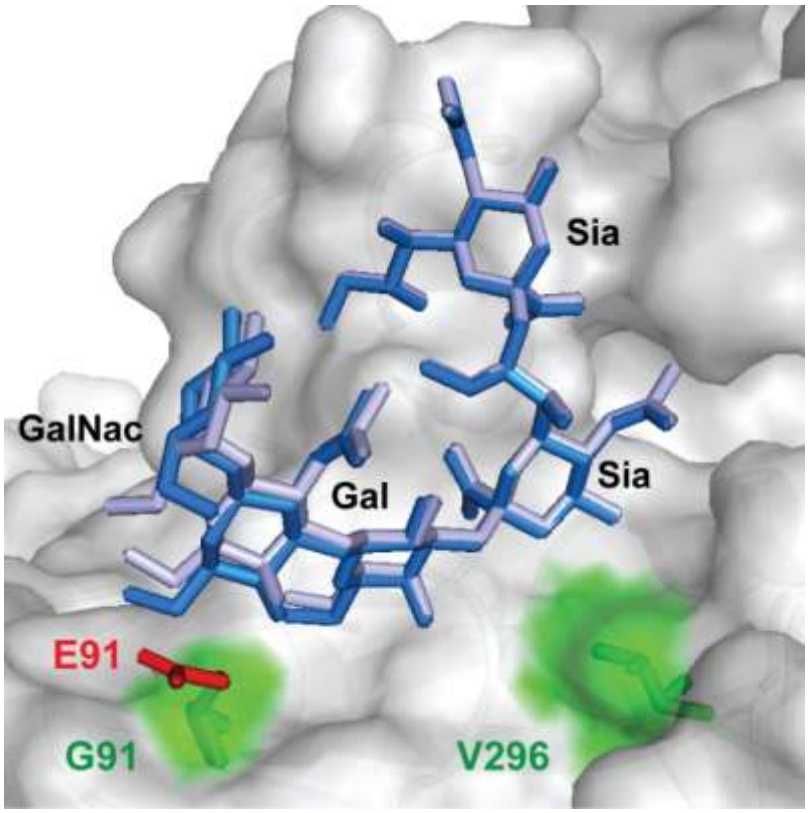

Figure 4.6: GT1a bound to the different MuPyV strains. Superposition of the GT1a-binding mode of RA (GT1a in dark blue) and PTA (light blue). The Sia-[α-2,8]-Sia-[α-2,3]-Gal-GalNac motif is shown as solid sticks. G91 and V296 shown in green. E91 mutation of PTA shown in red. All superpositionings were carried out in PyMOL using 'align' for the protein chains only (PDB 5CPW and 5CPZ).

Although gangliosides are ubiquitously expressed; the relative levels of different ganglioside receptors in tissues are not well understood (Saito & Sugiyama 2001; Maccioni et al. 1999). It is possible that GT1a is expressed at higher levels in certain tissues of mice *versus* GD1a and GT1b. LID and PTA were more sensitive to the GT1a ganglioside than RA, and this data may suggest that LID and PTA bind GT1a with higher affinity than GD1a or GT1b and could contribute to their altered tropism *in vivo*. The ability of MuPyV PTA and LID strains to bind GT1a more efficiently may be due to the additional [α2-8]-linked sialic acid that is distant from the G91 and V296 mutations, effectively stabilizing their binding to GT1a over GD1a/GT1b (Figure 4.6). Unfortunately, limitations of comparing infection levels across strains with vastly different PFU to particle ratios makes it impossible to determine if PTA and LID bind GT1a at higher affinity than RA based on our infection data alone (Figure 4.2). Dr. Buch's crystal soaking experiments were unable to demonstrate any significant differences between RA, PTA, and LID binding of GT1a; however, this method is also limited by the low affinity of VP1 for the ganglioside receptors. Thus, it remains to be determined exactly why RA, PTA, and LID MuPyV have such vastly different tropism and virulence. The MuPyV system remains a robust model for investigating the role of altered receptor binding in pathogenesis.

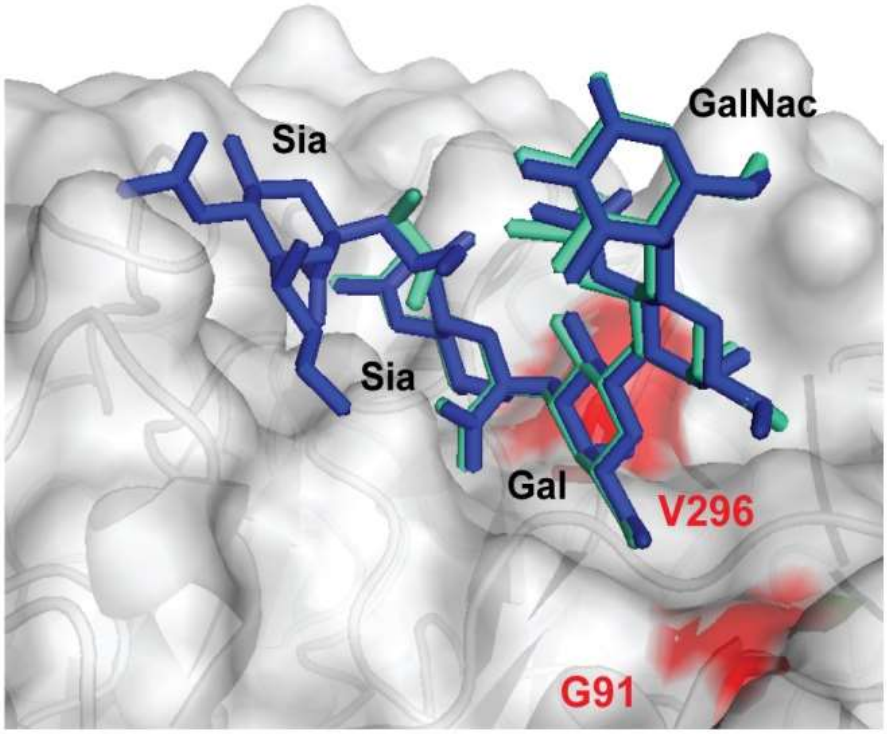

Figure 4.7: GT1a and GD1a Overlay of RA MuPyV VP1. Superposition of the GT1a-binding (dark blue) and GD1a-binding (light green) to MuPyV RA VP1 binding pocket. V296 and G91 are shown in red. All superpositionings were carried out in PyMOL using 'align' for the protein chains only (PDB 5CQO and 5CPZ).

Chapter 5: Murine Polyomavirus Cell Surface Receptors Activate Distinct Signaling Pathways Required for Infection

5.1 Introduction:

Virus binding to cell surface receptors often activates signaling cascades that promote virus entry (Greber 2002). Many enveloped viruses activate the PI3K pathway to facilitate virus entry and trafficking (Diehl et al. 2013). For example, Hepatitis C virus (HCV) binding to CD81 and claudin-1 transiently activates the PI3K pathway to enhance virus internalization, while the Zaire Ebola virus (ZEBOV) requires PI3K activation for virus release from endosomal compartments and trafficking (Liu et al. 2012; Saeed et al. 2008). How non-enveloped viruses use signaling during virus entry is less well understood.

Polyomaviruses (PyV) are non-enveloped, dsDNA viruses that rapidly induce primary response genes (*e.g., Myc, Fos, Jun*) upon binding to cells (Zullo et al. 1987; Glenn et al. 1990; Dangoria et al. 1996; You & O'Hara et al. 2015). Primary response genes are induced by mitogenic signals at the cell surface, such as growth factor ligand binding and subsequent growth factor receptor (GFR) activation. The rapidity of PyV primary response gene induction suggests that PyV cell surface binding may activate GFRs. Many GFRs are receptor tyrosine kinases and tyrosine kinase inhibition with genistein blocks SV40 and JCPyV infection, further suggesting that activation of GFRs is required for PyV infection (Querbes et al. 2004; Dangoria et al. 1996). However, PyVs are not known to bind GFRs directly, suggesting that other PyV receptor interactions may facilitate PyV-GFR activation.

Murine polyomavirus (MuPyV) binds to cell surface gangliosides and the α4-integrin receptor though specific sites on the VP1 capsid protein (Stehle & Harrison 1997; Stehle et al. 1994; Stehle & Harrison 1996), and both receptors are required for MuPyV infection (Tsai et al. 2003; Caruso et al. 2007; Caruso et al. 2003; You & O'Hara et al. 2015). Gangliosides are sialic acid-modified glycosphingolipids that reside in the outer leaflet of the plasma membrane. Mouse embryonic fibroblasts (MEFs) lacking gangliosides cannot be infected by MuPyV, but supplementation with specific gangliosides rescues infection (You & O'Hara et al. 2015). Integrins regulate cell attachment to the extracellular matrix, cytoskeletal organization, and proliferation (Srichai & Zent 2010). A point mutation in the VP1 α4-integrin binding motif or knockdown of the cellular α4-integrin reduces MuPyV infection by >60% (Caruso et al. 2007; Caruso et al. 2003). However, it is unclear how gangliosides or α4-integrin contribute to MuPyV infection, since MuPyV still binds to the cell surface and is internalized when these receptors are absent (You & O'Hara et al. 2015; Qian & Tsai 2010; Caruso et al. 2003; Caruso et al. 2007). Gangliosides have been shown to be required for trafficking of PyV to the endoplasmic reticulum, although the mechanism of this trafficking is unknown (Qian & Tsai 2010; Qian et al. 2009). Both gangliosides and integrins are important signaling molecules that may contribute to virus activation of GFRs required for virus entry or downstream trafficking.

Both gangliosides and integrins modulate GFR activation (Kaucic et al. 2006; Yates et al. 1995; Li et al. 2000; Liu et al. 2004; Miyamoto et al. 1996; Moro et al. 2002; Moro et al. 1998). Gangliosides interact with GFRs in lipid rafts and can activate GFRs even in the absence of a growth factor ligand (Liu et al. 2004). Clustering of integrins

though interactions with extracellular matrix proteins can also initiate and regulate signal transduction from GFRs (Legate et al. 2009; Srichai et al. 2010; Harburger & Calderwood 2009). Fibronectin binding to α4-integrin activates transcription of primary response genes, eliciting a similar transcriptional response as induced by MuPyV binding (Dike & Ingber 1996; Zullo et al. 1987; Glenn et al. 1990). Interestingly, MuPyV binds to α4-integrin though the same motif as fibronectin (Komoriyas et al. 1991), suggesting that MuPyV binding to α4-integrin could result in a similar mitogenic response. MuPyV multivalent binding to gangliosides and α4-integrin on the plasma membrane may therefore serve to *cluster* associated GFRs leading to their subsequent activation. Given their important role in cell signaling, gangliosides and α4-integrin likely contribute to MuPyV-induced signaling events, downstream transcriptional changes, and infectious entry.

We describe a diverse signaling network activated immediately following MuPyV-binding to the cell surface. We present evidence that interactions between VP1 and glycan receptors, gangliosides and integrins, stimulate specific signaling events required for MuPyV infection. Furthermore, we identified a subset of these signaling pathways that are critical for MuPyV entry and downstream trafficking of virus onto infectious pathways.

5.2 Materials and methods:

Cells: wild-type, gang-/-, and α4-integrin knock down MEFs: Mouse embryonic fibroblast (MEFs) and ganglioside knock out (gang-/-) MEFs, obtained from Thomas Benjamin at Harvard Medical School (You & O'Hara et al. 2015), were maintained in complete growth medium (10% FBS in DMEM). FAK +/+ and FAK -/- MEFs were

purchased from ATCC (CRL-2645, CRL-2644) and maintained in complete growth medium. The α4-integrin KD MEFs were generated in our laboratory. Lentiviruses containing sNAs directed against α4-integrin (refseq NM_010576) were prepared at from the Functional Genomics Facility at the University of Colorado (functionalgenomicsfacility.org).

Viruses and Pseudoviruses: Wild-type virus was NG59RA. Prior to addition to cells, the virus was sonicated at 70 watts for 1 min and incubated at 45°C for 20 min. The solution was centrifuged at 10,000 x g for 3 min. The virus supernatant was then dialyzed though a 100 kDa filter (Amicon Ultra URC510096) at 10,000 x g. The virus was then salt extracted (washed in 850 mM NaCl), followed by resuspension in PBS and washed an addition 2 x times though the 100 kDa filter to remove contaminants. Pseudoviruses were generated following the standard protocol (Buck & Thompson 2007) publically available at http://home.ccr.cancer.gov/lco/production.asp.

Gangliosides and Ganglioside Supplementation: Lyophilized gangliosides were obtained from Matreya LLC (GD1a #1062, GM1 #1061) and MyBiosource (GT1a MBS663096). Ganglioside supplementation was done as previously described in (You & O'Hara et al. 2015; Buch et al. 2015).

Immunoblotting and Antibodies: Cells were collected in RIPA buffer containing phosphatase inhibitors (NaF and Na_3VO_4) and a protease inhibitor cocktail (Roche 11836153001). Lysates were separated by 8-12% SDS-PAGE and transferred to a PVDF membrane. Membranes were incubated with primary antibody for 16 h at 4°C (Cell Signaling antibodies: anti-pERK #4695, anti-pAKT #4058, anti-AKT #9272, anti-p-cJun #3270/#9164, anti-α4-integrin #8440, p-EGFR #3777, anti-pFAK #3281, anti-pSRC

6943, anti-α-4-integrin #8440Abcam: pFAK #39967) or at 37°C for 1 h (Santa Cruz antibodies: anti-ERK sc-93, anti-Tubulin sc-8035). Immunoblots underwent chemiluminescent development and imaged on the Image Quant™ LAS400 imager. ImageJ was used to quantify the integrated density of bands.

Confocal Microscopy: MEFs were seeded onto glass coverslips in DMEM. At indicated times cells were washed in PBS and fixed with 4% paraformaldehyde. Cells were permeabilized with 0.1-0.5% Triton X-100 and stained for T-ag (E1)(Goldman & Benjamin 1975), GD1a (MAB5606, Millipore), or VP1 (I58). Samples were then incubated with Alexa Fluor labeled secondary antibodies. Cells were imaged on a Nikon A1R confocal microscope.

Flow Cytometry: Cells were dissociated from the plate with Versene solution at 25ºC. Suspended cells then washed in cold PBS. Samples were fixed with 0.5% paraformaldehyde (25ºC for 5 min) followed by incubation with primary antibodies. Cells were processed on a CyAn™ ADP Analyzer.

Small Molecule Inhibitor Treatment: MEFs were plated in 96-well plates at a density of 2000 cells/well in complete growth medium and grown overnight at 37°C. To test the effect of inhibitors on MuPyV entry, MEFs were starved for 6-12 h in serum free DMEM. The virus was premixed with the indicated concentration of DMSO (control) or inhibitor and added to MEFs for 2 h. The virus and inhibitor solution were then removed and the cells were washed with serum free DMEM, followed by addition of serum free DMEM supplemented with VP1 neutralizing antibody (I58) at a dilution of 1:5000. After 2 h fresh DMEM with VP1 neutralizing antibody (1:5000) was added to cells. 20 h later the media

was removed and the cells were washed with cold PBS followed by paraformaldehyde (PFA) fixation. To test the effect of inhibitors on MPyV targeting, MEFs were starved for 6 to 12 h in serum free complete medium followed by virus addition for 2 h. The virus solution was then removed and the cells were washed with serum free DMEM, followed by addition of serum free DMEM supplemented with either DMSO (control) or inhibitor and VP1 neutralizing antibody (I58) at a dilution of 1:5000. The VP1/inhibitor solution was removed after 2 h and cells were placed in serum free DMEM with VP1 antibody at 1:5000 dilution. 20 h later the media was removed and the cells were washed with cold PBS followed by PFA fixation. Plates were fixed in 4% paraformaldehyde at 25ºC for 10 min. Cells were then permeabilized with 0.5% Triton X-100 for 15 min at 25ºC followed by blocking in 10% FBS in PBS overnight at 4°C. Plates were then stained for the viral protein T-ag (E1 antibody) followed by incubation with Alexa Fluor labeled secondary antibody (546) and Hoechst DNA dye. The plate was then washed in PBS followed by imaging on the Molecular Devices ImageXpress Micro XL High-Content Screener. To quantify infection, T-ag staining was measured per each Hoechst stained nuclei. 5 images were collected per well, and each sample contained 3 replicates per plate. The DAPI channel on each image was thesholded and nuclei were counted using ImageJ (Analyze Particles). These particles were marked as “Regions of Interest” (ROI) and then the average pixel intensity of T-ag staining was measured for each nuclei (ROI). These were then binned into T-ag positive or T-ag negative nuclei to create % infected for each sample. The % infected reported is the average of the three plated replicates.

SIM Microscopy and Colocalization Analysis: For Structured Illumination Microscopy cells were plated on glass slides as previously described. Labeled virus was added at a

concentration of 1 µg/ mL of VP1. At indicated times slides were fixed in 4% PFA supplemented with 0.1% glutaraldehyde, followed by 0.5% TritonX-100 permeabilization. Slides were imaged on a Nikon N-structured illumination microscope (SIM) and images were reconstructed using the Nikon N-SIM elements module. Confocal images for co-localization analysis were obtained on a Nikon A1R laser scanning confocal, 100 X oil objectives. Co-localization analysis was carried out with Imaris Coloc Software. Intensity thresholds were set for the virus and tubulin/actin channels. The % of virus voxels above threshold that co-localized with tubulin or actin voxels was then calculated by the software. Over 50 cells were quantified from each slide, with two biological replicates were performed per sample.

Kinase Arrays: R&D Systems Proteome Profiler™ Antibody Array (Human Phospho-Kinase Array Catalog # ARY003B) were performed per manufacturer's instructions. Briefly, MEFs were plated on 10 cm dishes at 400,000 cells per dish in complete medium and grown to 80% confluence for 24 to 48 h. MEFs were then starved in serum free DMEM for 2 to 6 h followed by pseudovirus addition. Lysates were then collected at indicated times post pseudovirus addition. Protein concentration of the lysates was quantified using a BCA assay and each sample was normalized to equivalent protein concentration. Lysates were then either added to the prepared array or aliquoted and stored at -80°C until use per manufacturers recommendation. Arrays were then processed as directed by the manufacturer. Kinase arrays were quantified using the ImageQuant™ TL Array Analysis Software using the PBS control as the background subtraction.

Plasmids and Site Directed Mutagenesis to Generate Binding Mutants: The MPyV VP1 coding plasmid pwP, VP2 coding plasmid ph2p, and the VP3 coding plasmid ph3p were obtained from Chis Buck at the Cancer Research Center. The pwP plasmid codes for the LID strain of VP1 and was mutated to the RA strain. Further mutations in the receptor binding sites were introduced into pwP using the Quick Change Site-Directed Mutagenesis System and confirmed by sequencing.

Virus and Pseudovirus Labeling: Purified virus and Pseudovirus were labeled with ATTO 565 NHS-ester (Sigma 72464*)* or Biotin SS NHS-ester (ApexBio A8006). Labeling was carried out according to the manufactures suggestions and for desired theoretical molar ratio: $MR = (moles\ of\ dye)/(moles\ of\ virus)$. After the labeling reaction, free dye was quenched with hydroxylamine followed by removal using a 100 kDa spin column (Millipore UFC5100BK). Biotin-SS linkage was confirmed by pull down with streptavidin coated beads followed by SDS-PAGE and Coomassie stain (Figure 5.10A). ATTO-565 labeling was confirmed by Typhoon gel imager and infectivity for labeled virus was determined to a theoretical MR of 40 (Figure 5.10C).

Internalization Assay: Biotin-SS-MuPyV was added to cells at a concentration of 1 μg/mL of VP1 for 30 min or 3 h at 37°C. Cells were washed with 50mM TCEP to remove biotin from virus on the cell surface. Cells were washed with cold PBS followed by lysis in a pull down buffer (20 mM Tris-HCl pH 8, 140 mM NaCl, 1% TX-100, 1 mM EDTA, 0.05% sodium deoxycholate). The protein concentration of cell lysates was measured by BCA assay. Lysates were resuspended at a concentration of 1 mg/mL prior to streptavidin pull down. 30% of the lysate was reserved as whole cell lysate, while 70% was added to streptavidin coated beads and incubated for 1 h at 25ºC. The lysate-bead

solutions were then placed on a magnetic rack for 5 min and the supernatant was discarded. The beads were washed with PBS twice followed by resuspension in 100 uL of 50 mM TCEP in PBS and incubation for 5 min at 25ºC. The TCEP-bead solutions was placed on the magnetic rack for 5 min and the supernatant was collected (Streptavidin Pull Down). WCL and pulldowns were then separated by SDS-PAGE followed by immunoblotting for VP1 and tubulin.

Signaling Pathways Network Analysis: Interaction mapping between activated kinase identified in the kinase arrays was generated using SPRING and visualized using Cytoscape software. Active interactions sources for SPRING were experimental evidence, textmining, and database searching with a medium confidence level (>0.4) (Franceschini et al. 2013). Cytoscape generated a prefuse force directed layout based on the experimental evidence of interactions (Cistmas, Rowan; Avila-Campillo, Iliana; Bolouri, Hamid; Schwikowski, Benno; Anderson, Mark; Kelley, Ryan; Landys, Nerius; Workman, Cis; Ideker, Trey; Cerami, Ethan; Sheridan, Rob; Bader, Gary D.; Sander 2005).

5.3 Results

5.3.1 Mouse Polyomavirus activates multiple signaling pathways during virus attachment and entry.

Inhibition of tyrosine kinases during virus binding to the cell surface blocks JCPyV and SV40 infection, suggesting that PyV-early signaling events are essential for polyomavirus infection (Querbes et al. 2004; Dangoria et al. 1996). We confirmed that MuPyV infection also requires tyrosine kinase activity. Mouse embryonic fibroblasts (MEFs) were treated with the tyrosine kinase inhibitor, genistein, either during virus

attachment and entry (0-2 h), or post virus entry (2-4 h). After 2 h, virus was removed and a neutralizing antibody to VP1 was added to block additional virus binding (Figure 5.1B). The I58 VP1 antibody was 100% neutralizing out to a dilution of 12,500 (Figure 5.1A). This antibody also allowed us to track the rate of infection using a neutralizing antibody chase demonstrating the slow rate of endocytosis in MuPyV infection (Figure 5.1A). T-ag (T-ag) nuclear staining 24 h post infection quantified the percentage of cells infected during the inhibitor treatment (Figure 5.1). Consistent with results with JCPyV and SV40 (Querbes et al. 2004; Dangoria et al. 1996), genistein treatment inhibited MuPyV infection. Genistein was most effective when administered during virus entry (0-2 h) and blocked MuPyV infection in a dose-responsive manner (Figure 5.1 C and 5.2 A), but had little effect on MuPyV infectivity when the drug was added after virus entry (2-4 h) (Figure 5.2 A). These results confirm that activation of tyrosine kinases during virus entry is required for MuPyV infection.

In order to identify specific signaling pathways activated during MuPyV binding and entry we profiled the phosphorylation of 43 different tyrosine, theonine, and serine kinases using a Phospho-Kinase Array (R&D Systems) after pseudovirus addition to MEFs. Pseudoviruses (PsVs) are virus-like particles assembled from the major (VP1) and minor (VP2/3) capsid proteins but lacking an encapsidated viral genome (Buck & Thompson 2007). Using the Phospho-Kinase Array, we detected four kinases phosphorylated within 30 min of pseudovirus addition (Figure 5.2 B), including the MAP kinases ERK1/2 and JNK, as well as the PI3K target, AKT. Kinases phosphorylated within 2 h of pseudovirus addition included Focal Adhesion Kinase (FAK), many of the SRC family kinases (SFKs), as well as PI3K/AKT targets: MTOR, PRAS40, and WNK1

(Figure 5.2 B). We validated these array results by infecting MEFs with MuPyV and analyzing cell lysates by immunoblots with phospho-specific antibodies. We observed phosphorylation of the earliest pathways, such as PI3K/AKT and the MAPK (ERK1/2), within 5 min of virus addition (Figure 5.2 C). SRC family kinases were phosphorylated between 15 min and 2 h after virus addition, while both FAK and C-JUN phosphorylation increased thoughout the course of infection (Figure 5.2 C). FAK phosphorylation was detected by 15 min, and C-JUN phosphorylation was detected as early as 1 h after virus addition. Thus, diverse signaling networks were activated similarly by both pseudovirions and wild-type MuPyV. Network analysis of kinases detected in the array identified tee major signaling pathways that were activated during virus attachment and entry: MAPK, PI3K, and FAK/SRC.

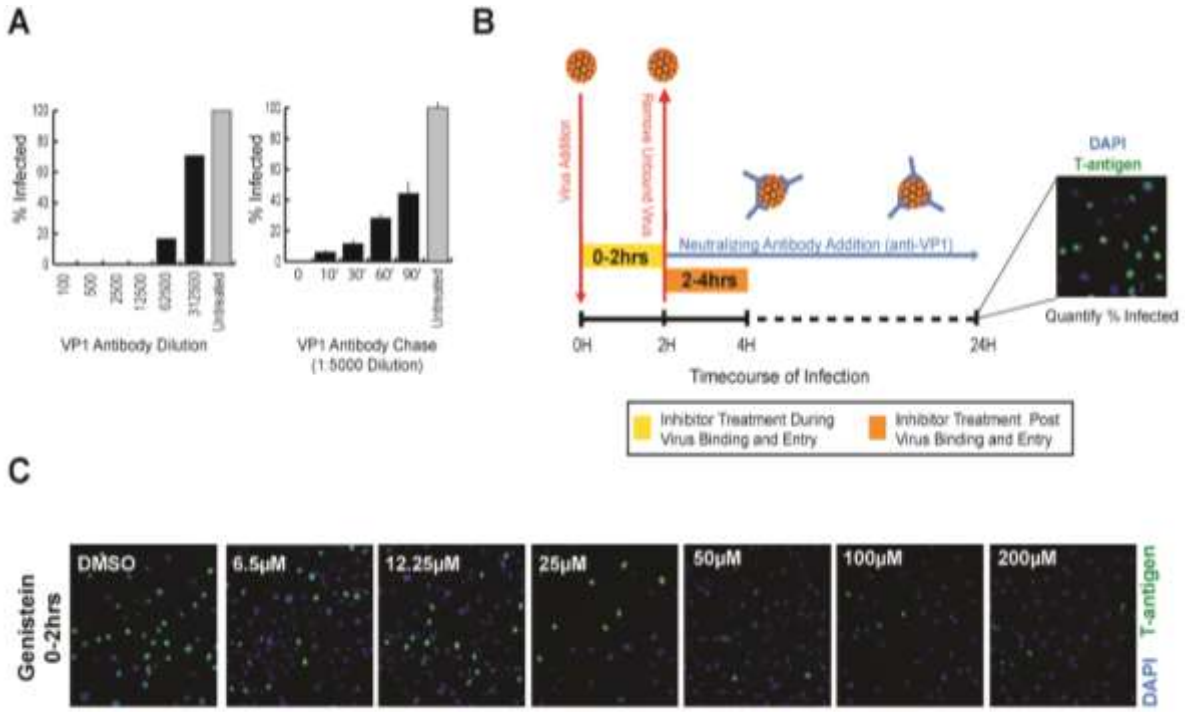

Figure 5.1 Medium-thoughput screening method to identify required MuPyV signaling pathways during virus entry and trafficking. A) Bar graph (left) shows dose response of neutralizing I58-VP1 antibody. Virus was mixed with antibody prior to addition to cells. I58 antibody was 100% neutralizing out to a dilution of 12,500. Bar graph (right) shows time course of infection at the time of neutralizing antibody addition. **B)** Diagram of drug treatment experimental protocol. These experiments were carried out on 96 well imaging dishes. **C)** Genistein, a tyrosine kinase inhibitor, blocked MuPyV infection in a dose responsive manner when treated during virus binding and entry (0-2 h). Infection was quantified at 24 h PI with immunofluorescence as the percent of T-ag positive nuclei and treatments were normalized to a DMSO control. T-ag is in green, DAPI is in blue.

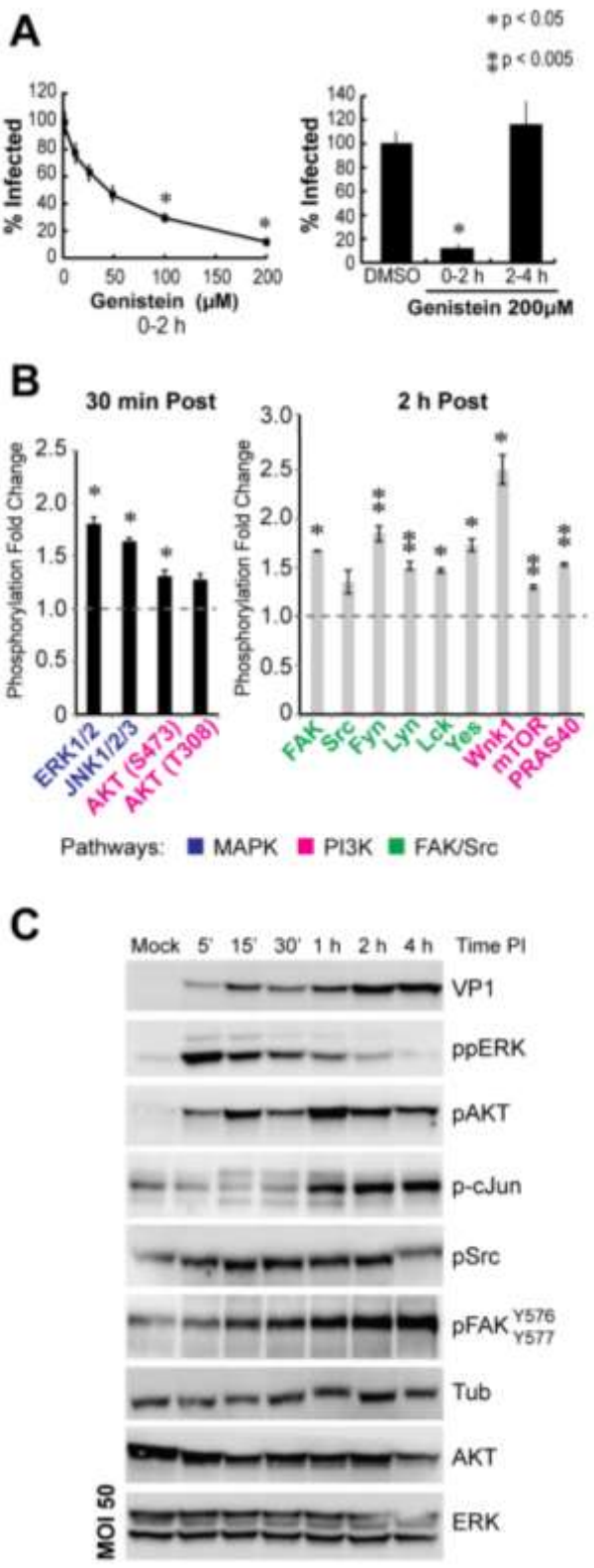

Figure 5.2: MuPyV activates required signaling pathways for infection during virus binding and entry. A) Cells were treated with genistein during virus binding and entry (0-2 h) or post virus entry (2-4 h). A neutralizing antibody was added after the 0-2 h period. Infection was quantified at 24 h PI as the percent of T-ag positive nuclei, normalized to a DMSO control. A paired *t* test was performed, n=3. **B)** Phospho-Kinase arrays obtained at 30 min (black bars) and 2 h (grey bars) post pseudovirus addition. Members of the MAPK, PI3K, and FAK/SRC pathways are shown in blue, pink, and in green respectively. **C)** Immunoblot of MuPyV time course in wild-type MEFs, MOI 50.

5.3.2 The ganglioside receptors GD1a and GT1a enhance PI3K activation by MuPyV.

MuPyV does not contain known binding sites for GFRs, but MuPyV binds to gangliosides *via* a VP1 sialic acid binding pocket. Gangliosides are important modulators of GFR signaling (Li et al. 2000; Liu et al. 2004; Kaucic et al. 2006; Yates et al. 1995) and MuPyV-ganglioside interactions could mediate MuPyV activation of GFRs and downstream signaling. Using a cell line deficient in ganglioside synthesis (ganglioside -/- MEFs) that are resistant to MuPyV infection (You & O'Hara et al. 2015), we first assayed for MuPyV-induced activation of signaling pathways in presence or absence of GD1a, a known MuPyV ganglioside receptor, which restores infection of these cells (Tsai et al. 2003; You & O'Hara et al. 2015). Ganglioside -/- MEFs were supplemented with 5 μM GD1a (Figure 5.3 A), and signaling was measured 30 min after addition of virus (Figure 5.3 B). GD1a supplementation alone did not alter phosphorylation of ERK or AKT as demonstrated by the base-line activation of the mocks (Figure 5.3 B). Virus addition to DMSO-treated and GD1a-supplemented ganglioside -/- MEFs displayed activation of MAPK with slightly higher levels of ERK phosphorylation in the GD1a-supplemented cells (Figure 5.3 B), indicating that MAPK activation is not solely dependent on MuPyV-GD1a interactions. In contrast, AKT phosphorylation was increased 5 to 10 fold in GD1a supplemented cells over that in the DMSO control (Figure 5.3 B), suggesting that GD1a mediates MuPyV activation of the PI3K pathway. Finally, to determine whether MuPyV ganglioside receptors activate specific signaling pathways compared to non-MuPyV ganglioside receptors we compared virus signal activation after supplementation with different gangliosides. The

gangliosides GD1a and GT1a are receptors for MuPyV, whereas GM1 is a receptor for SV40 PyV (Tsai et al. 2003; Buch et al. 2015). Virus addition to GD1a- and GT1a-supplemented ganglioside -/- MEFs resulted in increased ERK phosphorylation compared to the DMSO control (Figure 5.3C), similar to the increased MAPK activation in Figure 5.3B. Interestingly, virus addition to GM1-supplemented cells resulted in ERK phosphorylation higher than the DMSO control (Figure 5.3C) despite the lack of interaction between VP1 and GM1, suggesting that GM1 supplementation alone may increase MAPK activation In contrast, only the GD1a- or GT1a-supplemented cells had increased phosphorylation of AKT (Figure 5.3 C). Taken together, these results suggest that MuPyV-specific ganglioside receptors promote activation of the PI3K/AKT pathway.

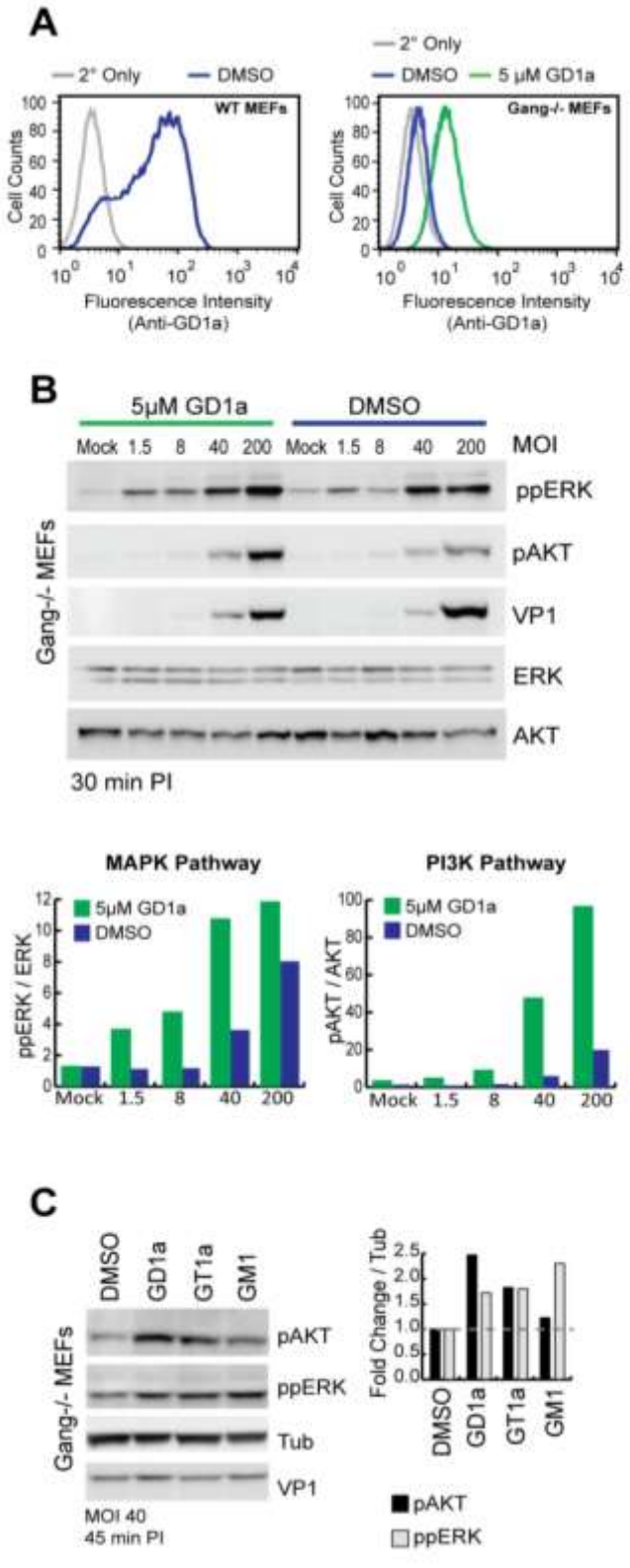

Figure 5.3: MuPyV ganglioside receptors enhance PI3K activation. A) Flow cytometry displaying cell surface GD1a levels of DMSO controls in blue for wild-type and ganglioside -/- MEFs. 5 µM GD1a-supplemented ganglioside -/- MEFs are shown in green. Secondary (2°) only controls are in grey. **B)** Immunoblot of MuPyV dose responses in DMSO or 5 µM GD1a supplemented gang -/- MEFs. Bar graphs are quantification of integrated density of ppERK and pAKT bands normalized to mock. **C)** Ganglioside -/- MEFs supplemented with GD1a, GT1a, or GM1 were analyzed for signal activation after MuPyV addition (MOI 40; 45 min PI). Bar graphs are integrated density normalized to mock.

5.3.3 α4-Integrin contributes to MuPyV signaling and infection.

In addition to specific gangliosides, MuPyV binding to α4-integrin (α4) also contributes to infection (Caruso et al. 2007; Caruso et al. 2003). Integrins can activate downstream signaling independently as well as though crosstalk with associated GFRs, thus we determined whether MuPyV interactions with α4-integrin mediate MuPyV-induced signaling events. We generated two α4-integrin knockdown (α4-integrin KD) MEF cell lines that expressed ~30% of wild-type α4-integrin protein levels (Figure 5.4A). Consistent with previous results (Caruso et al. 2003), the α4-integrin KD MEFs showed a 60% decrease in MuPyV infection with no reduction in virus cell surface binding or ganglioside levels compared to control cells (Figure 5.4B-D). We then determined whether MuPyV-mediated signaling was altered in the α4-integrin KD MEFs. Although ERK was transiently phosphorylated between 15 and 30 min after virus addition to the α4-integrin KD MEFs, the extent of ERK activation was limited suggesting that α4-integrin binding contributes to MuPyV activation of MAPK (Figure 5.4E). The PI3K pathway was activated in control MEFs between 15 min and 2 h after virus addition; however, in the α4-integrin KD cells AKT phosphorylation was observed between 15 min and 30 min after virus addition. These data suggest that α4-integrin may sustain PI3K signaling after virus binding. Interestingly, C-JUN, a downstream target of many signaling pathways, showed delayed phosphorylation in the α4-integrin KD cells relative to control MEFs (Figure 5.4E) further supporting a defect in MuPyV signaling. Although these data suggest a role for α4-integrin in MuPyV signal activation, it is possible that reducing α4-integrin levels nonspecifically alters signaling pathways, and the defect we observed was not a consequence of MuPyV binding (Gonzalez et al. 2010). Therefore,

we next tested whether pseudoviruses that are unable to bind integrins or gangliosides affected signal activation, without modifying cell surface receptor expression or cellular signaling pathways.

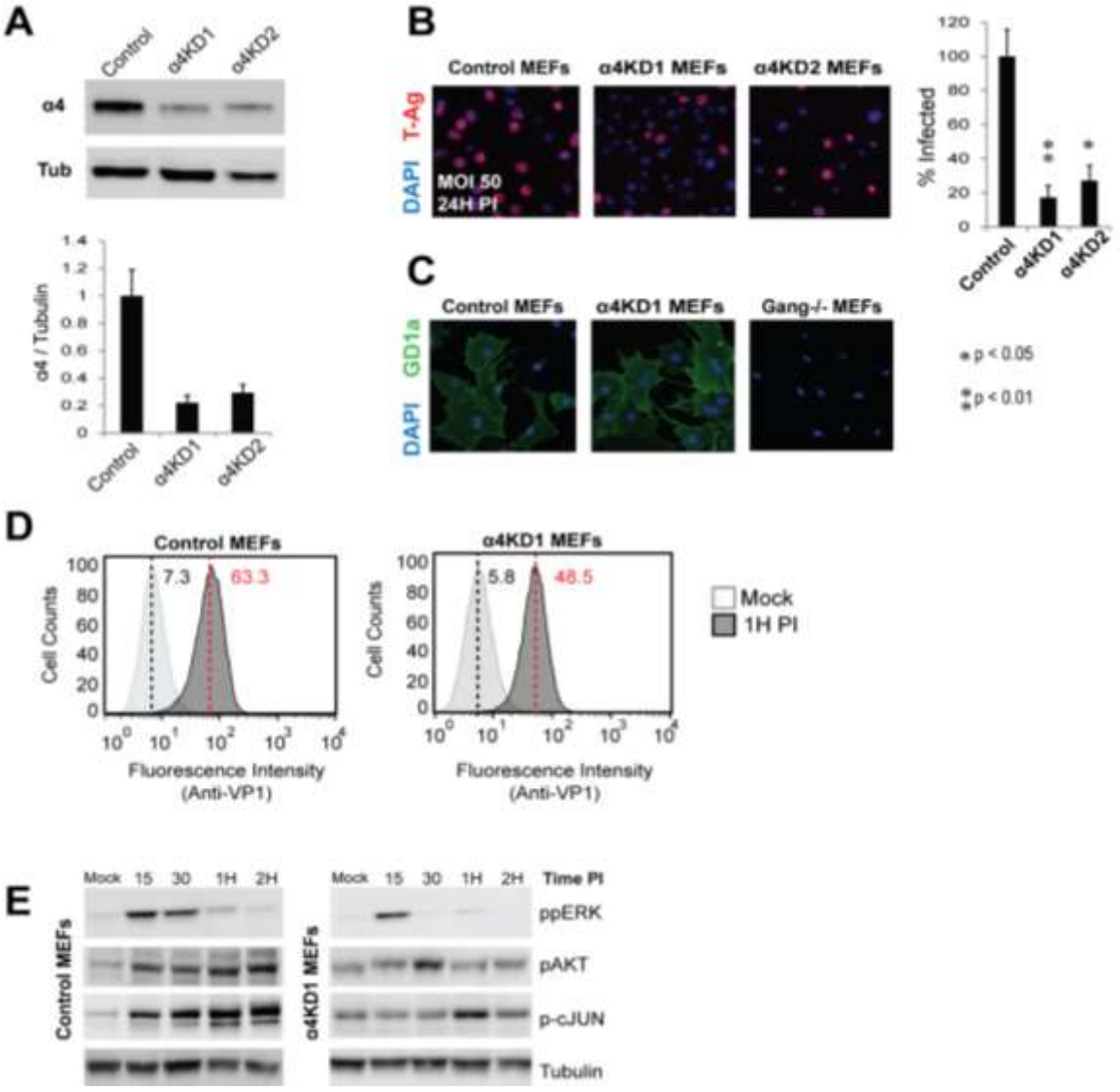

Figure 5.4 α4-Integrin contributes to MuPyV signaling and infection. **A)** Immunoblot for α4-integrin of KD1, KD2, and Control MEF lysates. Bar graph shows integrated density of bands normalized to control, error bars are standard error. **B)** Representative immunofluorescence images of infection, nuclei are labeled by DAPI (blue) and T-ag (red). Bar graph shows quantification of infection at 24 h PI. *T* test values p = 0.009 and p = 0.016. **C)** Immunofluorescence images for GD1a (green) and DAPI (blue). **D)** Flow cytometry staining for cell surface VP1 30 min post virus addition in control and α4-integrin KD1 MEFs. Geometric mean of uninfected and 30 min PI were plotted by dashed lines shown in black and red, respectively. **E)** Immunoblot of MuPyV time course in control and α4-

5.3.4 VP1 binding to gangliosides and α4-integrin contributes to signal activation.

To confirm that gangliosides and α4-integrin binding mediate MuPyV-induced signaling, we generated mutant pseudoviruses altered by single amino acid residues in specific receptor binding sites on the VP1 capsid protein. Two residues in the sialic acid binding site of VP1 are required for sialic acid binding, H298 and R77 (Bauer et al. 1999). Mutation of these amino acids (H298Q and R77Q) abrogated sialic acid binding as shown by loss of agglutination of red blood cells (SA-/-, Figure 5.5 B). The MuPyV α4-integrin binding site is an LDV motif within VP1 that is distinct from the sialic acid binding site of VP1(Caruso et al. 2003; Caruso et al. 2007). It has been shown that changing the VP1 LDV sequence to LNV abolishes α4-integrin binding and results in a 60% decrease in MuPyV infection (Caruso et al. 2007). Mutation of the integrin binding motif did not alter ganglioside (sialic acid) binding (LNV, Figure 5.5 B). We also generated a mutant pseudovirus lacking both ganglioside and α4-integrin binding (LNV SA-/-). Electron micrographs of purified wild-type and mutant pseudoviruses showed intact 50 nM capsids (Figure 5.5 A).

Addition of the pseudovirus mutants to wild-type MEFs activated the MAPK/ERK pathway (Figure 5.5 C). Wild-type pseudovirus induced robust AKT phosphorylation; however, induction of AKT by integrin (LNV) or ganglioside (SA-/-) mutant pseudoviruses was greatly reduced. Furthermore, the LNV SA-/- mutant pseudovirus elicited little to no AKT phosphorylation (Figure 5.5 C) even though high levels of virus were detected as shown by VP1 staining of whole cell lysates (Figure 5.5 C). These data confirm that both ganglioside and α4-integrin binding are required for activation of the PI3K/AKT pathway, but either interaction is sufficient for MAPK activation.

In addition to PI3K and MAPK, we observed EGFR phosphorylation after MuPyV addition to wild-type MEFs (Figure 5.5 E). We tested whether MuPyV activation of the EGFR was ganglioside dependent as GD1a has been shown to alter EGFR signaling (Liu et al. 2004). The EGFR was activated in a dose responsive manner in ganglioside -/- MEFs by wild-type pseudoviruses (RA and LID strains) indicating that MuPyV activation of the EGFR does not require ganglioside interactions (Figure 5.5D). Integrin clustering can also induce EGFR activation (Moro et al. 2002). Using the integrin-mutant pseudovirus (LNV) we tested whether integrin binding contributed to EGFR activation. Addition of the LNV pseudovirus, which retains sialic acid binding, did not result in EGFR phosphorylation in ganglioside -/- MEFs (Figure 5.5D). These results indicate that MuPyV binding to α4-integrin can activate the EGFR.

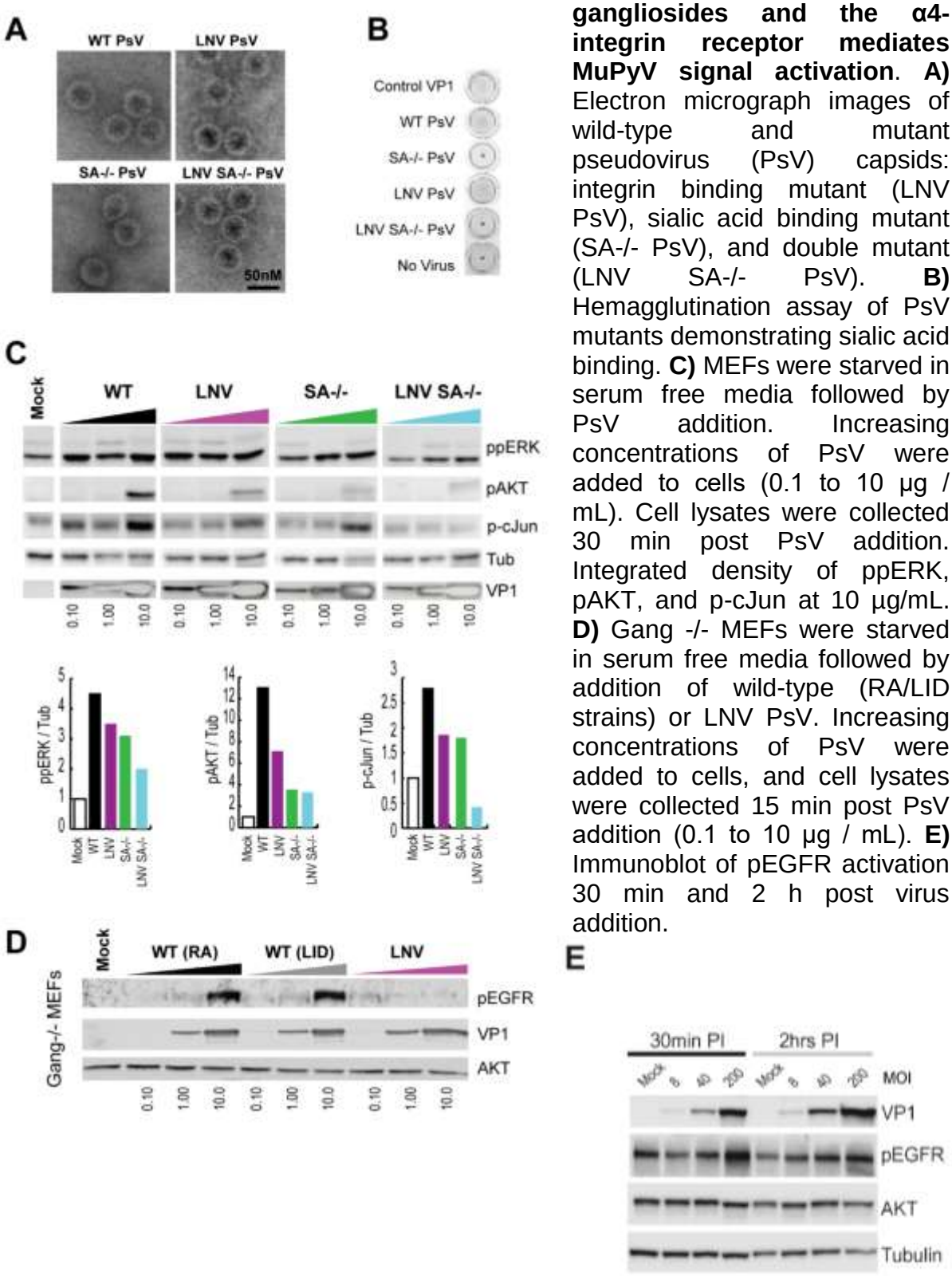

Figure 5.5: Virus binding to gangliosides and the α4-integrin receptor mediates MuPyV signal activation. **A)** Electron micrograph images of wild-type and mutant pseudovirus (PsV) capsids: integrin binding mutant (LNV PsV), sialic acid binding mutant (SA-/- PsV), and double mutant (LNV SA-/- PsV). **B)** Hemagglutination assay of PsV mutants demonstrating sialic acid binding. **C)** MEFs were starved in serum free media followed by PsV addition. Increasing concentrations of PsV were added to cells (0.1 to 10 μg / mL). Cell lysates were collected 30 min post PsV addition. Integrated density of ppERK, pAKT, and p-cJun at 10 μg/mL. **D)** Gang -/- MEFs were starved in serum free media followed by addition of wild-type (RA/LID strains) or LNV PsV. Increasing concentrations of PsV were added to cells, and cell lysates were collected 15 min post PsV addition (0.1 to 10 μg / mL). **E)** Immunoblot of pEGFR activation 30 min and 2 h post virus addition.

5.3.5 The PI3K and the FAK/SRC pathways are required for MuPyV infection.

MuPyV cell surface binding activated the MAPK, PI3K, and FAK/SRC pathways (Figure 5.2). To determine which of these signaling pathways might be required for MuPyV infection, we used pathway specific small molecule inhibitors. Small molecule inhibitors allowed timed inhibition of signaling specifically during early events of virus infection, without disrupting important signaling occurring during virus replication (Meili et al. 1998).Wild-type MEFs were treated with the inhibitors during virus binding (0-2 h), or after virus entry (2-4 h). The PI3K target AKT was phosphorylated within 5 min of virus addition to cells, suggesting that PI3K may be important for very early steps of virus infection (Figure 5.1C). Two PI3K inhibitors, wortmannin and LY294002, blocked MuPyV infection when added during virus attachment and entry, but not when added at later time points (Figure 5.6A), suggesting that PI3K-mediated signaling may be important for initial steps of virus entry.

FAK and SRC family kinases were activated between 15 min and 4 h after virus addition to cells (Figure 5.1B,5.1C) suggesting that these pathways may be important for both entry and virus trafficking. We used the FAK inhibitor 14 (FAK14) and the SRC family kinase inhibitor (AZM475271) to determine whether FAK/SRC activation is required for infection. Similar to the PI3K inhibitor results, inhibition of the FAK or SRC kinases during virus entry blocked infection (Figure 5.6B). Inhibition of FAK/SRC post virus entry (2-4 h) resulted in decreased infection, but not to the extent as seen if added during virus entry (Figure 5.6B). These results suggest that the FAK/SRC pathway is important for either virus entry and/or trafficking.

MuPyV binding activated the MAPK pathway (Figure 5.2B, 5.2C). However, MAPK inhibition with two MEK1 inhibitors, U0126 and PD98059, had no effect on MuPyV infection (Figure 5.7A), although these two inhibitors completely blocked the MAPK signal induced by MuPyV (Figure 5.7B) indicating that MuPyV-activation of the MAPK pathway is not required for early events of MuPyV entry. To control for possible modulation of receptor expression by these inhibitors (Swimm et al. 2010), we confirmed that ganglioside levels on the cell surface were at wild-type levels and there were no changes in virus binding to the cell surface (Figure 5.7C). Together, these data show that although several signaling pathways are activated by MuPyV binding and entry, only the PI3K and FAK/SRC pathways are required for initial steps of infection.

Many polyomaviruses activate signaling during virus entry (Querbes et al. 2004; Dangoria et al. 1996; Butin-Israeli et al. 2010), yet it is unclear whether the signaling pathways required for infection are conserved across species. For example, EGFR activation is required for JCPyV infection (Querbes et al. 2004) and we found that the EGFR was also activated by MuPyV. However, EGFR inhibition by AG555 did not affect MuPyV infection (Figure 5.7D). SV40, a monkey polyomavirus, requires caspase activation during entry (Butin-Israeli et al. 2010). We tested whether caspases were functioning during MuPyV infection using a caspase inhibitor, Z-VAD-FMK. Unlike SV40, caspase activation was not required for MuPyV infection (Figure 5.7D). Taken together, these data suggest that different PyV species utilize unique signaling pathways during virus entry.

Because the PI3K and FAK/SRC pathway are both required for infection, it is possible that these pathways are undergoing synergistic crosstalk with both contributing

to a single step of infection. For example, the FAK/SRC pathway has been shown to activate PI3K (Xia et al. 2004). However, it is also possible that these pathways are functioning independently and contribute to separate steps of infection. To determine whether crosstalk was occurring between the pathways during MuPyV entry, we inhibited PI3K or FAK/SRC and probed for activation of AKT, FAK, or SRC at 30 min and 2 h post-virus addition (Figure 5.6C). As expected, PI3K inhibition abolished AKT phosphorylation at both 30 min and 2 h PI. In contrast, PI3K inhibition did not decrease FAK/SRC activation. SRC kinase phosphorylated FAK at residues Y576 and Y577 (Calalb et al. 1995). SRC inhibition blocked SRC phosphorylation of FAK Y576/577 within 30 min PI, indicating robust inhibition of SRC kinase. SRC inhibition did not decrease AKT phosphorylation. Furthermore, treating simultaneously with the FAK and SRC inhibitors, which blocks FAK phosphorylation of SRC and SRC phosphorylation of FAK, we observed decreased FAK and SRC phosphorylation within 30 min PI (Figure 5.6C); however, there was no decrease in AKT phosphorylation. Taken together, these results indicate that while the PI3K and FAK/SRC pathways are both required for infection, they are not synergistic and likely contribute to distinct steps of virus entry.

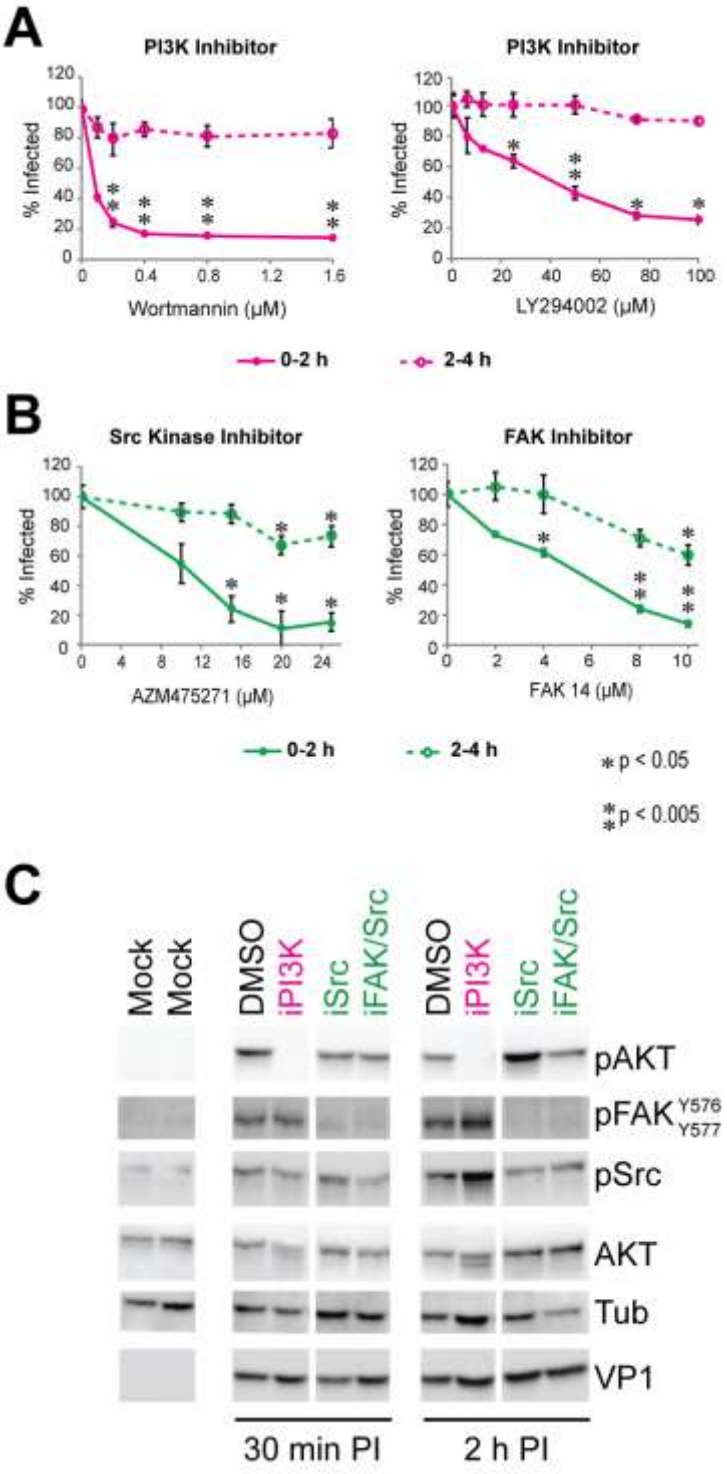

Figure 5.6: Both the PI3K and FAK/SRC pathways are required for early steps of MuPyV infection. **A)** Dose response curves of inhibitor treatments. Inhibitors were present either during virus binding (0-2 h, solid lines) or post virus binding (2-4 h, dashed lines). The PI3K pathway was inhibited with wortmannin or LY294002. Infection was quantified at 24 h PI by the percent T-ag positive nuclei. A paired *t* test was performed, n=3. **B)** Dose response curves of infection with SRC Kinase Inhibitor, AZM475271, or FAK inhibitor 14 normalized to DMSO controls. Graphs are normalized to DMSO controls and error bars are standard error. A paired *t* test was performed, n=3. **C)** Immunoblot of cells treated with virus at an MOI 50 in either the presence or absence of inhibitors for 30 min or 2 h PI.

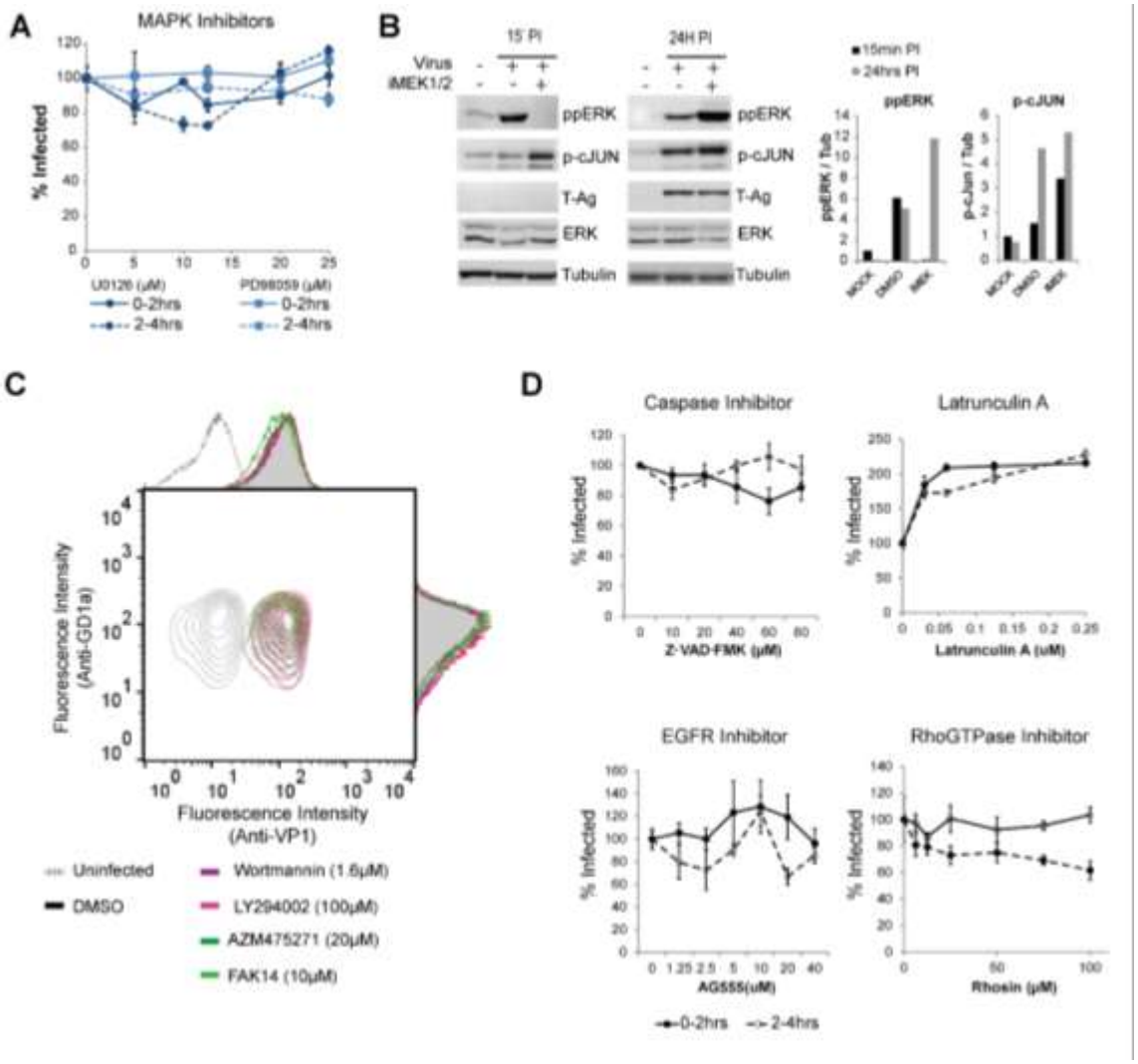

Figure 5.7 Signaling pathways not required for MuPyV entry. A) Dose response curves of MAPK inhibitor treatments (U0126, PD98059). Inhibitors were present either during virus binding (0-2 h, solid lines) or post virus binding (2-4 h, dashed lines). Graphs are normalized to DMSO controls and error bars are standard error, n=3. **B)** Immunoblot of ppERK and p-cjun 15 min and 24 h PI in the presence or absence of MEK1/2 inhibitor U0126 (20 μM). ERK was phosphorylated at 15 min PI. The MEK1/2 inhibitor U0126 blocked ERK phosphorylation when added with the virus. However, this had no effect on virus infection as shown by T-ag staining of lysates 24 h PI. C-JUN was phosphorylated in both DMSO and iMEK1/2 samples at 15 min and 24 h PI. **C)** MEFs were treated with virus either in the presence or absence of inhibitors for 30 min at 4°C. Cells were fixed and stained for cell surface bound virus (anti-VP1) and the receptor GD1a (anti-GD1a). **D)** Inhibition of the EGFR, caspases, Rho-GTPases, or actin polymerization (Latrunculin) during virus binding and entry (0-2 h) or post virus entry (0-4 h). Infection was quantified at 24 h PI as the percent of T-ag positive nuclei and treatments were compared to a DMSO control. Error bars are standard error. n=3.

5.3.6 FAK -/- MEFs are resistant to MuPyV signaling and infection.

Pharmacological inhibition of FAK/SRC blocked MuPyV infection (Figure 5.6B). In order to confirm that FAK is required we tested MuPyV infection in FAK -/- MEFs (Ilić et al. 1995; Sieg et al. 1998). We first determined whether these cells expressed the MuPyV ganglioside receptor GD1a. Although, the FAK +/+ MEFs showed a heterogeneous expression of GD1a, with some cells expressing high levels of GD1a and others lacking the GD1a receptor (y-axis, Figure 5.8A), the FAK -/- MEFs unexpectedly displayed a complete loss of GD1a (y-axis, Figure 5.8A), rendering them uninfectable by MuPyV (Figure 5.8A). FAK -/- MEFs have not been previously reported to lack cell surface gangliosides. However, even after ganglioside supplementation, confirmed by flow cytometry with a GD1a antibody (Figure 5.8B), the FAK -/- MEFs remained uninfectable, suggesting that FAK is required for MuPyV infection (Figure 5.8C). Finally, we tested whether signaling pathways activated in FAK +/+ MEFs were activated in the absence of FAK. As expected, there was no detectable induction of SRC or AKT phosphorylation in the ganglioside null FAK -/- MEFs compared to their FAK+/+ controls after virus addition (Figure 5.8D). However, there were elevated levels of phosphorylated SRC in the FAK-/- MEFs as previously reported (Sieg et al. 1998), although this activation was insufficient to restore infection of these cells. These results further support the conclusion that FAK is critical for virus-induced signaling events and infection.

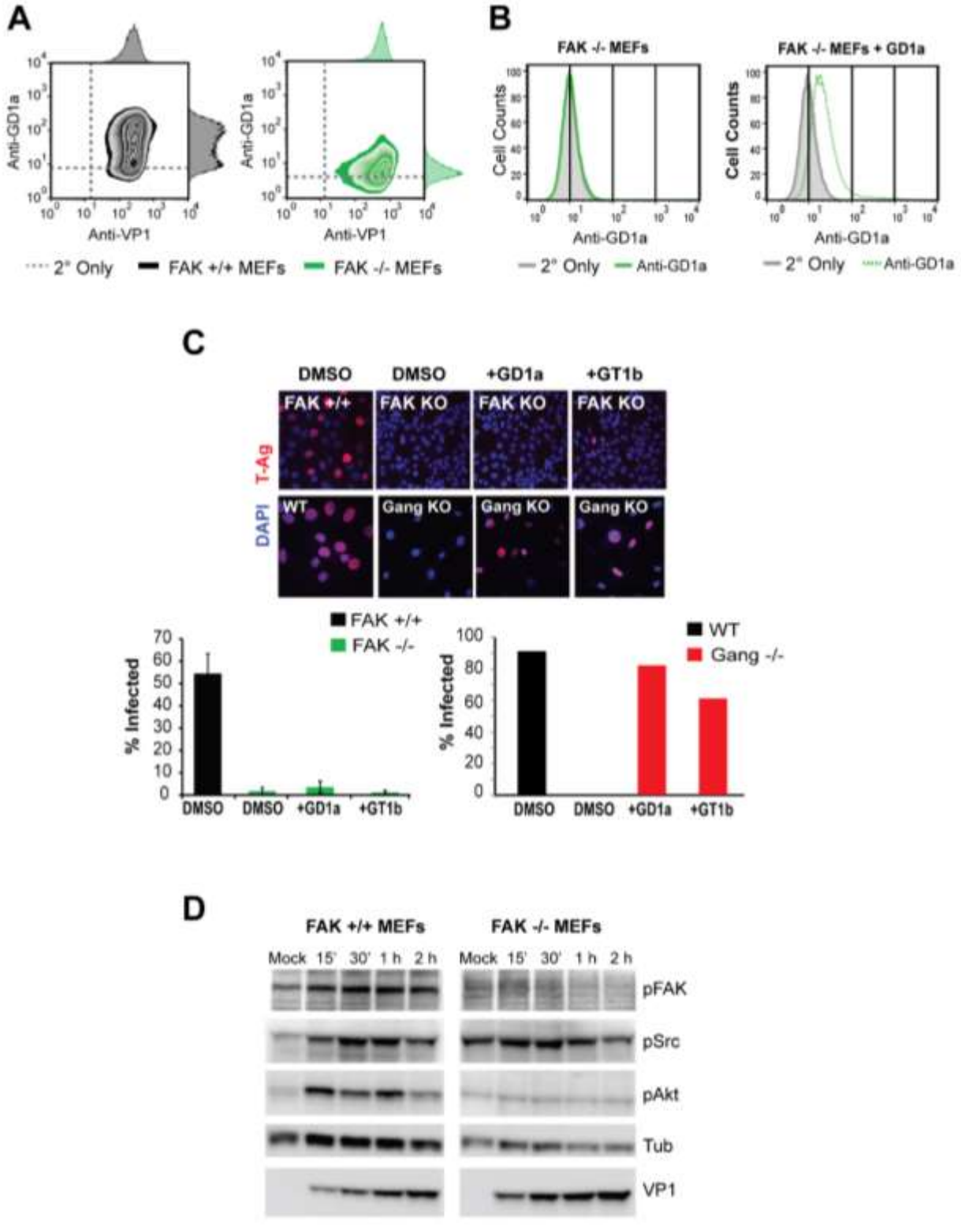
A
Anti-GD1a
Anti-VP1
2° Only
FAK +/+ MEFs
FAK -/- MEFs
B
FAK -/- MEFs
FAK -/- MEFs + GD1a
Cell Counts
Anti-GD1a
2° Only
Anti-GD1a
C
DMSO
DMSO
+GD1a
+GT1b
FAK +/+
FAK KO
FAK KO
FAK KO
T-Ag
DAPI
WT
Gang KO
Gang KO
Gang KO
FAK +/+
FAK -/-
% Infected
DMSO
DMSO
+GD1a
+GT1b
WT
Gang -/-
D
FAK +/+ MEFs
FAK -/- MEFs
Mock
15'
30'
1 h
2 h
pFAK
pSrc
pAkt
Tub
VP1

Figure 5.8 FAK -/- MEFs are resistant to MuPyV signaling and infection. A) Flow cytometry data of FAK +/+ MEFs (black) and FAK -/- MEFs (green) 30 min post virus addition (MOI 50) displayed as a contour plot with GD1a levels on the y-axis (anti-GD1a) and virus binding on the x-axis (anti-VP1). The geometric mean of the negative controls are plotted by the grey dashed line. **B)** Flow cytometry data showing GD1a staining of FAK -/- MEFs and GD1a-supplemented FAK -/- MEFs 5 h post ganglioside addition. **C)** Infection of FAK +/+ MEFs, FAK -/- MEFs, and FAK -/- MEFs supplemented with gangliosides GD1a or GT1b. Nuclei are stained with DAPI (blue) and T-ag (Red). The bar graph is quantification of infection of T-ag positive nuclei at 24 h PI, n=3, the right hand panel are representative slides from the infections. Also shown are infections of wild-type, ganglioside-/- MEFs, and ganglioside-/- MEFs supplemented with GD1a or GT1b prior to infection. These infections were carried out alongside FAK -/- infections as a positive control. **C)** Immunoblot of MuPyV time course in FAK +/+ and FAK -/- MEFs.

5.3.7 PI3K is important for early steps in virus entry.

We next sought to understand how the PI3K and FAK/SRC pathways contribute to early steps in MuPyV infection. Specifically, we determined whether signal inhibition caused defects in virus endocytosis. In order to measure virus internalization, virus was covalently linked to a disulfide-biotin tag prior to addition to cells. Confirmation of the specificity of biotin labeled virus pull down and tris-2-carboxyethylphosphine (TCEP) reduction is demonstrated in Figure 5.10A. Biotin-SS-virus was added to cells for 30 min or 3 h at 37°C. Cells were washed with 50 mM tris-2-carboxyethylphosphine (TCEP), a non-cell permeable reducing agent that removed biotin from virus on the cell surface while internalized virus retained the biotin tag at indicated times. Whole cell lysates (WCL) were collected and incubated with streptavidin-coated beads. The virus bound to the streptavidin-coated beads (pull-down) was eluted in 50 mM TCEP to isolate the

internalized fraction. Whole cell lysates (total virus) and the streptavidin pull-downs (internalized virus) were then immunoblotted with anti-VP1. As expected, we observed that the fraction of internalized virus increased from 30 min to 3 h in the DMSO control (Figure 5.9A). However, the PI3K inhibited sample showed no increase in internalized VP1 from 30 min to 3 h, indicating that PI3K inhibition likely reduced virus entry. It is also possible that the virus in the PI3K inhibited samples is being trafficked to lysosomes leading to loss of the biotin tag and decreased pull-down; however, no increased virus degradation was detected in the WCL of the PI3K inhibited samples (Figure 5.9A), confirming an internalization defect during PI3K inhibition. The SRC-inhibited cells did not show a defect in virus internalization (Figure 5.9A), indicating that FAK/SRC activation is not required for initial virus endocytosis, and therefore is required for a later step in infection.

Ganglioside -/- MEFs internalize MuPyV, although this internalization does not lead to infection (You & O'Hara et al. 2015). Using the internalization assay, we measured virus endocytosis in ganglioside -/- MEFs compared to wild-type. Wild-type cells displayed increased virus internalization (pull-down) from 1 h to 5 h post virus addition with only one degradation band at less than 42 kDa (Figure 5.9B). Ganglioside -/- MEFs displayed high levels of virus internalization at 1 h; however, the amount of virus internalized (pull-down) did not increase from 1 h to 5 h (Figure 5.9B). Additionally, degradation of the virus was apparent at 3 h and 5 h post virus addition and may be due to lysosomal trafficking of the virus and subsequent loss of the biotin tag. Degradation of the virus in ganglioside -/- MEFs was apparent in the WCL, which showed many VP1 bands less than 42kDa in size (Figure 5.9B). Additionally, when a

lysosome inhibitor, chloroquine diphosphate (CQ), was added to ganglioside -/- MEFs the amount of virus pulled-down increased from 1 h to 5 h PI, and virus degradation was blocked (Figure 5.9B), confirming that lysosomal degradation of the virus was occurring in the ganglioside -/- MEFs. These results provide evidence that in the absence of gangliosides, MuPyV undergoes an alternative entry pathway that leads to increased lysosomal degradation. We also tested internalization in α4-integrin KD MEFs; however, there was no defect in virus internalization in these cells suggesting that α4-integrin may be important for a later step in infection (Figure 5.10B).

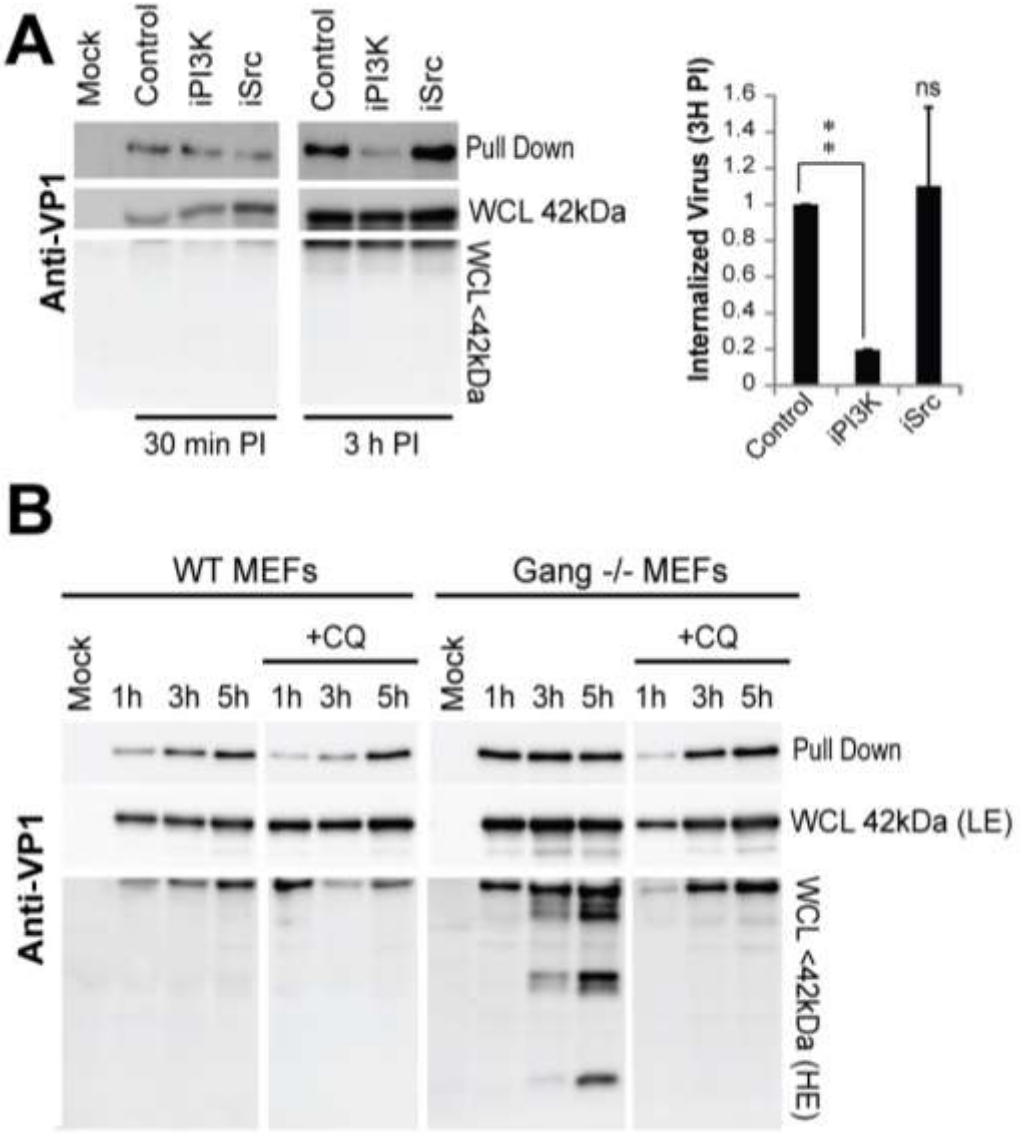

Figure 5.9: PI3K activation is required for virus internalization. A) Internalization assays in wild-type MEFs with or without inhibitor treatment. The virus present in the whole cell lysate (WCL) and the streptavidin pull-down (pull down) were detected by immunoblotting with anti-VP1 for each time point. Bar graph displays the average internalization of n=2 bio replicates, error bars are standard error. A paired *t* test was performed. **B)** Internalization assays in wild-type and ganglioside -/- MEFs with or without the lysosomal degradation inhibitor, 100 µM chloroquine diphosphosphate (CQ). The virus present in the whole cell lysate (WCL) and streptavidin pull-downs (pull down) was detected by immunoblotted with anti-VP1 for each time point. WCL chemiluminescence low exposure (LE) and high exposure (HE) are shown.

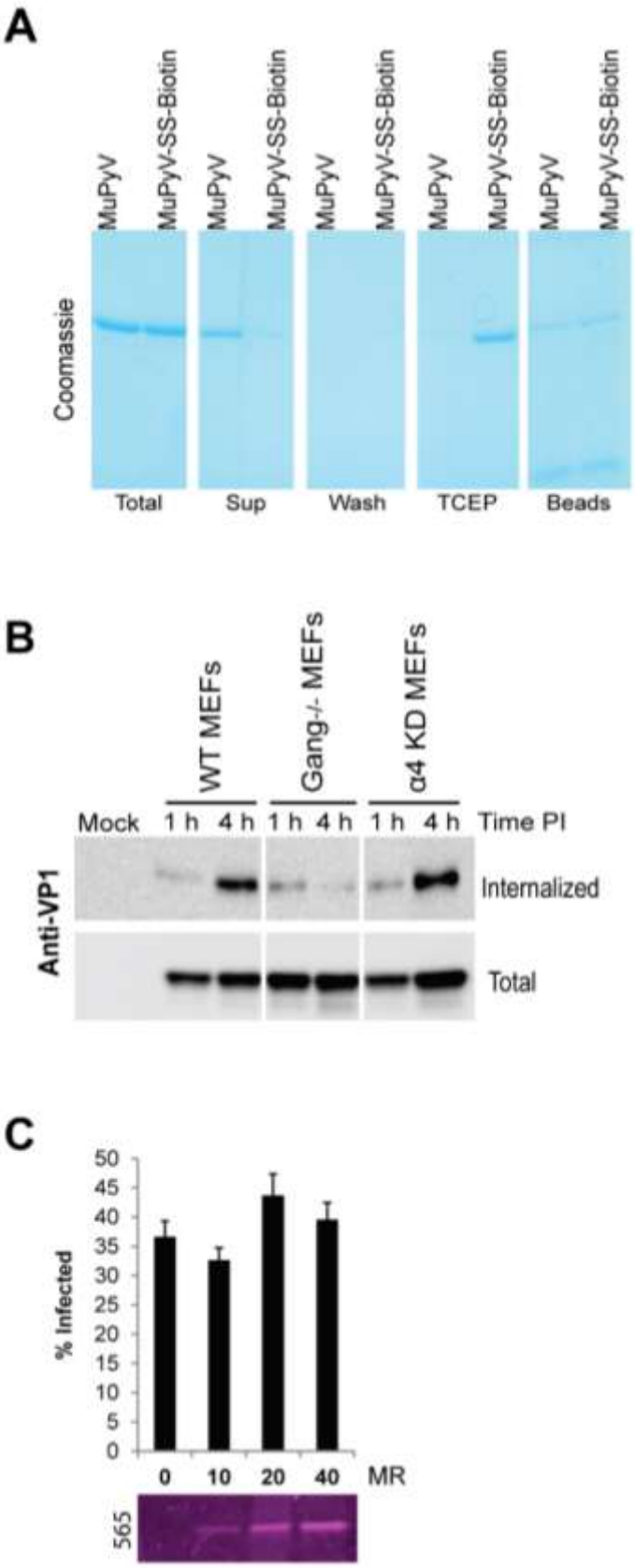

Figure 5.10 Biotin and dye labeled virus and pseudovirus.

A**)** Confirmation of Biotin-SS-MuPyV linkage by SDS-PAGE electrophoresis and Coomassie staining after pull down with streptavidin coated beads. MuPyV or MuPyV covalently inked to disulfide biotin were incubated with streptavidin beads. The beads were pellected and the supernatant (Sup) shows only MuPyV did not bind the beads. TCEP was added to the beads and the supernatant (TCEP) shows releases of the virus from the biotin tag. The beads show very little nonspecific virus binding. **B)** Internalization assay in wild-type, ganglioside -/-, and α4-integrin knock down MEFs. **C)** Infectivity of ATTO-565 labeled MuPyV at molar ratio of 0, 10, 20, and 40. Gel shows typhoon scanner image with the 560 laser.

5.3.8 FAK/SRC is important for steps in virus trafficking.

SRC inhibition blocked infection but not MuPyV internalization, suggesting that this pathway may contribute to a subsequent step in the virus life cycle such as virus trafficking. Microtubules have been shown to be required for MuPyV trafficking to the ER (Gilbert et al. 2003; Zila et al. 2014). The microtubule polymerization antagonist, nocodazole, inhibited MuPyV infection when added during virus entry and this inhibition increased when nocodazole was added during virus trafficking (Figure 5.11C). In contrast, inhibition of actin polymerization increased MuPyV infection, suggesting that actin breakdown may be required for efficient virus trafficking (Gilbert et al. 2003) (Figure 5.7D). Using confocal and super-resolution structured illumination microscopy (SIM) we imaged ATTO565-labeled virus, microtubules, and actin filaments (Figure 5.11A). We quantified virus association with microtubules and actin filaments 1 h post virus addition (Figure 5.11B). We also observed cortical actin depolymerization at the edge of the infected cell as previously reported (Control, Figure 5.11A) (Stergiou et al. 2013). As expected, nocodazole treatment decreased virus association with microtubules due to microtubule depolymerization (Figure 5.11B). Interestingly, nocodazole treatment increased virus association with actin at 1 h PI (Figure 5.11B), further supporting actin depolymerization as important for MuPyV trafficking. Because the FAK/SRC pathway is known to regulate microtubule and actin dynamics (Ezratty et al. 2005; Schaller 2010; Hamadi et al. 2005), we tested virus association with microtubules and actin during FAK/SRC inhibition. We found a 40% decrease in microtubule association when cells were treated with the SRC inhibitor (Figure 5.11A and quantification shown in 5.11B), although the microtubule network of the cell

remained intact (Figure 5.11A). We also observed a concurrent 2-fold increase in actin association due to SRC inhibition, indicative of virus undergoing non-productive trafficking (Figure 5.11B). These data suggest that the FAK/SRC pathway is important for virus trafficking along microtubules or actin depolymerization and suggest that intracellular trafficking, rather than entry, is defective in the absence of FAK/SRC signaling.

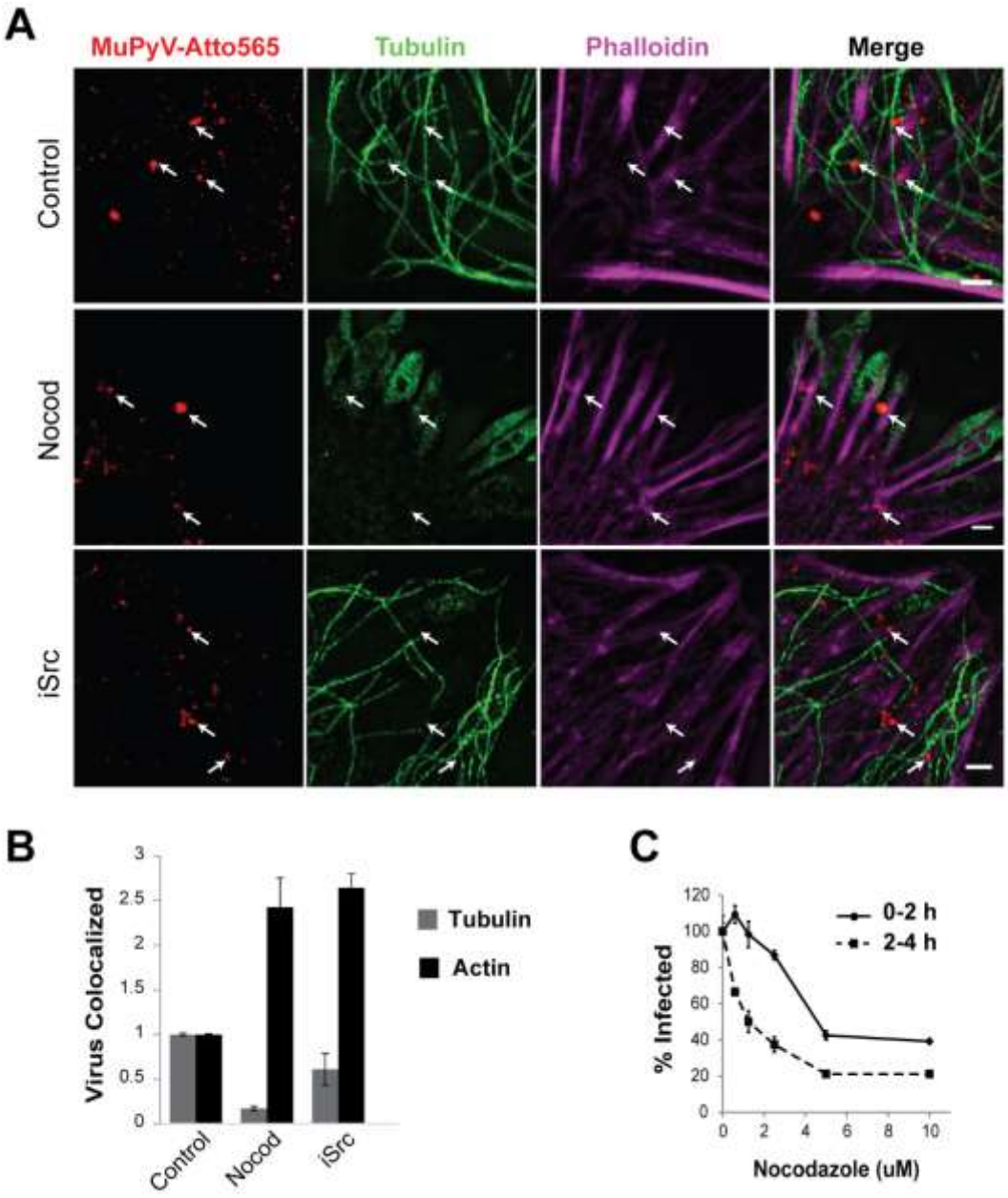

Figure 5.11 The FAK/SRC pathway is important for virus trafficking on microtubules. A) SIM images of virus treated samples 1 h post infection: MuPyV labeled with ATTO-565 (red), microtubules (green), and phalloidin staining actin filaments (magenta). Scale bars are 2.5 μM. **B)** Colocalization analysis of confocal images taken from experiments shown in Figure 5.11A. Bar graphs plots virus voxels colocalized with tubulin voxels (grey bars) or actin voxels (black bars) normalized to the control. Error bars are standard error, n=2. **C)** Nocodazole treatment of MEFs during virus binding and entry (0-2 h, solid black line) or post virus binding and entry (2-4 h, dashed line). Infection was quantified at 24 h PI by the percent T-ag positive nuclei and treatments were normalized to the DMSO control. Error bars are standard error, n=3.

5.4 **Discussion**

We identified a diverse signaling network activated by MuPyV cell surface binding, including the MAPK, PI3K, and FAK/SRC pathways. Activation of the PI3K and FAK/SRC pathways were required for early steps of MuPyV infection, while the MAPK pathway was not essential. PI3K activation was dependent upon VP1 interactions with both cell-surface gangliosides and the α4-integrin receptor, while VP1 interactions with either gangliosides or α4-integrin were sufficient to activate the MAPK pathway. Finally, we defined the contribution of each signaling pathway to early steps of infection. We found that PI3K activation was required for virus internalization, whereas the FAK/SRC pathway contributed to virus trafficking along microtubules. These results indicate that VP1 cell surface binding activates specific signaling pathways essential for early steps of MuPyV infection.

MuPyV activation of the MAPK, PI3K, and FAK/SRC pathways is likely initiated by GFRs on the cell surface, but how the virus may activate GFR signaling is unclear given that the capsid does not contain specific GFR binding sites. A likely possibility is that MuPyV multivalent binding to gangliosides and α4-integrin could facilitate activation by indirectly clustering GFRs located in cholesterol-rich microdomains of the plasma membrane. For example, previous results showing increased transcriptional responses to complete viral capsids *versus* capsomere subunits suggested that clustering could be important for signaling (Zullo et al. 1987). In support of MuPyV-GFR activation, we found that the EGFR was rapidly phosphorylated upon virus addition (Figure 5.5E). Cell surface gangliosides were not required for EGFR activation by virus, although loss of both integrin and ganglioside binding abrogated EGFR phosphorylation (Figure 5.5C).

These results demonstrate that MuPyV activation of GFRs can be mediated by VP1 interactions with other cell surface receptors, such as α4-integrin. Sialic acid binding alone was not sufficient to activate EGFR (Figure 5.5C), thus MuPyV does not appear to be binding to the EGFR though sialic acid modifications on the extracellular domain of this receptor or this binding is not sufficient for activation (Qian & Tsai 2010). Finally, although general tyrosine kinase inhibition by genistein blocked MuPyV infection, inhibition of EGFR phosphorylation alone had no effect on MuPyV infection (Figure 5.7C), suggesting that multiple GFRs may contribute to signaling events required for infection.

The MAPK pathway was activated rapidly upon virus addition to cells (Figure 5.1C), measured by ppERK, though *either* ganglioside or integrin interactions. However, loss of both interactions resulted in decreased ppERK without loss of virus binding to the cell surface (Figure 5.5C). Although rapidly activated, the MAPK pathway was not required for the early steps of MuPyV infection (Figure 5.7A). It has been previously reported that capsid binding to cells results in increased incorporation of BrdU into cellular DNA (Zullo et al. 1987), and it is possible that the MAPK and other mitogenic signaling occurring during entry may be important for subsequent stages of infection such viral DNA replication.

MuPyV rapidly induces the transcription of primary response genes (*Myc, Fos*, and *Jun*) upon cell surface binding (Zullo et al. 1987; Glenn & Eckhart 1990). Consistent with these observations MuPyV binding induced C-JUN phosphorylation (Figure 5.1C), which is a precursor to induction of *Jun* transcription. MuPyV binding to both ganglioside and integrins led to the highest levels of C-JUN activation, and loss of either VP1

interaction reduced phosphorylation of C-JUN (Figure 5.5C). These results suggest possible cooperativity between MuPyV ganglioside and integrin binding in the activation of C-JUN. We also tested inhibition of JNK kinase and found decreased infection. However, the JNK inhibitors we tested had off target effects, and thus it is unclear whether the JNK pathway specifically impacts infection.

The PI3K pathway, measured by pAKT, was activated rapidly upon virus addition and required *both* ganglioside and integrin interactions. If either interaction was lost, AKT phosphorylation was greatly reduced (Figure 5.3C). It is possible that the signaling theshold required for PI3K activation is attained only when both receptors are engaged, or that a specific combination of signals is necessary. Inhibition of the PI3K pathway during virus entry blocked infection by preventing virus internalization, while inhibition post-entry had no effect (Figure 5.6A, 5.9A). Interestingly, we found that the essential MuPyV ganglioside receptors (GD1a, GT1a) increased activation of the PI3K pathway, while non-MuPyV ganglioside receptors or ganglioside -/- cells alone retained only MAPK signaling (Figure 5.3B, C). These data suggest that specific VP1-ganglioside interactions may induce particular signaling pathways required for productive trafficking of virus and subsequent infection. It is important to note that even when infection-related receptors are not present, the virus still binds the cell surface and is internalized (You & O'Hara et al. 2015; Tsai et al. 2003). Thus the productive entry pathway is a subset of the possible routes engaged by the virus. In the absence of gangliosides virus was trafficked to the lysosome, leading to its degradation (Figure 5.6B), but how gangliosides mediate trafficking of the virus to non-lysosomal or productive pathways of infection is unclear (Qian et al. 2009). In the absence of gangliosides, we see rapid

endocytosis with much faster kinetics than observed in wild-type MEFs (Figure 5.6C). In wild-type MEFs there may be competition for virus binding between gangliosides and other receptors, such as Toll Like Receptor 4 (TLR4) (Velupillai et al. 2012; You & O'Hara et al. 2015). In ganglioside null cells, this competition would not exist and increased binding to TLR4 may induce rapid endocytosis. Interestingly, inhibition of lysosomal maturation by chloroquine diphosphate reduced the rate of endocytosis in ganglioside null cells and restored wild-type kinetics of endocytosis (Figure 5.6B), indicating that alternative pathways are dependent on endosomal maturation and trafficking to the lysosome. Gangliosides have been previously implicating in virus escape from the endolysosome to the ER; however, it is unclear how these receptors mediate this trafficking event (Qian et al. 2009). MuPyV binding to gangliosides and the subsequent activation of the PI3K pathway may define the subpopulation of virus that escape the endolysosome, and are trafficked to productive pathways for infection.

The FAK/SRC pathway modulates microtubules and actin dynamics (Schaller 2010) and MuPyV requires intact microtubules and disrupted actin fibers for virus trafficking (Figure 5.11C, 5.7D) (Gilbert et al. 2003). MuPyV activated FAK after the MAPK/PI3K pathways, and phospho-FAK accumulated thoughout virus entry (Figure 1C). Inhibition of the FAK/SRC pathway either during virus entry or trafficking reduced MuPyV infection (Figure 5.6B). FAK/SRC inhibition did not affect virus internalization (Figure 5.9A), but decreased MuPyV-microtubule association and increased MuPyV-actin association (Figure 5.11B) further implicating FAK/SRC as important for MuPyV trafficking. MuPyV activation of the FAK/SRC pathway may mediate polymerization or recruitment of microtubules to sites of virus endocytosis. Further studies investigating

how microtubules are recruited to the plasma membrane during infection, as well as the role of FAK/SRC in this process could elucidate an important step in intracellular virus trafficking.

Signaling at the cell surface appears to be a critically conserved step in PyV entry, although different PyV species may utilize distinct signaling pathways for infection (Zullo et al. 1987; Glenn & Eckhart 1990; Dangoria et al. 1996; Querbes et al. 2004; Butin-Israeli et al. 2010). For example, JCPyV infection of human glial cells requires activation of the EGFR and the MAPK pathway (Querbes et al. 2004), whereas MuPyV also activates the EGFR and MAPK, but this activation is not required for infection. SV40 also induces phosphorylation of AKT after virus binding, but unlike MuPyV, activation of PI3K does not appear to be required for SV40 infection (Butin-Israeli et al. 2010). Differences in signaling between PyVs may be due to the distinct cell surface receptors found on the host cells for these viruses. Most PyVs bind specific gangliosides as primary cell attachment receptors and it is possible that ganglioside binding induces host- or cell-specific signaling pathways. Recently, the SV40 VP1-GM1 interaction has been shown to be essential for SV40-induced vacuolization (Luo et al. 2016). Thus, SV40 binding to GM1 may induce cellular signaling pathways that cause host cell vacuolization though a similar mechanism as mediated by GD1a and GT1a activation of PI3K after MuPyV binding.

Human PyV infections, such as those caused by BKPyV and JCPyV, can lead to major complications in immunosuppressed patients (Jiang et al. 2009). Thus, understanding the signaling pathways required for these PyV infections could lead to new therapeutics. It is possible that PyV species that use the same ganglioside

receptors may have similar signaling requirements. For example, BKPyV binds GT1b, a receptor used by MuPyV (Erickson et al. 2009; Low et al. 2006), and thus the PI3K and FAK/SRC pathways may also play a role in BKPyV infection and could be therapeutic targets.

Chapter 6 Conclusions and Future Directions:

6.1 Conclusions

6.1.1 Need for PyV Therapeutics and Entry Inhibitor Potential

Human Polyomaviruses are ubiquitous in the population. JCPyV and BKPyV establish an asymptomatic infection of the kidney and urinary tract and have a seroprevalance ranging from 55%-90%, respectively (Jiang et al. 2009; DeCaprio & Garcea 2013). Although these infections are asymptomatic in healthy individuals, HuPyVs can cause significant diseases under conditions of immunosuppression. For example, in immunosuppressed patients JCPyV can infect oligodendrocytes leading to a deadly condition known as progressive multifocal leukoencephalopathy (PML) (Jiang et al. 2009). BKPyV lytic infection of the kidney can lead to kidney allograft loss after solid organ kidney transplant and has been implicated in the etiology of bladder carcinoma (Fernandez Rivera et al. 2010). The rise in efficacy of immunosuppressive drugs in the last decade has increased the prevalence of BKPyV and JCPyV infections, and no treatments or vaccines are available to date (DeCaprio et al. 2013; Jiang et al. 2009; Gorelik et al. 2011; Uettwiller et al. 2011). Thus, the need for antiviral therapies for treatment of PyV infections under conditions of immunosuppression is significant.

Virus entry inhibitors are a promising therapeutics to inhibit human polyomavirus infections and could span multiple steps of virus entry, from attachment to internalization. Identifying the cell surface receptors required for PyV infection could lead to development of functional blocking molecules that inhibit virus attachment. These types of inhibitors are attractive for drug development as they block the virus life

cycle before it begins and do not need to enter the cell to exert their activity (Zhou & Simmons 2012). For PyVs, the carbohydrate portion of gangliosides could be pre-bound to virus, thus blocking virus interactions with ganglioside receptors, effectively inhibiting infection. Cancer cells shed gangliosides into the extracellular space, possibly altering the tumor microenvironment and increasing mitogenic signaling in neighboring cells where gangliosides incorporate (Kaucic et al. 2006). However, cleaving the ceramide tail from gangliosides would block cellular incorporation while retaining interactions with the sialic acid binding pocket of VP1. Investigating the use of ganglioside fragments of GT1b to block BKPyV infection may be an effective treatment option in kidney transplant patients. JCPyV isolates from PML patients have shown that mutations in the VP1 capsid disrupt sialic acid binding, indicating that gangliosides (or the glycan portion of LSTc) are not the receptors mediating JCPyV oligodendrocyte infection (Reid et al. 2011). A possible protein receptor for JCPyV is discussed in section 6.1.2.

Targeting internalization pathways could also be a viable option for antiviral therapies; however, due to the importance of these signaling pathways in cellular processes, inhibition of cell signaling may be toxic to the host. One advantage to targeting cellular signaling pathways is that many of these pathways have been implicated in cancer, and thus many small molecule inhibitors to these pathways are already in development. We found that the PI3K and FAK/SRC pathways to be important for MuPyV infection (Chapter 5) and these signaling pathways could also function in HuPyV infections. PI3K and its targets, AKT/MTOR, are overexpressed or have gain of function mutations in a wide range of human cancers (Fruman & Rommel 2014). PI3K inhibitors in clinical trials have largely proven to be ineffective; however,

less toxic and more specific small molecules are in development (Han et al. 2016). Additionally, failed PI3K inhibitors in cancer treatment may still hold therapeutic potential as antivirals. In our studies we used two pan-PI3K inhibitors to inhibit MuPyV entry, thus it is unclear which specific isoform of PI3K is required for MuPyV entry (Chapter 5). An siRNA screen investigating JCPyV identified a specific subunit of PI3K that is important for JCPyV infection (Walter Atwood, personal communication). It is possible that inhibitors to specific PI3K isoforms or subunits could be potent antivirals for JCPyV infection without the toxicity demonstrated by pan-PI3K inhibition.

The signaling pathways required for BKPyV infection remain unknown. However, BKPyV binds to a common ganglioside receptor as MuPyV, GT1b, further suggesting that the PI3K or FAK/SRC pathways may function in BKPyV infection. There are FAK and SRC inhibitors currently in clinical trials for a wide range of cancers (Tai et al. 2015). Further investigation of these pathways in BKPyV infection are needed. It is possible that small molecules developed for cancer therapy could be leveraged to prevent PyV infections in immunosuppressed individuals.

6.1.2 Possible JCPyV protein receptor in Natalizumab-associated PML infections

Over 50% of the population is seropositive for JCPyV, a typically asymptomatic infection of the kidneys and urinary tract (Maginnis & Atwood 2010; Kean et al. 2009). In severely immune-compromised individuals JCPyV can infect oligodendrocytes and astrocytes leading to progressive multifocal leukoencephalopathy (PML). In 2005, a multiple sclerosis drug, Natalizumab (NTM), was recalled due to increased rates of PML in NTM treated patients. Multiple sclerosis (MS) is an immune-mediated disorder in

which leukocytes attack the protective myelin sheath of nerve cells leading to loss of synaptic transmission. NTM was approved for MS treatment in 2004 and is a IgG4 humanized monoclonal antibody directed against the α4-integrin subunit of α4β1-integrin receptor (Schwab et al. 2014). Integrin receptors are cell-adhesion molecules that facilitate cell binding to the extracellular matrix and have roles in leukocyte trafficking (Hynes 2002). On leukocytes, chemokine stimulation activates α4β1-integrin, enabling integrin binding to vascular cell adhesion molecule-1 (VCAM-1) on activated endothelial cells of the blood brain barrier (BBB)(Schwab et al. 2014; Uettwiller et al. 2011). NTM blocks α4β1-integrin/VCAM-1 interactions, preventing leukocyte trafficking across the BBB (Gorelik et al. 2011; Schwab et al. 2014; Uettwiller et al. 2011). NTM was successful in phase III clinical trials, where it resulted in a 68% decrease in MS relapses (Schwab et al. 2014). However, in 2005 three NTM treated patients developed progressive multifocal encephalopathy (PML), a rare and severe condition caused by JC polyomavirus (JCPyV) infection of oligodendrocytes, leading to NTM recall (Reid et al. 2011; Gorelik et al. 2011).

Despite the connection between NTM and PML, the FDA re-approved NTM in 2008 for severely affected MS patients where the benefits of NTM might outweigh the risk of PML (Reid et al. 2011; Gorelik et al. 2011; Schwab et al. 2014). NTM treated patients must be regularly screened for the presence of JCPyV DNA in cerebral spinal fluid (CSF) (Vallefuoco et al. 2014). Over 400 cases of NTM-associated PML have subsequently been reported, with an increased PML incidence correlating with extended NTM-treatment (Schwab et al. 2014). PML development in NTM-patients may be due to lack of immune surveillance in the CNS; however, the rate of NTM-associated PML is

much higher than what has been reported for other immunosuppressive drugs (Schwab et al. 2014; Uettwiller et al. 2011). Additionally, JCPyV DNA sequences extracted from the CSF of NTM-associated PML patients frequently acquire mutations in the viral capsid, specifically in the receptor-binding loops of the major capsid protein VP1 (Reid et al. 2011). These mutations are absent in JCPyV harvested from the kidneys and urinary tract (Reid et al. 2011; Gorelik et al. 2011).

JCPyV is known to bind sialylated-oligosaccharides that are ubiquitously expressed on the plasma membrane of cells (O'Hara et al. 2014). However, JCPyV extracted from the CSF of NTM-associated PML patients lack the ability to bind these receptors (Reid et al. 2011; Gorelik et al. 2011). These data suggest that altered JCPyV-receptor binding may affect PML development in NTM-treated patients. A similar phenomenon has been described in mouse polyomavirus (MuPyV), a virus closely related to JCPyV, where decreased receptor binding has been shown to increase MuPyV spread, tissue tropism, and pathogenesis (Bauer et al. 1995; O'Hara et al. 2014). Additionally, α4-integrin is a receptor for MuPyV and loss of α4-integrin binding decreases infection *ex vivo* and alters tissue tropism *in vivo* (Caruso et al. 2007; Caruso et al. 2003; O'Hara et al. 2014). MuPyV contains two predicted α4-integrin binding motifs located on the virus capsid. One motif, LDV, has been confirmed to be a functional binding site; however, mutation of LDV only decreases mPyV infection by 60% (Caruso et al. 2007; Caruso et al. 2003). An additional α4-integrin binding motif, DSP, is located in the binding loops of the virus capsid and is the minimum required motif for VCAM-1 binding to α4-integrin (Clements et al. 1994; Meyer 2013), the very same interaction blocked by NTM. The DSP motif is conserved across many PyV

species, including mouse, simian virus 40 (SV40), BKPyV, and JCPyV (Meyer 2013). The DSP motif may be the primary PyV-integrin binding site, as the LDV motif is not conserved across virus species. The DSP site in JCPyV may be important for α4-integrin binding and may be the primary receptor in the absence of sialic acid interactions.

The loss of SA-binding in JCPyV mutants extracted from PML patients supports altered-receptor binding as a mechanism for virus dissemination (Gorelik et al. 2011). If JCPyV binds α4-integrin, NTM treatment could further increase JCPyV spread while maintaining its ability to bind integrin receptors and be infectious in the CNS. Only low levels of NTM can cross the BBB, thus NTM would be decreased in its ability to prevent JCPyV infection of oligodendrocytes (Dennis & Watts 2012). NTM treatment may inhibit JCPyV-α4-integrin interactions in NTM-saturated (IgG4-accessible) tissues, allowing for increased spread of the virus throughout the organism. NTM treatment causes loss of immune surveillance in the CNS and may increase virus spread creating a prime environment for PML development. Modifying NTM to increase trafficking across the BBB could reduce JCPyV infection in oligodendrocytes and there are mechanisms to increase antibody transfer across the BBB currently in development (Jones & Shusta 2007).

6.2 Future Directions

6.2.1 The importance of multivalent binding in MuPyV signal activation

The sialic acid binding pocket of VP1 is a shallow surface pocket that has a low affinity interaction with the sialic acid head group of the ganglioside receptor (Stehle et al. 1994; Stehle & Harrison 1996; Buch et al. 2015). The dissociation constant for sialic acid binding to a single VP1 pentamer is estimated to be 5mM. However, the virus capsid contains 360 sialic acid binding sites and thus multivalent binding to receptors is important for stabilizing VP1-receptor interactions (Ewers et al. 2005). The avidity of PyV multivalent binding to gangliosides is thought to reach the strength of a covalent bond (Szklarczyk et al. 2013; Ewers et al. 2010).

Cholesterol depletion of cellular membranes results in increased virus diffusion along the plasma membrane, suggesting that lipid rich micro-domains enriched for ganglioside receptors could maintain receptor concentrations important for inducing multivalent VP1-ganglioside interactions (Ewers et al. 2005; Szklarczyk et al. 2013). These lipid-rich microdomains are also enriched for important signaling molecules, such as growth factor receptors and integrins. The MuPyV protein receptor, α4β1-integrin, likely also undergoes multivalent VP1-interactions. Canonically, integrin receptors are activated though clustering induced by multivalent binding to extracellular matrix proteins like fibronectin (Hynes 2002; Del Pozo 2004; Srichai & Zent 2010). In Chapter 5 I demonstrated that ganglioside and integrin binding are important for MuPyV signaling events; however, the mechanism by which these receptors induce signal activation is still unclear. Integrins may self-activate upon virus clustering, but

gangliosides do not have intrinsic signaling properties. However, gangliosides have been shown to induce activation of associated growth factor receptors and multivalent binding of virus to gangliosides may cluster associated GFRs, leading to their activation (Liu et al. 2004; Kaucic et al. 2006; Yates et al. 1995; Li et al. 2000). Previous work has shown that mitogenic gene expression is increased for virions more so than for individual viral pentamers, suggesting that multivalent binding may be important for MuPyV signaling events.

In order to test the role of multivalent binding in MuPyV signaling events we have generated full length and truncated VP1 pentamers. Full-length pentamers can form pentamer-pentamer interactions though their c-terminal regions, leading to high avidity interactions with cell surface receptors. Truncated pentamers have a 30 amino acid deletion of their c-terminus. These CΔ30 VP1 mutants still form pentamers, but cannot form pentamer-pentamer interactions, reducing the avidity or valency of cell surface receptor binding. VP1 pentamers will be purified from 293TT cells (VP1 purification process is in covered in Appendix I). We will then probe for signal activation by phospho-immunoblot after addition of high and low valency pentamers to mouse embryonic fibroblast (MEFs). Pentamers will be added to MEFs in dose-response with the expectation that high valency pentamers, full length, will activate signaling at lower protein concentrations than low valency, CΔ30 pentamers. It is also possible to assemble pentamers into virus like particles in vitro, providing the highest valency interaction. These experiments will provide insight into the role of multivalent receptor binding in MuPyV signal activation.

Bibliography

Anderson, H. a, Chen, Y. & Norkin, L.C., 1996. Bound simian virus 40 translocates to caveolin-enriched membrane domains, and its entry is inhibited by drugs that selectively disrupt caveolae. *Molecular biology of the cell*, 7(11), pp.1825–34. Available at: http://www.pubmedcentral.nih.gov/articlerender.fcgi?artid=276029&tool=pmcentrez&rendertype=abstract.

Bauer, P.H. et al., 1999. Discrimination between sialic acid-containing receptors and pseudoreceptors regulates polyomavirus spread in the mouse. *Journal of virology*, 73(7), pp.5826–32. Available at: http://www.pubmedcentral.nih.gov/articlerender.fcgi?artid=112643&tool=pmcentrez&rendertype=abstract.

Bauer, P.H. et al., 1995. Genetic and structural analysis of a virulence determinant in polyomavirus VP1. *Journal of virology*, 69(12), pp.7925–31. Available at: http://www.pubmedcentral.nih.gov/articlerender.fcgi?artid=189737&tool=pmcentrez&rendertype=abstract.

Bennett, S.M. et al., 2015. Role of a nuclear localization signal on the minor capsid Proteins VP2 and VP3 in BKPyV nuclear entry. *Virology*, 474, pp.110–116. Available at: http://dx.doi.org/10.1016/j.virol.2014.10.013.

Bolen, J.B. et al., 1985. A Determinant of Polyomavirus Virulence Enhances Virus Growth in Cells of Renal Origin. , 53(1), pp.335–339.

Breau, W.C., Atwood, W.J. & Norkinl, L.C., 1992. Class I major histocompatibility proteins are an essential component of the simian virus 40 Receptor. *Journal of virology*, 66(4), pp.2037–2045.

Buch, M.H.C. et al., 2015. Structural and functional analysis of murine polyomavirus capsid proteins establish the determinants of ligand recognition and pathogenicity. *PLOS Pathogens*, 11(10), p.e1005104. Available at: http://dx.plos.org/10.1371/journal.ppat.1005104.

Buck, C.B. & Thompson, C.D., 2007. Production of papillomavirus-based gene transfer vectors. In *Current protocols in Cell Biology*.

Butin-Israeli, V., Drayman, N. & Oppenheim, A., 2010. Simian virus 40 infection triggers a balanced network that includes apoptotic, survival, and stress pathways. *Journal of virology*, 84(7), pp.3431–3442.

Calalb, M.B., Polte, T.R. & Hanks, S.K., 1995. Tyrosine phosphorylation of focal adhesion kinase at sites in the catalytic domain regulates kinase activity: a role for Src family kinases. *Molecular and Cellular Biology*, 15(2), pp.954–963. Available at: http://mcb.asm.org/content/15/2/954.abstract.

Carroll, J. et al., 2007. Receptor-binding and oncogenic properties of polyoma viruses isolated from feral mice. *PLoS pathogens*, 3(12), p.e179. Available at: http://www.pubmedcentral.nih.gov/articlerender.fcgi?artid=2134959&tool=pmcentrez&rendertype=abstract [Accessed December 5, 2013].

Caruso, M. et al., 2003. Alpha-4 Beta-1 Integrin acts as a cell receptor for Murine Polyomavirus at the postattachment level. *Journal of Virology*, 77(7), pp.3913–3921.

Caruso, M. et al., 2007. Mutation in the VP1-LDV motif of the murine polyomavirus affects viral infectivity and conditions virus tissue tropism in vivo. *Journal of molecular biology*, 367(1), pp.54–64. Available at: http://www.ncbi.nlm.nih.gov/pubmed/17239397 [Accessed November 8, 2012].

Cheng, J. et al., 2009. Cellular transformation by Simian Virus 40 and Murine Polyoma Virus T antigens. *Seminars in cancer biology*, 19(4), pp.218–28. Available at: http://www.pubmedcentral.nih.gov/articlerender.fcgi?artid=2694755&tool=pmcentrez&rendertype=abstract [Accessed February 12, 2013].

Christmas, Rowan; Avila-Campillo, Iliana; Bolouri, Hamid; Schwikowski, Benno; Anderson, Mark; Kelley, Ryan; Landys, Nerius; Workman, Chris; Ideker, Trey; Cerami, Ethan; Sheridan, Rob; Bader, Gary D.; Sander, C., 2005. Cytoscape: a software environment for integrated models of biomolecular interaction networks. *American Association for Cancer Research Education Book*, (Karp 2001), pp.12–16.

Clements, J.M. et al., 1994. Identification of a key integrin-binding sequence in VCAM-1 homologous to the LDV active site in fibronectin. , 2135, pp.2127–2135.

Damm, E.-M. et al., 2005. Clathrin- and caveolin-1-independent endocytosis: entry of simian virus 40 into cells devoid of caveolae. *The Journal of cell biology*, 168(3), pp.477–88. Available at: http://www.pubmedcentral.nih.gov/articlerender.fcgi?artid=2171728&tool=pmcentrez&rendertype=abstract [Accessed October 16, 2012].

Dangoria, N.S. et al., 1996. Extracellular simian virus 40 induces an ERK/MAP kinase-independent signalling pathway that activates primary response genes and promotes virus entry. *The Journal of general virology*, 77 (Pt 9), pp.2173–82. Available at: http://www.ncbi.nlm.nih.gov/pubmed/8811017.

DeCaprio, J. a & Garcea, R.L., 2013. A cornucopia of human polyomaviruses. *Nature reviews. Microbiology*, 11(4), pp.264–76. Available at: http://www.ncbi.nlm.nih.gov/pubmed/23474680 [Accessed November 20, 2013].

Dennis, M.S. & Watts, R.J., 2012. Transferrin antibodies into the brain. *Neuropsychopharmacology : official publication of the American College of Neuropsychopharmacology*, 37(1), pp.302–3.

Diehl, N. & Schaal, H., 2013. Make yourself at home: Viral hijacking of the PI3K/Akt

signaling pathway. *Viruses*, 5(12), pp.3192–3212.

Dike, L.E. & Ingber, D.E., 1996. Integrin-dependent induction of early growth response genes in capillary endothelial cells. , 2863, pp.2855–2863.

Dubensky, T.W. et al., 1991. Polyomavirus replication in mice: influences of VP1 type and route of inoculation. *Journal of virology*, 65(1), pp.342–9. Available at: http://www.ncbi.nlm.nih.gov/pubmed/1845895\nhttp://www.pubmedcentral.nih.gov/articlerender.fcgi?artid=PMC240523.

Elphick, G.F. et al., 2004. The human polyomavirus, JCV, uses serotonin receptors to infect cells. *Science (New York, N.Y.)*, 306(5700), pp.1380–3. Available at: http://www.ncbi.nlm.nih.gov/pubmed/15550673 [Accessed January 26, 2014].

Erickson, K.D., Garcea, R.L. & Tsai, B., 2009. Ganglioside GT1b is a putative host cell receptor for the Merkel cell polyomavirus. *Journal of virology*, 83(19), pp.10275–9. Available at: http://www.pubmedcentral.nih.gov/articlerender.fcgi?artid=2748031&tool=pmcentrez&rendertype=abstract [Accessed December 4, 2013].

Ewers, H. et al., 2010. GM1 structure determines SV40-induced membrane invagination and infection. *Nature cell biology*, 12(1), pp.11-8-12. Available at: http://www.ncbi.nlm.nih.gov/pubmed/20023649 [Accessed November 5, 2012].

Ewers, H. et al., 2005. Single-particle tracking of murine polyoma virus-like particles on live cells and artificial membranes. *Proceedings of the National Academy of Sciences of the United States of America*, 102(42), pp.15110–5. Available at: http://www.pubmedcentral.nih.gov/articlerender.fcgi?artid=1257700&tool=pmcentrez&rendertype=abstract.

Ewers, H. & Helenius, A., 2011. Lipid-mediated endocytosis. *Cold Spring Harbor perspectives in biology*, 3(8), p.a004721. Available at: http://www.ncbi.nlm.nih.gov/pubmed/21576253 [Accessed October 16, 2012].

Ezratty, E.J., Partridge, M.A. & Gundersen, G.G., 2005. Microtubule-induced focal adhesion disassembly is mediated by dynamin and focal adhesion kinase. *Nature cell biology*, 7(6), pp.581–590.

Fernandez Rivera, C. et al., 2010. Association of bladder adenocarcinoma and BK virus infection in a pancreatico-renal transplant recipient. *NDT Plus*, 3(3), pp.300–302. Available at: http://ckj.oxfordjournals.org/cgi/doi/10.1093/ndtplus/sfq042 [Accessed November 27, 2012].

Franceschini, A. et al., 2013. STRING v9.1: Protein-protein interaction networks, with increased coverage and integration. *Nucleic Acids Research*, 41(D1), pp.808–815.

Freund, R. et al., 1991. Polyomavirus tumor induction in mice: effects of polymorphisms of VP1 and large T antigen. *Journal of Virology*, 65(1), pp.335–341.

Fruman, D.A. & Rommel, C., 2014. PI3K and cancer: lessons, challenges and

opportunities. *Nat Rev Drug Discov*, 13(2), pp.140–156. Available at: http://www.ncbi.nlm.nih.gov/pubmed/24481312.

Gilbert, J. et al., 2006. Downregulation of protein disulfide isomerase inhibits infection by the mouse polyomavirus. *Journal of virology*, 80(21), pp.10868–10870.

Gilbert, J. et al., 2005. Ganglioside GD1a restores infectibility to mouse cells lacking functional receptors for polyomavirus. *Journal of virology*, 79(1), pp.615–8. Available at: http://www.pubmedcentral.nih.gov/articlerender.fcgi?artid=538744&tool=pmcentrez&rendertype=abstract.

Gilbert, J. & Benjamin, T., 2004. Uptake Pathway of Polyomavirus via Ganglioside GD1a. *Journal of Virology*, 78(22), pp.12259–12267.

Gilbert, J.M. & Benjamin, T.L., 2000. Early steps of polyomavirus entry into cells. *Journal of virology*, 74(18), pp.8582–8. Available at: http://www.pubmedcentral.nih.gov/articlerender.fcgi?artid=116371&tool=pmcentrez&rendertype=abstract.

Gilbert, J.M., Goldberg, I.G. & Benjamin, T.L., 2003. Cell penetration and trafficking of polyomavirus. *Journal of virology*, 77(4), pp.2615–22. Available at: http://www.pubmedcentral.nih.gov/articlerender.fcgi?artid=141103&tool=pmcentrez&rendertype=abstract.

Glenn, G.M. & Eckhart, W., 1990. Transcriptional regulation of early-response genes during Polyomavirus infection. *Journal of virology*, 64(5), pp.2193–2201.

Goldman, E. & Benjamin, T.L., 1975. Analysis of host range of nontransforming polyoma virus mutants. *Virology*, 66(2), pp.372–384.

Gonzalez, A.M. et al., 2010. Transdominant regulation of integrin function: Mechanisms of crosstalk. *Cellular Signalling*, 22(4), pp.578–583. Available at: http://dx.doi.org/10.1016/j.cellsig.2009.10.009.

Goodwin, E.C. et al., 2011. BiP and Multiple DNAJ Molecular Chaperones in the Endoplasmic Reticulum Are Required for Efficient Simian Virus 40 Infection. *mBio*, 2(3), pp.1–9.

Gorelik, L. et al., 2011. Progressive multifocal leukoencephalopathy (PML) development is associated with mutations in JC virus capsid protein VP1 that change its receptor specificity. *The Journal of infectious diseases*, 204(1), pp.103–14. Available at: http://www.pubmedcentral.nih.gov/articlerender.fcgi?artid=3307153&tool=pmcentrez&rendertype=abstract [Accessed December 4, 2013].

Greber, U.F., 2002. Signaling in viral entry. *Cellular and Molecular Life Sciences*, 59, pp.608–626.

Gross, L., 1953. Neck tumors, or leukemia, developing in adult C3H mice following inoculation, in early infancy, with filtered (Berkefeld N), or centrifugated (144,000 X

g), Ak-leukemic extracts. *Cancer*, 6(5), pp.948–58. Available at: http://www.ncbi.nlm.nih.gov/pubmed/13094642.

Hamadi, A. et al., 2005. Regulation of focal adhesion dynamics and disassembly by phosphorylation of FAK at tyrosine 397. *Journal of cell science*, 118(Pt 19), pp.4415–4425.

Han, J. et al., 2016. Structure-based optimization leads to the discovery of NSC765844 , a highly potent , less toxic and orally efficacious dual PI3K / mTOR inhibitor. *European journal of medicinal chemistry*, 122, pp.684–701.

Harburger, D.S. & Calderwood, D.A., 2009. Integrin signalling at a glance. *Journal of Cell Science*, 122(9), pp.1472–1472. Available at: http://jcs.biologists.org/cgi/doi/10.1242/jcs.052910 [Accessed November 2, 2012].

Heiser, K., Nicholas, C. & Garcea, R.L., 2016. Activation of DNA damage repair pathways by murine polyomavirus. *Virology*, 497, pp.346–356. Available at: http://dx.doi.org/10.1016/j.virol.2016.07.028.

Horvath, C. a J. et al., 2010. Mechanisms of cell entry by human papillomaviruses: an overview. *Virology journal*, 7, p.11. Available at: http://www.pubmedcentral.nih.gov/articlerender.fcgi?artid=2823669&tool=pmcentrez&rendertype=abstract.

Hynes, R.O., 2002. Integrins : Bidirectional , Allosteric Signaling Machines In their roles as major adhesion receptors , integrins. *Cell*, 110(Table 1), pp.673–687.

Ilić, D. et al., 1995. Reduced cell motility and enhanced focal adhesion contact formation in cells from FAK-deficient mice. *Nature*, 377(6549), pp.539–544.

Jiang, M. et al., 2009. The role of polyomaviruses in Human disease. *Virology*, 384(2), pp.266–273.

Jones, R.A. & Shusta, V.E., 2007. Blood-brain barrier transport of therapeutics cia receptor-mediation. *Pharm Res.*, 24(9), pp.1759–1771.

Kaucic, K., Liu, Y. & Ladisch, S., 2006. Modulation of growth factor signaling by gangliosides : positive or negative? *Methods in Enzymology*, 417(6), pp.168–185.

Kean, J.M. et al., 2009. Seroepidemiology of human polyomaviruses. *PLoS pathogens*, 5(3), p.e1000363.

Khan, Z.M. et al., 2014. Crystallographic and glycan microarray analysis of Human Polyomavirus 9 VP1 identifies N-Glycolyl Neuraminic Acid as a receptor candidate. *Journal of Virology*, 88(11), pp.6100–6111.

Komoriyas, A. et al., 1991. The minimal essential sequence for a major cell type-specific adhesion site (CS1) within the alternatively spliced type I11 connecting segment domain of fibronectin is Leucine-Aspartic Acid- Valine. *The Journal of Biological Chemistry*, 266(23), pp.15075–15079.

Legate, K.R., Wickstrom, S.A. & Fassler, R., 2009. Genetic and cell biological analysis of integrin outside-in signaling. *Genes & Development*, 23(4), pp.397–418. Available at: http://genesdev.cshlp.org/cgi/doi/10.1101/gad.1758709 [Accessed October 25, 2012].

Li, R. et al., 2000. Cellular gangliosides promote growth factor-induced proliferation of fibroblasts. *The Journal of biological chemistry*, 275(44), pp.34213–23. Available at: http://www.ncbi.nlm.nih.gov/pubmed/10859325 [Accessed November 4, 2012].

Liebl, D. et al., 2006. Mouse polyomavirus enters early endosomes, requires their acidic pH for productive infection, and meets transferrin cargo in Rab11-positive endosomes. *Journal of virology*, 80(9), pp.4610–4622.

Lilley, B.N. et al., 2006. Murine polyomavirus requires the endoplasmic reticulum protein Derlin-2 to initiate infection. *Journal of virology*, 80(17), pp.8739–8744.

Liu, Y., Li, R. & Ladisch, S., 2004. Exogenous ganglioside GD1a enhances epidermal growth factor receptor binding and dimerization. *The Journal of biological chemistry*, 279(35), pp.36481–9. Available at: http://www.ncbi.nlm.nih.gov/pubmed/15215248 [Accessed October 8, 2012].

Liu, Z. et al., 2012. Transient activation of the PI3K-AKT pathway by HCV to enhance viral entry. *Journal of Biological Chemistry*, 287(50), pp.41922–41930.

Low, J.A. et al., 2006. Identification of Gangliosides GD1b and GT1b as Receptors for BK Virus. *Journal of Virology*, 80(3), pp.1361–1366.

Luo, Y. et al., 2016. Interaction between Simian Virus 40 Major Capsid Protein VP1 and Cell Surface Ganglioside GM1 Triggers Vacuole Formation. *mBio*, 7(2), pp.e00297-16. Available at: http://mbio.asm.org/lookup/doi/10.1128/mBio.00297-16.

Maccioni, H.J., Daniotti, J.L. & Martina, J. a, 1999. Organization of ganglioside synthesis in the Golgi apparatus. *Biochimica et biophysica acta*, 1437(2), pp.101–18. Available at: http://www.ncbi.nlm.nih.gov/pubmed/10064894.

Maginnis, M.S. et al., 2013. Progressive Multifocal Leukoencephalopathy-Associated Mutations in the JC Polyomavirus Capsid Disrupt Lactoseries Tetrasaccharide c Binding. *mBio*, 4(3).

Maginnis, M.S. & Atwood, W.J., 2010. JCV: AN ONCOGENIC VIRUS IN ANIMALS AND HUMANS. , 19(4), pp.261–269.

Mannová, P. & Forstová, J., 2003. Mouse polyomavirus utilizes recycling endosomes for a traffic pathway independent of COPI vesicle transport. *Journal of virology*, 77(3), pp.1672–1681.

Meili, R. et al., 1998. Protein kinase B/Akt is activated by polyomavirus middle-T antigen via a phosphatidylinositol 3-kinase-dependent mechanism. *Oncogene*, 16(7), pp.903–7. Available at: http://www.ncbi.nlm.nih.gov/pubmed/9484781.

Meyer, M.A., 2013. Amino Acid Sequences Mediating Vascular Cell Adhesion Molecule 1 Binding to Integrin Alpha 4: Homologous DSP Sequence Found for JC Polyoma VP1 Coat Protein. *Neurology international*, 5(3), p.e14. Available at: http://www.pubmedcentral.nih.gov/articlerender.fcgi?artid=3794449&tool=pmcentrez&rendertype=abstract [Accessed December 5, 2013].

Miyamoto, S. et al., 1996. Integrins can collaborate with growth factors for phosphorylation of receptor tyrosine kinases and MAP kinase activation: roles of integrin aggregation and occupancy of receptors. *The Journal of cell biology*, 135(6 Pt 1), pp.1633–42. Available at: http://www.pubmedcentral.nih.gov/articlerender.fcgi?artid=2133938&tool=pmcentrez&rendertype=abstract.

Moro, L. et al., 2002. Integrin-induced epidermal growth factor (EGF) receptor activation requires c-Src and p130Cas and leads to phosphorylation of specific EGF receptor tyrosines. *The Journal of biological chemistry*, 277(11), pp.9405–14. Available at: http://www.ncbi.nlm.nih.gov/pubmed/11756413 [Accessed November 8, 2012].

Moro, L. et al., 1998. Integrins induce activation of EGF receptor: role in MAP kinase induction and adhesion-dependent cell survival. *The EMBO journal*, 17(22), pp.6622–32. Available at: http://www.pubmedcentral.nih.gov/articlerender.fcgi?artid=1171008&tool=pmcentrez&rendertype=abstract.

Neu, U., Allen, S.-A. a, et al., 2013. A Structure-Guided Mutation in the Major Capsid Protein Retargets BK Polyomavirus. *PLoS pathogens*, 9(10), p.e1003688. Available at: http://www.pubmedcentral.nih.gov/articlerender.fcgi?artid=3795024&tool=pmcentrez&rendertype=abstract [Accessed November 11, 2013].

Neu, U. et al., 2008. Structural basis of GM1 ganglioside recognition by simian virus 40. *Proceedings of the National Academy of Sciences of the United States of America*, 105(13), pp.5219–24. Available at: http://www.pubmedcentral.nih.gov/articlerender.fcgi?artid=2278218&tool=pmcentrez&rendertype=abstract.

Neu, U. et al., 2010. Structure-function analysis of the human JC polyomavirus establishes the LSTc pentasaccharide as a functional receptor motif. *Cell host & microbe*, 8(4), pp.309–19. Available at: http://www.pubmedcentral.nih.gov/articlerender.fcgi?artid=2957469&tool=pmcentrez&rendertype=abstract [Accessed December 4, 2013].

Neu, U., Khan, Z.M., et al., 2013. Structures of B-Lymphotropic Polyomavirus VP1 in complex with oligosaccharide ligands. *PLoS pathogens*, 9(10), p.e1003714. Available at: http://www.pubmedcentral.nih.gov/articlerender.fcgi?artid=3814675&tool=pmcentrez&rendertype=abstract [Accessed December 5, 2013].

Neu, U. et al., 2012. Structures of Merkel cell polyomavirus VP1 complexes define a

sialic acid binding site required for infection. *PLoS pathogens*, 8(7), p.e1002738. Available at: http://www.pubmedcentral.nih.gov/articlerender.fcgi?artid=3406085&tool=pmcentrez&rendertype=abstract [Accessed December 5, 2013].

Neu, U. et al., 2011. Structures of the major capsid proteins of the human Karolinska Institutet and Washington University polyomaviruses. *Journal of virology*, 85(14), pp.7384–92. Available at: http://www.pubmedcentral.nih.gov/articlerender.fcgi?artid=3126572&tool=pmcentrez&rendertype=abstract [Accessed January 10, 2014].

O'Hara, S.D., Stehle, T. & Garcea, R.L., 2014. Glycan receptors of the Polyomaviridae: structure, function, and pathogenesis. *Current opinion in virology*, 7, pp.73–78. Available at: http://dx.doi.org/10.1016/j.coviro.2014.05.004\nfile:///Users/geogheganem/Library/Application Support/Papers2/Articles/2014/O?Hara/Curr Opin Virol 2014 O?Hara.pdf\npapers2://publication/doi/10.1016/j.coviro.2014.05.004\nhttp://www.sciencedirect.com/scienc.

Oyelaran, O. & Gildersleeve, J., 2009. Glycan Arrays: Recent Advances and Future Challenges. *Current Opinion in Chemical Biology*, 13(4), pp.406–413.

Pastrana, D. V et al., 2013. BK polyomavirus genotypes represent distinct serotypes with distinct entry tropism. *Journal of virology*, 87(18), pp.10105–13. Available at: http://www.ncbi.nlm.nih.gov/pubmed/23843634 [Accessed January 8, 2014].

Pastrana, D. V et al., 2012. Neutralization serotyping of BK polyomavirus infection in kidney transplant recipients. *PLoS pathogens*, 8(4), p.e1002650. Available at: http://www.pubmedcentral.nih.gov/articlerender.fcgi?artid=3325208&tool=pmcentrez&rendertype=abstract [Accessed January 27, 2014].

Pho, M.T., Ashok, a & Atwood, W.J., 2000. JC virus enters human glial cells by clathrin-dependent receptor-mediated endocytosis. *Journal of virology*, 74(5), pp.2288–2292.

Del Pozo, M.A., 2004. Integrin signaling and lipid rafts. *Cell Cycle*, 3(6), pp.725–728. Available at: http://www.ncbi.nlm.nih.gov/pubmed/15197344\nhttps://www.landesbioscience.com/journals/cc/delpozoCC3-6.pdf.

Qian, M. et al., 2009. A lipid receptor sorts polyomavirus from the endolysosome to the endoplasmic reticulum to cause infection. *PLoS Pathogens*, 5(6), p.e1000465.

Qian, M. & Tsai, B., 2010. Lipids and proteins act in opposing manners to regulate polyomavirus infection. *Journal of virology*, 84(19), pp.9840–52. Available at: http://www.pubmedcentral.nih.gov/articlerender.fcgi?artid=2937789&tool=pmcentrez&rendertype=abstract [Accessed November 8, 2012].

Querbes, W. et al., 2004. A JC virus-induced signal is required for infection of glial cells

by a clathrin- and eps15-dependent pathway. *Journal of virology*, 78(1), pp.250–256.

Reid, C.E. et al., 2011. Sequencing and analysis of JC virus DNA from natalizumab-treated PML patients. *The Journal of infectious diseases*, 204(2), pp.237–44. Available at: http://www.pubmedcentral.nih.gov/articlerender.fcgi?artid=3114470&tool=pmcentrez&rendertype=abstract [Accessed December 5, 2013].

Saeed, M.F. et al., 2008. Phosphoinositide-3 kinase-akt pathway controls cellular entry of ebola virus. *PLoS Pathogens*, 4(8), p.e1000141.

Saito, M. & Sugiyama, K., 2001. Gangliosides in rat kidney: composition, distribution, and developmental changes. *Archives of biochemistry and biophysics*, 386(1), pp.11–6. Available at: http://www.ncbi.nlm.nih.gov/pubmed/11360994 [Accessed January 11, 2014].

Schaller, M.D., 2010. Cellular functions of FAK kinases: insight into molecular mechanisms and novel functions. *Journal of cell science*, 123(Pt 7), pp.1007–1013.

Schelhaas, M. et al., 2007. Simian Virus 40 depends on ER protein folding and quality control factors for entry into host cells. *Cell*, 131(3), pp.516–29. Available at: http://www.ncbi.nlm.nih.gov/pubmed/17981119 [Accessed July 23, 2012].

Schowalter, R.M., Pastrana, D. V & Buck, C.B., 2011. Glycosaminoglycans and sialylated glycans sequentially facilitate Merkel cell polyomavirus infectious entry. *PLoS pathogens*, 7(7), p.e1002161. Available at: http://www.pubmedcentral.nih.gov/articlerender.fcgi?artid=3145800&tool=pmcentrez&rendertype=abstract [Accessed January 10, 2014].

Schwab, N., Schneider-Hohendorf, T. & Wiendl, H., 2014. Therapeutic uses of anti-α4-integrin (anti-VLA-4) antibodies in multiple sclerosis. *International immunology*, 1, pp.1–7. Available at: http://www.ncbi.nlm.nih.gov/pubmed/25326459 [Accessed November 25, 2014].

Sieg, D.J. et al., 1998. Pyk2 and Src-family protein-tyrosine kinases compensate for the loss of FAK in fibronectin-stimulated signaling events but Pyk2 does not fully function to enhance FAK- cell migration. *EMBO Journal*, 17(20), pp.5933–5947.

Srichai, M.B. & Zent, R., 2010. Integrin Structure and Function. In *Cell-Extracellular Matrix Interactions in Cancer*. pp. 19–41.

Stehle, T. et al., 1994. Structure of murine polyomavirus complexed with oligosaccharide receptor fragment. *Nature*, 369, pp.160–163.

Stehle, T. & Harrison, S.C., 1996. Crystal structures of murine polyomavirus in complex with straight-chain and branched-chain sialyloligosaccharide receptor fragments. *Structure*, 4, pp.183–194.

Stehle, T. & Harrison, S.C., 1997. High-resolution structure of a polyomavirus VP1-

oligosaccharide complex: implications for assembly and receptor binding. *The EMBO journal*, 16(16), pp.5139–48. Available at: http://www.pubmedcentral.nih.gov/articlerender.fcgi?artid=1170147&tool=pmcentrez&rendertype=abstract.

Stergiou, L. et al., 2013. Integrin-Mediated Signaling Induced by Simian Virus 40 Leads to Transient Uncoupling of Cortical Actin and the Plasma Membrane. *PLoS ONE*, 8(2), p.e55799.

Swimm, A.I. et al., 2010. Abl family tyrosine kinases regulate sialylated ganglioside receptors for polyomavirus. *Journal of virology*, 84(9), pp.4243–51. Available at: http://www.pubmedcentral.nih.gov/articlerender.fcgi?artid=2863717&tool=pmcentrez&rendertype=abstract [Accessed July 30, 2012].

Szklarczyk, O.M. et al., 2013. Receptor concentration and diffusivity control multivalent binding of Sv40 to membrane bilayers. *PLoS computational biology*, 9(11), p.e1003310. Available at: http://www.pubmedcentral.nih.gov/articlerender.fcgi?artid=3828148&tool=pmcentrez&rendertype=abstract [Accessed January 9, 2014].

Tai, Y.-L., Chen, L.-C. & Shen, T.-L., 2015. Emerging roles of focal adhesion kinase in cancer. *BioMed research international*, 2015, p.690690. Available at: http://apps.webofknowledge.com.proxy.library.cornell.edu/full_record.do?product=UA&search_mode=GeneralSearch&qid=1&SID=2CLUzMiGCzMnkMsBrqx&page=1&doc=2.

Taube, S., Jiang, M. & Wobus, C.E., 2010. Glycosphingolipids as receptors for non-enveloped viruses. *Viruses*, 2(4), pp.1011–49. Available at: http://www.pubmedcentral.nih.gov/articlerender.fcgi?artid=3185660&tool=pmcentrez&rendertype=abstract [Accessed October 6, 2012].

Tsai, B. et al., 2003. Gangliosides are receptors for murine polyoma virus and SV40. *The EMBO journal*, 22(17), pp.4346–55. Available at: http://www.pubmedcentral.nih.gov/articlerender.fcgi?artid=202381&tool=pmcentrez&rendertype=abstract.

Uettwiller, F., Rigal, E. & Hoarau, C., 2011. Infections associated with monoclonal antibody and fusion protein therapy in humans. *mAbs*, 3(5), pp.461–466.

Vallefuoco, L. et al., 2014. JC virus antibody index in natalizumab-treated patients : correlations with John Cunningham virus DNA and C-reactive protein level. , pp.807–814.

Varki, A., 2001. Loss of N-Glycolylneuraminic Acid in Humans : Mechanisms , Consequences , and Implications for Hominid Evolution. , 69, pp.54–69.

Velupillai, P. et al., 2012. Polymorphisms in toll-like receptor 4 underlie susceptibility to tumor induction by the mouse polyomavirus. *Journal of virology*, 86(21), pp.11541–7. Available at:

http://www.pubmedcentral.nih.gov/articlerender.fcgi?artid=3486304&tool=pmcentrez&rendertype=abstract.

Walczak, C.P. et al., 2014. A Cytosolic Chaperone Complexes with Dynamic Membrane J-Proteins and Mobilizes a Nonenveloped Virus out of the Endoplasmic Reticulum. *PLoS Pathogens*, 10(3).

Xia, H. et al., 2004. Focal adhesion kinase is upstream of phosphatidylinositol 3-kinase/Akt in regulating fibroblast survival in response to contraction of type I collagen matrices via a beta-1 integrin viability signaling pathway. *Journal of Biological Chemistry*, 279(31), pp.33024–33034.

Yates, A.J., Saqr, H.E. & Van Brocklyn, J., 1995. Ganglioside modulation of the PDGF receptor. *Journal of neuro-oncology*, 24(1), pp.65–73. Available at: http://www.ncbi.nlm.nih.gov/pubmed/8523078.

You & O'Hara, S.D. et al., 2015. Ganglioside and non-ganglioside mediated host responses to the Mouse Polyomavirus. *PLOS Pathogens*, 11(10), p.e1005175. Available at: http://dx.plos.org/10.1371/journal.ppat.1005175.

Zhou, Y. & Simmons, G., 2012. Development of novel entry inhibitors targeting emerging viruses. *Expert review of anti-infective therapy*, 10(10), pp.1129–38. Available at: http://informahealthcare.com/doi/abs/10.1586/eri.12.104#.VXFrEIg7M4c.mendeley.

Zila, V. et al., 2014. Involvement of microtubular network and its motors in productive endocytic trafficking of mouse polyomavirus. *PLoS ONE*, 9(5), p.e96922.

Zullo, J., Stiles, C.D. & Garcea, R.L., 1987. Regulation of c-myc and c-fos mRNA levels by polyomavirus: distinct roles for the capsid protein VP1 and the viral early proteins. *Proceedings of the National Academy of Sciences of the United States of America*, 84(5), pp.1210–4. Available at: http://www.pubmedcentral.nih.gov/articlerender.fcgi?artid=304396&tool=pmcentrez&rendertype=abstract.

Appendix I: VP1 Purification from Mammalian Cells

Recombinant MuPyV VP1 pentamers have traditionally been purified from *E.coli*. This system is robust, producing high levels of VP1 at low cost. However, VP1 pentamers produced in *E.coli* are coated with endotoxin (lipopolysaccharide, LPS) and are not suitable for all research purposes. Many endotoxin removal methods are commercially available; however, none of these methods reliably separate endotoxin from VP1. Thus, a new purification system was necessary. Mammalian protein purification systems can produce large quantities of protein without endotoxin contamination. We generated a construct that expressed VP1 linked to a glutathione transferase (GST) though a thrombin cleavage site (Figure A.1B). A diagram of the protein purification process is shown in Figure A.1A. The plasmid contains a SV40 origin of replication (VP1-GST FL pwP) and upon transfections into 293TT cells, which contain 2 copies of SV40 T-ag, leads to high levels of plasmid replication and protein expression. Two transfection reagents were tested: Lipofectamine 2000 (LIPO2000) and polyethylenimine (PEI). Cells were collected 72 h post transfection and frozen at -80° C until cell lysis. Cells are lysed in a TRIS buffer solution (Buffer L) containing 5mM DTT to prevent protein aggregation and 0.1% Triton-X 100 to permeabilize cell membranes. Cells were homogenized in a dounce homogenizer to further break up cells followed by sonication to shear DNA. Cell debris was then pelleted and the supernatant containing the cellular proteins and VP1 (WCL, Figure A.1C) were incubated with glutathione sepharose beads overnight. The VP1-GST will bind the glutathione beads while cellular proteins will remain in suspension. 24 h after addition, the cellular proteins are eluted and the VP1-GST/beads complexes are washed with Buffer L containing 5 mM DTT. Thrombin is then added to the beads to cleave the

thrombin site linking VP1 to GST and incubated for 2 h at room temperature. The cleaved VP1 pentamers are then eluted (Figure A.1D). Pentamers produced show a characteristic 5-point donut shape when imaged by EM (Figure A.1E). This system produced high levels of pure endotoxin free VP1, approximately 2 mg / 182 cM dish with LIPO2000 transfection reagent (Figure A1.1E). PEI transfection, a much cheaper reagent than LIPO2000, can also be used; however, produces 75% less than LIPO2000.

Figure A1.1: VP1 Purification from 293TTs

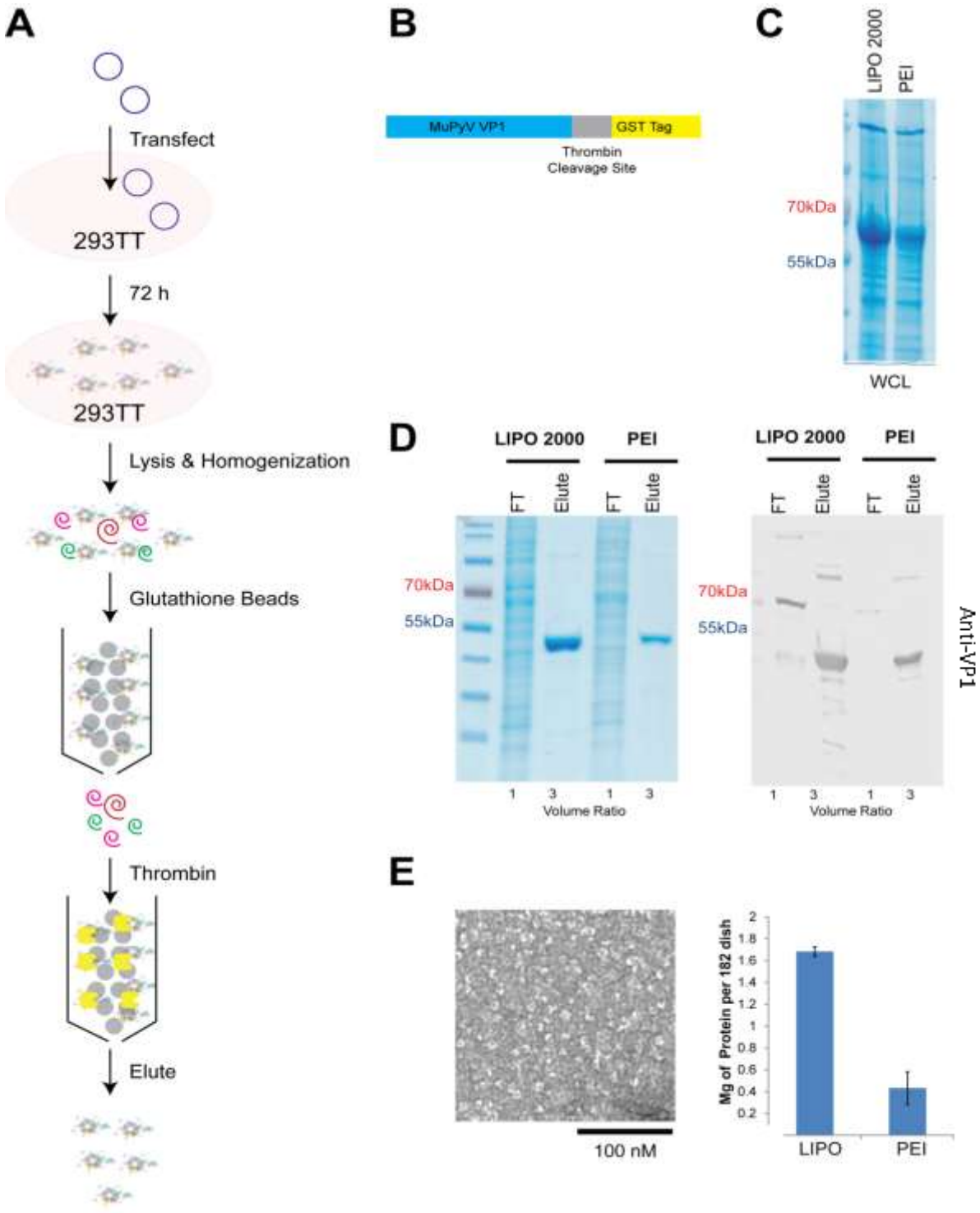

Protocol:

1. **Plate Dishes**
    a. Calculate number of dishes desired. 182cM will produce approximately 2mg of purified protein.
    b. Prior to counting 293TT cells, transfer cells though cell filter to remove clumps of cells, this will increase transfection levels by increasing exposed membrane edges.
    c. Plate 17.5 million 293TTs per 182cM dish 24 h prior to transfection
2. **Transfect with VP1-GST pwP**

Per 182cM Dish
17.5 Million 293TTs
60ug DNA
200uL Lipofectamine 2000
4mL OPTI MEM

    a. Incubate 60 µg of DNA with 2mL of OPTI MEM at RT for 10min
    b. Incubate 200 µL Lipofectamine 2000 with 2mL of OPTI MEM at RT for 10min
    c. Mix DNA and Lipofectamine solution together and incubate at RT for 10min
    d. Add DNA/LIPO solutions to 182 cM dish
    e. Incubate DNA/LIPO with cells overnight (12 h)
    f. Change media and incubate for additional 72 h
3. **Harvest Cells**
    a. Cells can usually be displaced from plate by agitating the plate. If this is not sufficient use a scraper to collect the cells and place in conical tube. Wash the plate with PBS to collect any additional cells.
    b. Pellet cells at 500xG for 10min at RT
    c. Remove media and place cells in -80°C until lysis
4. **Cell Lysis and Homogenization**
    a. Resuspend cells in 5mL of cold Buffer L with 5mM DTT and 0.1% TX-100 and 1x protease inhibitor
        i. Buffer L: 2M TRIS, pH 7.5, 5M NaCl, 0.5M EDTA, 5% Glycerol
    b. Transfer cell solution to cold dounce homogenizer
    c. Dounce 15-20 times while keeping cool
    d. Transfer lysate to conical tube for sonication
    e. Sonicate at 3 times at 30% Amp for 15 s and 15 s off
    f. Pellet cell debris at max speed for 15 min in table top centrifuge and reserve supernatant
5. **Glutathione Beads**

a. Wash glutathione sepharose beads in ddH2O and Buffer L /5mM DTT
b. Mix supernatant with washed glutathione sepharose beads and incubate overnight
    i. 182cM dish with 1.5mL of 80% beads
c. Elute non-bound proteins, collect 50uL of Flow Though for SDS page
d. Wash beads with Buffer L/5mM DTT - 3 column volumes
e. Add 25U of Thrombin to beads in Buffer L/DTT in one column volume and incubate for 2 h at RT
f. Elute VP1 with a 1mL wash of Buffer L/DTT
g. Run SDS-PAGE and Immunoblot to check for VP1 purity
h. Run Bradford assay to determine VP1 concentration

Appendix II : Plasmids Generated

RApwP

Plasmid containing mouse polyomavirus (strain RA) VP1. This plasmid was generated by site directed mutagenesis of three nucleotides (C3593T A3594C T2979A) of pwP (strain LID) (addgene #22519) resulting in two amino acids changes A296V and E91G. This plamsid is used in combination with ph2p (addgene #22520) and ph3p (addgene # 22521) to generate pseudovirus in 293TT cells.

Figure A2.1: RApwP

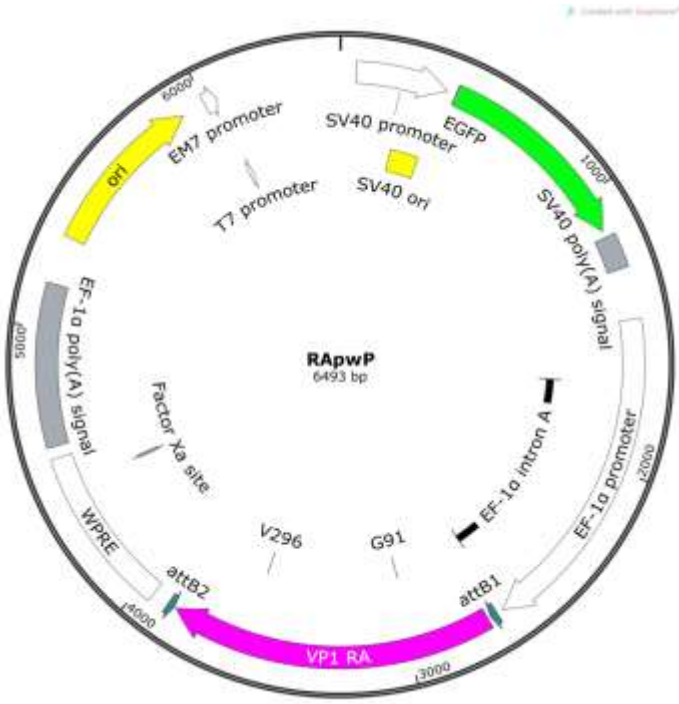

Sequence:

CCCTGCAGGGCCTGAAATAACCTCTGAAAGAGGAACTTGGTTAGGTACCTGTGGAATGTGTGTCAGTTAGGGTGTGGAAAGTC
CCCAGGCTCCCCAGCAGGCAGAAGTATGCAAAGCATGCATCTCAATTAGTCAGCAACCAGGTGTGGAAAGTCCCCAGGCTCCC
CAGCAGGCAGAAGTATGCAAAGCATGCATCTCAATTAGTCAGCAACCATAGTCCCGCCCCTAACTCCGCCCATCCCGCCCCTA
ACTCCGCCCAGTTCCGCCCATTCTCCGCCCCATGGCTGACTAATTTTTTTTATTTATACAGAGGCCGAGGCCGCCTCGGCCTCT
GAGCTATTCCAGAAGTAGTGAGGAGGCTTTTTTGGAGGCCTAGGCTTTTGCAAAAAGCTTGATTGGGATCCACCGGTCGCCAC
CATGGTGAGCAAGGGCGAGGAGCTGTTCACCGGGGTGGTGCCCATCCTGGTCGAGCTGGACGGCGACGTAAACGGCCACAA
GTTCAGCGTGTCCGGCGAGGGCGAGGGCGATGCCACCTACGGCAAGCTGACCCTGAAGTTCATCTGCACCACCGGCAAGCTG
CCCGTGCCCTGGCCCACCCTCGTGACCACCCTGACCTACGGCGTGCAGTGCTTCAGCCGCTACCCCGACCACATGAAGCAGC
ACGACTTCTTCAAGTCCGCCATGCCCGAAGGCTACGTCCAGGAGCGCACCATCTTCTTCAAGGACGACGGCAACTACAAGACC
CGCGCCGAGGTGAAGTTCGAGGGCGACACCCTGGTGAACCGCATCGAGCTGAAGGGCATCGACTTCAAGGAGGACGGCAAC
ATCCTGGGGCACAAGCTGGAGTACAACTACAACAGCCACAACGTCTATATCATGGCCGACAAGCAGAAGAACGGCATCAAGGT

GAACTTCAAGATCCGCCACAACATCGAGGACGGCAGCGTGCAGCTCGCCGACCACTACCAGCAGAACACCCCCATCGGCGAC
GGCCCCGTGCTGCTGCCCGACAACCACTACCTGAGCACCCAGTCCGCCCTGAGCAAAGACCCCAACGAGAAGCGCGATCACA
TGGTCCTGCTGGAGTTCGTGACCGCCGCCGGGATCACTCTCGGCATGGACGAGCTGTACAAGTAAAGCGGCCGCTTCGAGCA
GACATGATAAGATACATTGATGAGTTTGGACAAACCACAACTAGAATGCAGTGAAAAAAATGCTTTATTTGTGAAATTTGTGATG
CTATTGCTTTATTTGTAACCATTATAAGCTGCAATAAACAAGTTAACAACAACAATTGCATTCATTTTATGTTTCAGGTTCAGGGG
GAGGTGTGGGAGGTTTTTTAAAGCAAGTAAAACCTCTACAAATGTGGTAAAATCGATAAGGATCCGGGCTGGCGTAATAGCGAA
GAGGCCCGCACCGATCGCCCTTCCCAACAGTTGCGGTGGAGAAGAGCATGCGTGAGGCTCCGGTGCCCGTCAGTGGGCAGA
GCGCACATCGCCCACAGTCCCCGAGAAGTTGGGGGGGAGGGGTCGGCAATTGAACCGGTGCCTAGAGAAGGTGGCGCGGGGT
AAACTGGGAAAGTGATGTCGTGTACTGGCTCCGCCCTTTTCCCGAGGGTGGGGGAGAACCGTATATAAGTGCAGTAGTCGCTG
TGAACGTTCTTTTTCGCAACGGGTTTGCCGCCAGAACACAGGTAAGTGCCGTGTGTGGTTCCCGCGGGCCTGGCCTCTTTACG
GGTTATGGCCCTTGCGTGCCTTGAATTACTTCCACCTGGCTGCAGTACGTGATTCTTGATCCCGAGCTTCGGGTTGGAAGTGG
GTGGGAGAGTTCGAGGCCTTGCGCTTAAGGAGCCCCTTCGCCTCGTGCTTGAGTTGAGGCCTGGCCTGGGCGCTGGGGCCG
CCGCGTGCGAATCTGGTGGCACCTTCGCGCCTGTCTCGCTGCTTTCGATAAGTCTCTAGCCATTTAAAATTTTTGATGACCTGC
TGCGACGCTTTTTTTCTGGCAAGATAGTCTTGTAAATGCGGGCCAAGATCTGCACACTGGTATTTCGGTTTTTGGGGCCGCGGG
CGGCGACGGGGCCCGTGCGTCCCAGCGCACATGTTCGGCGAGGCGGGGCCTGCGAGCGCGGCCACCGAGAATCGGACGGG
GGTAGTCTCAAGCTGGCCGGCCTGCTCTGGTGCCTGGCCTCGCGCCGCCGTGTATCGCCCCGCCCTGGGCGGCAAGGCTGG
CCCGGTCGGCACCAGTTGCGTGAGCGGAAAGATGGCCGCTTCCCGGCCCTGCTGCAGGGAGCTCAAAATGGAGGACGCGGC
GCTCGGGAGAGCGGGCGGGTGAGTCACCCACACAAAGGAAAAGGGCCTTTCCGTCCTCAGCCGTCGCTTCATGTGACTCCAC
GGAGTACCGGGCGCCGTCCAGGCACCTCGATTAGTTCTCGAGCTTTTGGAGTACGTCGTCTTTAGGTTGGGGGGAGGGGTTTT
ATGCGATGGAGTTTCCCCACACTGAGTGGGTGGAGACTGAAGTTAGGCCAGCTTGGCACTTGATGTAATTCTCCTTGGAATTTG
CCCTTTTTGAGTTTGGATCTTGGTTCATTCTCAAGCCTCAGACAGTGGTTCAAAGTTTTTTTCTTCCATTTCAGGTGTCGTGAGGA
ATTCTCTAGAGCTTGATCAAACAAGTTTGTACAAAAAAGCAGGCTTCCGGAACCACCATGGCACCAAAGCGCAAGTCAGGGGTC
AGCAAATGTGAAACCAAGTGCACCAAGGCATGCCCCCGCCCTGCACCCGTCCCAAAGCTCTTGATCAAGGGCGGCATGGAAG
TCCTCGATCTGGTCACCGGCCCCGATTCCGTCACCGAGATCGAGGCATTCCTGAATCCACGCATGGGCCAACCCCCAACACCC
GAGTCACTGACCGAAGGCGGCCAGTATTACGGCTGGAGCCGCGGCATCAACCTCGCCACCAGCGACACCGAAGACAGTCCCG
GAAACAACACCTTGCCAACCTGGTCCATGGCCAAACTGCAACTGCCAATGCTGAACGAAGATCTGACATGCGATACATTGCAAA
TGTGGGAAGCCGTCAGCGTCAAGACAGAAGTCGTCGGGAGCGGGAGCCTGCTCGATGTCCACGGCTTCAACAAGCCAACCGA
CACCGTGAACACCAAGGGCATCAGTACCCCGGTTGAGGGGTCACAGTACCACGTCTTCGCCGTCGGGGGCGAGCCCCTGGAT
CTGCAAGGCTTGGTCACCGACGCACGCACCAAGTTCAAAGAGGAGGGCGTGGTCACCATCAAGACCATTACCAAGAAGGACAT
GGTCAACAAGGATCAGGTGCTCAACCCCATCTCAAAAGCAAAGCTCGACAAGGATGGCATGTACCCCGTCGAGATTTGGCACC
CCGACCCCGCCAAGAACGAAAACACCCGCTACTTCGGGAACTATACCGGCGGGACCACCACCCCACCGGTGCTCCAATTCAC
CAATACACTCACCACCGTCCTGCTGGACGAGAACGGCGTCGGCCCACTGTGCAAGGGCGAAGGGTTGTATCTGAGTTGCGTG
GACATCATGGGGTGGCGCGTCACCCGCAACTACGACGTCCACCATTGGCGCGGCCTGCCACGCTACTTCAAGATTACACTCC
GCAAGCGCTGGGTCAAGAACCCATACCCAATGGCAAGTCTGATCTCGAGTCTGTTCAACAATATGTTGCCACAAGTCCAGGGG
CAGCCAATGGAGGGCGAAAACACACAAGTGGAAGAAGTCCGCGTCTACGACGGCACCGAGCCCGTGCCCGGCGATCCCGAC
ATGACCAGATACGTCGATAGGTTCGGCAAGACCAAAACCGTGTTCCCAGGAAACTGAGCCTAGGACCCAGCTTTCTTGTACAAA
GTGGTTCGATCTAGAATGGCTAGTGGATCCCCCGGGCTGCAGGAATTCGATATCAAGCTTATCGATAATCAACCTCTGGATTAC
AAAATTTGTGAAAGATTGACTGGTATTCTTAACTATGTTGCTCCTTTTACGCTATGTGGATACGCTGCTTTAATGCCTTTGTATCA
TGCTATTGCTTCCCGTATGGCTTTCATTTTCTCCTCCTTGTATAAATCCTGGTTGCTGTCTCTTTATGAGGAGTTGTGGCCCGTTG
TCAGGCAACGTGGCGTGGTGTGCACTGTGTTTGCTGACGCAACCCCCACTGGTTGGGGCATTGCCACCACCTGTCAGCTCCTT
TCCGGGACTTTCGCTTTCCCCCTCCCTATTGCCACGGCGGAACTCATCGCCGCCTGCCTTGCCCGCTGCTGGACAGGGGCTC
GGCTGTTGGGCACTGACAATTCCGTGGTGTTGTCGGGGAAATCATCGTCCTTTCCTTGGCTGCTCGCCTGTGTTGCCACCTGG
ATTCTGCGCGGGACGTCCTTCTGCTACGTCCCTTCGGCCCTCAATCCAGCGGACCTTCCTTCCCGCGGCCTGCTGCCGGCTCT
GCGGCCTCTTCCGCGTCTTCGCCTTCGCCCTCAGACGAGTCGGATCTCCCTTTGGGCCGCCTCCCCGCATCGATACCGTCGG
CCCACTGCTCCCTAAACCTGAGCTAGCATTATCCCTAATACCTGCCACCCCACTCTTAATCAGTGGTGGAAGAACGGTCTCAGA
ACTGTTTGTTTCAATTGGCCATTTAAGTTTAGTAGTAAAAGACTGGTTAATGATAACAATGCATCGTAAAACCTTCAGAAGGAAAG
GAGAATGTTTTGTGGACCACTTTGGTTTTCTTTTTTGCGTGTGGCAGTTTTAAGTTATTAGTTTTTAAAATCAGTACTTTTTAATGG
AAACAACTTGACCAAAAATTTGTCACAGAATTTTGAGACCCATTAAAAAAGTTAAATGAGAAACCTGTGTGTTCCTTTGGTCAACA
CCGAGACATTTAGGTGAAAGACATCTAATTCTGGTTTTACGAATCTGGAAACTTCTTGAAAATGTAATTCTTGAGTTAACACTTCT
GGGTGGAGAATAGGGTTGTTTTCCCCCCACATAATTGGAAGGGGAAGGAATATCATTTAAAGCTATGGGAGGGTTTCTTTGATT
ACAACACTGGAGAGAAATGCAGCATGTTGCTGATTGCCTGTCACTAAAACAGGCCAAAAACTGAGTCCTTGGGTTGCATAGAAA
GCTTCATGTTGCTAAACCAATGTTAAGTGAATCTTTGGAAACAAAATGTTTCCAAATTACTGGGATGTGCATGTTGAAACGTGGG
TTAATTAACTAGCCATGACCAAAATCCCTTAACGTGAGTTTTCGTTCCACTGAGCGTCAGACCCCGTAGAAAAGATCAAAGGATC
TTCTTGAGATCCTTTTTTTTCTGCGCGTAATCTGCTGCTTGCAAACAAAAAAACCACCGCTACCAGCGGTGGTTTGTTTGCCGGAT
CAAGAGCTACCAACTCTTTTTCCGAAGGTAACTGGCTTCAGCAGAGCGCAGATACCAAATACTGTTCTTCTAGTGTAGCCGTAG
TTAGGCCACCACTTCAAGAACTCTGTAGCACCGCCTACATACCTCGCTCTGCTAATCCTGTTACCAGTGGCTGCTGCCAGTGGC
GATAAGTCGTGTCTTACCGGGTTGGACTCAAGACGATAGTTACCGGATAAGGCGCAGCGGTCGGGCTGAACGGGGGGTTCGT
GCACACAGCCCAGCTTGGAGCGAACGACCTACACCGAACTGAGATACCTACAGCGTGAGCTATGAGAAAGCGCCACGCTTCC
CGAAGGGAGAAAGGCGGACAGGTATCCGGTAAGCGGCAGGGTCGGAACAGGAGAGCGCACGAGGGAGCTTCCAGGGGGAA
ACGCCTGGTATCTTTATAGTCCTGTCGGGTTTCGCCACCTCTGACTTGAGCGTCGATTTTTGTGATGCTCGTCAGGGGGGCGGA
GCCTATGGAAAAACGCCAGCAACGCGGCCTTTTTACGGTTCCTGGCCTTTTGCTGGCCTTTTGCTCACATGTTCTTAATTAAATT

TTTCAAAAGTAGTTGACAATTAATCATCGGCATAGTATATCGGCATAGTATAATACGACTCACTATAGGAGGGCCATCATGGCCA
AGTTGACCAGTGCTGTCCCAGTGCTCACAGCCAGGGATGTGGCTGGAGCTGTTGAGTTCTGGACTGACAGGTTGGGGTTCTCC
AGAGATTTTGTGGAGGATGACTTTGCAGGTGTGGTCAGAGATGATGTCACCCTGTTCATCTCAGCAGTCCAGGACCAGGTGGT
GCCTGACAACACCCTGGCTTGGGTGTGGGTGAGAGGACTGGATGAGCTGTATGCTGAGTGGAGTGAGGTGGTCTCCACCAAC
TTCAGGGATGCCAGTGGCCCTGCCATGACAGAGATTGGAGAGCAGCCCTGGGGGAGAGAGTTTGCCCTGAGAGACCCAGCAG
GCAACTGTGTGCACTTTGTGGCAGAGGAGCAGGACTGAGGATAAGAATTGTAACAAAAAACCCCGCCCCGGCGGGGTTTTTTG
TTAATTAA

LNVpwP

Plasmid containing mouse polyomavirus (strain RA) VP1 with point mutation abrograting the integrin binding site. This plasmid was generated by site directed mutagenesis at two nucleotides (G3115A and T3117C) of RApwP resulting in one amino acid change D138V. This plamsid is used in combination with ph2p (addgene #22520) and ph3p (addgene # 22521) to generate pseudovirus in 293TT cells.

Figure A2.2: LNVpwP

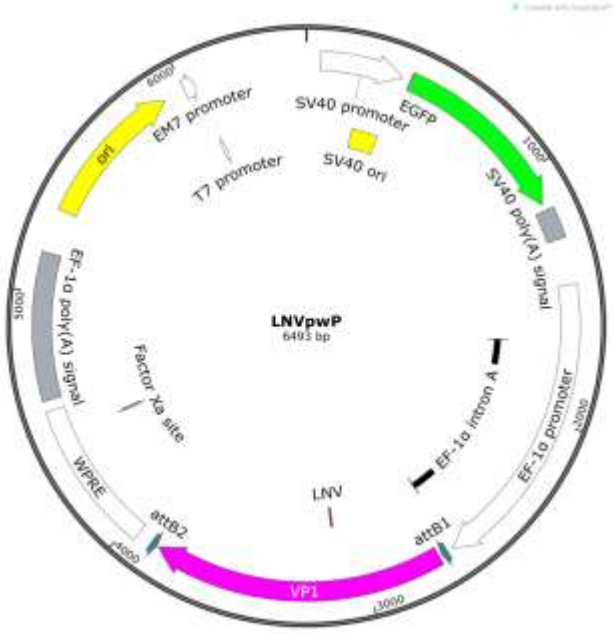

Sequence:

CCCTGCAGGGCCTGAAATAACCTCTGAAAGAGGAACTTGGTTAGGTACCTGTGGAATGTGTGTCAGTTAGGGTGTGGAAAGTC
CCCAGGCTCCCCAGCAGGCAGAAGTATGCAAAGCATGCATCTCAATTAGTCAGCAACCAGGTGTGGAAAGTCCCCAGGCTCCC
CAGCAGGCAGAAGTATGCAAAGCATGCATCTCAATTAGTCAGCAACCATAGTCCCGCCCCTAACTCCGCCCATCCCGCCCCTA
ACTCCGCCCAGTTCCGCCCATTCTCCGCCCCATGGCTGACTAATTTTTTTTATTTATACAGAGGCCGAGGCCGCCTCGGCCTCT
GAGCTATTCCAGAAGTAGTGAGGAGGCTTTTTTGGAGGCCTAGGCTTTTGCAAAAAGCTTGATTGGGATCCACCGGTCGCCAC
CATGGTGAGCAAGGGCGAGGAGCTGTTCACCGGGGTGGTGCCCATCCTGGTCGAGCTGGACGGCGACGTAAACGGCCACAA
GTTCAGCGTGTCCGGCGAGGGCGAGGGCGATGCCACCTACGGCAAGCTGACCCTGAAGTTCATCTGCACCACCGGCAAGCTG
CCCGTGCCCTGGCCCACCCTCGTGACCACCCTGACCTACGGCGTGCAGTGCTTCAGCCGCTACCCCGACCACATGAAGCAGC
ACGACTTCTTCAAGTCCGCCATGCCCGAAGGCTACGTCCAGGAGCGCACCATCTTCTTCAAGGACGACGGCAACTACAAGACC
CGCGCCGAGGTGAAGTTCGAGGGCGACACCCTGGTGAACCGCATCGAGCTGAAGGGCATCGACTTCAAGGAGGACGGCAAC
ATCCTGGGGCACAAGCTGGAGTACAACTACAACAGCCACAACGTCTATATCATGGCCGACAAGCAGAAGAACGGCATCAAGGT
GAACTTCAAGATCCGCCACAACATCGAGGACGGCAGCGTGCAGCTCGCCGACCACTACCAGCAGAACACCCCCATCGGCGAC
GGCCCCGTGCTGCTGCCCGACAACCACTACCTGAGCACCCAGTCCGCCCTGAGCAAAGACCCCAACGAGAAGCGCGATCACA

TGGTCCTGCTGGAGTTCGTGACCGCCGCCGGGATCACTCTCGGCATGGACGAGCTGTACAAGTAAAGCGGCCGCTTCGAGCA
GACATGATAAGATACATTGATGAGTTTGGACAAACCACAACTAGAATGCAGTGAAAAAAATGCTTTATTTGTGAAATTTGTGATG
CTATTGCTTTATTTGTAACCATTATAAGCTGCAATAAACAAGTTAACAACAACAATTGCATTCATTTTATGTTTCAGGTTCAGGGG
GAGGTGTGGGAGGTTTTTTAAAGCAAGTAAAACCTCTACAAATGTGGTAAAATCGATAAGGATCCGGGCTGGCGTAATAGCGAA
GAGGCCCGCACCGATCGCCCTTCCCAACAGTTGCGGTGGAGAAGAGCATGCGTGAGGCTCCGGTGCCCGTCAGTGGGCAGA
GCGCACATCGCCCACAGTCCCCGAGAAGTTGGGGGGGAGGGGTCGGCAATTGAACCGGTGCCTAGAGAAGGTGGCGCGGGGT
AAACTGGGAAAGTGATGTCGTGTACTGGCTCCGCCCTTTTCCCGAGGGTGGGGGAGAACCGTATATAAGTGCAGTAGTCGCTG
TGAACGTTCTTTTTCGCAACGGGTTTGCCGCCAGAACACAGGTAAGTGCCGTGTGTGGTTCCCGCGGGCCTGGCCTCTTTACG
GGTTATGGCCCTTGCGTGCCTTGAATTACTTCCACCTGGCTGCAGTACGTGATTCTTGATCCCGAGCTTCGGGTTGGAAGTGG
GTGGGAGAGTTCGAGGCCTTGCGCTTAAGGAGCCCCTTCGCCTCGTGCTTGAGTTGAGGCCTGGCCTGGGCGCTGGGGCCG
CCGCGTGCGAATCTGGTGGCACCTTCGCGCCTGTCTCGCTGCTTTCGATAAGTCTCTAGCCATTTAAAATTTTTGATGACCTGC
TGCGACGCTTTTTTTCTGGCAAGATAGTCTTGTAAATGCGGGCCAAGATCTGCACACTGGTATTTCGGTTTTTGGGGCCGCGGG
CGGCGACGGGGCCCGTGCGTCCCAGCGCACATGTTCGGCGAGGCGGGGCCTGCGAGCGCGGCCACCGAGAATCGGACGGG
GGTAGTCTCAAGCTGGCCGGCCTGCTCTGGTGCCTGGCCTCGCGCCGCCGTGTATCGCCCCGCCCTGGGCGGCAAGGCTGG
CCCGGTCGGCACCAGTTGCGTGAGCGGAAAGATGGCCGCTTCCCGGCCCTGCTGCAGGGAGCTCAAAATGGAGGACGCGGC
GCTCGGGAGAGCGGGCGGGTGAGTCACCCACACAAAGGAAAAGGGCCTTTCCGTCCTCAGCCGTCGCTTCATGTGACTCCAC
GGAGTACCGGGCGCCGTCCAGGCACCTCGATTAGTTCTCGAGCTTTTGGAGTACGTCGTCTTTAGGTTGGGGGGAGGGGTTTT
ATGCGATGGAGTTTCCCCACACTGAGTGGGTGGAGACTGAAGTTAGGCCAGCTTGGCACTTGATGTAATTCTCCTTGGAATTTG
CCCTTTTTGAGTTTGGATCTTGGTTCATTCTCAAGCCTCAGACAGTGGTTCAAAGTTTTTTTCTTCCATTTCAGGTGTCGTGAGGA
ATTCTCTAGAGCTTGATCAAACAAGTTTGTACAAAAAAGCAGGCTTCCGGAACCACCATGGCACCAAAGCGCAAGTCAGGGGTC
AGCAAATGTGAAACCAAGTGCACCAAGGCATGCCCCCGCCCTGCACCCGTCCCAAAGCTCTTGATCAAGGGCGGCATGGAAG
TCCTCGATCTGGTCACCGGCCCCGATTCCGTCACCGAGATCGAGGCATTCCTGAATCCACGCATGGGCCAACCCCCAACACCC
GAGTCACTGACCGAAGGCGGCCAGTATTACGGCTGGAGCCGCGGCATCAACCTCGCCACCAGCGACACCGAAGACAGTCCCG
GAAACAACACCTTGCCAACCTGGTCCATGGCCAAACTGCAACTGCCAATGCTGAACGAAGATCTGACATGCGATACATTGCAAA
TGTGGGAAGCCGTCAGCGTCAAGACAGAAGTCGTCGGGAGCGGGAGCCTGCTCAACGTCCACGGCTTCAACAAGCCAACCGA
CACCGTGAACACCAAGGGCATCAGTACCCCGGTTGAGGGGTCACAGTACCACGTCTTCGCCGTCGGGGGCGAGCCCCTGGAT
CTGCAAGGCTTGGTCACCGACGCACGCACCAAGTTCAAAGAGGAGGGCGTGGTCACCATCAAGACCATTACCAAGAAGGACAT
GGTCAACAAGGATCAGGTGCTCAACCCCATCTCAAAAGCAAAGCTCGACAAGGATGGCATGTACCCCGTCGAGATTTGGCACC
CCGACCCCGCCAAGAACGAAAACACCCGCTACTTCGGGAACTATACCGGCGGGACCACCACCCCACCGGTGCTCCAATTCAC
CAATACACTCACCACCGTCCTGCTGGACGAGAACGGCGTCGGCCCACTGTGCAAGGGCGAAGGGTTGTATCTGAGTTGCGTG
GACATCATGGGGTGGCGCGTCACCCGCAACTACGACGTCCACCATTGGCGCGGCCTGCCACGCTACTTCAAGATTACACTCC
GCAAGCGCTGGGTCAAGAACCCATACCCAATGGCAAGTCTGATCTCGAGTCTGTTCAACAATATGTTGCCACAAGTCCAGGGG
CAGCCAATGGAGGGCGAAAACACACAAGTGGAAGAAGTCCGCGTCTACGACGGCACCGAGCCCGTGCCCGGCGATCCCGAC
ATGACCAGATACGTCGATAGGTTCGGCAAGACCAAAACCGTGTTCCCAGGAAACTGAGCCTAGGACCCAGCTTTCTTGTACAAA
GTGGTTCGATCTAGAATGGCTAGTGGATCCCCCGGGCTGCAGGAATTCGATATCAAGCTTATCGATAATCAACCTCTGGATTAC
AAAATTTGTGAAAGATTGACTGGTATTCTTAACTATGTTGCTCCTTTTACGCTATGTGGATACGCTGCTTTAATGCCTTTGTATCA
TGCTATTGCTTCCCGTATGGCTTTCATTTTCTCCTCCTTGTATAAATCCTGGTTGCTGTCTCTTTATGAGGAGTTGTGGCCCGTTG
TCAGGCAACGTGGCGTGGTGTGCACTGTGTTTGCTGACGCAACCCCCACTGGTTGGGGCATTGCCACCACCTGTCAGCTCCTT
TCCGGGACTTTCGCTTTCCCCCTCCCTATTGCCACGGCGGAACTCATCGCCGCCTGCCTTGCCCGCTGCTGGACAGGGGCTC
GGCTGTTGGGCACTGACAATTCCGTGGTGTTGTCGGGGAAATCATCGTCCTTTCCTTGGCTGCTCGCCTGTGTTGCCACCTGG
ATTCTGCGCGGGACGTCCTTCTGCTACGTCCCTTCGGCCCTCAATCCAGCGGACCTTCCTTCCCGCGGCCTGCTGCCGGCTCT
GCGGCCTCTTCCGCGTCTTCGCCTTCGCCCTCAGACGAGTCGGATCTCCCTTTGGGCCGCCTCCCCGCATCGATACCGTCGG
CCCACTGCTCCCTAAACCTGAGCTAGCATTATCCCTAATACCTGCCACCCCACTCTTAATCAGTGGTGGAAGAACGGTCTCAGA
ACTGTTTGTTTCAATTGGCCATTTAAGTTTAGTAGTAAAAGACTGGTTAATGATAACAATGCATCGTAAAACCTTCAGAAGGAAAG
GAGAATGTTTTGTGGACCACTTTGGTTTTCTTTTTTGCGTGTGGCAGTTTTAAGTTATTAGTTTTTAAAATCAGTACTTTTTAATGG
AAACAACTTGACCAAAAATTTGTCACAGAATTTTGAGACCCATTAAAAAAGTTAAATGAGAAACCTGTGTGTTCCTTTGGTCAACA
CCGAGACATTTAGGTGAAAGACATCTAATTCTGGTTTTACGAATCTGGAAACTTCTTGAAAATGTAATTCTTGAGTTAACACTTCT
GGGTGGAGAATAGGGTTGTTTTCCCCCCACATAATTGGAAGGGGAAGGAATATCATTTAAAGCTATGGGAGGGTTTCTTTGATT
ACAACACTGGAGAGAAATGCAGCATGTTGCTGATTGCCTGTCACTAAAACAGGCCAAAAACTGAGTCCTTGGGTTGCATAGAAA
GCTTCATGTTGCTAAACCAATGTTAAGTGAATCTTTGGAAACAAAATGTTTCCAAATTACTGGGATGTGCATGTTGAAACGTGGG
TTAATTAACTAGCCATGACCAAAATCCCTTAACGTGAGTTTTCGTTCCACTGAGCGTCAGACCCCGTAGAAAAGATCAAAGGATC
TTCTTGAGATCCTTTTTTTTCTGCGCGTAATCTGCTGCTTGCAAACAAAAAAACCACCGCTACCAGCGGTGGTTTGTTTGCCGGAT
CAAGAGCTACCAACTCTTTTTCCGAAGGTAACTGGCTTCAGCAGAGCGCAGATACCAAATACTGTTCTTCTAGTGTAGCCGTAG
TTAGGCCACCACTTCAAGAACTCTGTAGCACCGCCTACATACCTCGCTCTGCTAATCCTGTTACCAGTGGCTGCTGCCAGTGGC
GATAAGTCGTGTCTTACCGGGTTGGACTCAAGACGATAGTTACCGGATAAGGCGCAGCGGTCGGGCTGAACGGGGGGTTCGT
GCACACAGCCCAGCTTGGAGCGAACGACCTACACCGAACTGAGATACCTACAGCGTGAGCTATGAGAAAGCGCCACGCTTCC
CGAAGGGAGAAAGGCGGACAGGTATCCGGTAAGCGGCAGGGTCGGAACAGGAGAGCGCACGAGGGAGCTTCCAGGGGGAA
ACGCCTGGTATCTTTATAGTCCTGTCGGGTTTCGCCACCTCTGACTTGAGCGTCGATTTTTGTGATGCTCGTCAGGGGGGCGGA
GCCTATGGAAAAACGCCAGCAACGCGGCCTTTTTACGGTTCCTGGCCTTTTGCTGGCCTTTTGCTCACATGTTCTTAATTAAATT
TTTCAAAAGTAGTTGACAATTAATCATCGGCATAGTATATCGGCATAGTATAATACGACTCACTATAGGAGGGCCATCATGGCCA
AGTTGACCAGTGCTGTCCCAGTGCTCACAGCCAGGGATGTGGCTGGAGCTGTTGAGTTCTGGACTGACAGGTTGGGGTTCTCC

AGAGATTTTGTGGAGGATGACTTTGCAGGTGTGGTCAGAGATGATGTCACCCTGTTCATCTCAGCAGTCCAGGACCAGGTGGT
GCCTGACAACACCCTGGCTTGGGTGTGGGTGAGAGGACTGGATGAGCTGTATGCTGAGTGGAGTGAGGTGGTCTCCACCAAC
TTCAGGGATGCCAGTGGCCCTGCCATGACAGAGATTGGAGAGCAGCCCTGGGGGAGAGAGTTTGCCCTGAGAGACCCAGCAG
GCAACTGTGTGCACTTTGTGGCAGAGGAGCAGGACTGAGGATAAGAATTGTAACAAAAAACCCCGCCCCGGCGGGGTTTTTTG
TTAATTAA

SApwP

Plasmid containing mouse polyomavirus (strain RA) VP1 with point mutation abrograting the sialic acid binding site. This plasmid was generated by site directed mutagenesis at three nucleotides (g2935a c2936g t3600g) of RApwP resulting in two amino acid changes R77Q and H298Q. This plamsid is used in combination with ph2p (addgene #22520) and ph3p (addgene # 22521) to generate pseudovirus in 293TT cells.

Figure A2.3: SApwP

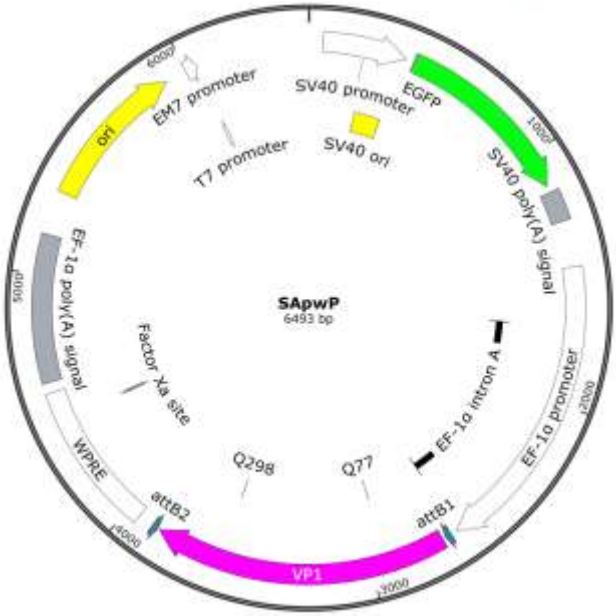

Sequence:

CCCTGCAGGGCCTGAAATAACCTCTGAAAGAGGAACTTGGTTAGGTACCTGTGGAATGTGTGTCAGTTAGGGTGTGGAAAGTC
CCCAGGCTCCCCAGCAGGCAGAAGTATGCAAAGCATGCATCTCAATTAGTCAGCAACCAGGTGTGGAAAGTCCCCAGGCTCCC
CAGCAGGCAGAAGTATGCAAAGCATGCATCTCAATTAGTCAGCAACCATAGTCCCGCCCCTAACTCCGCCCATCCCGCCCCTA
ACTCCGCCCAGTTCCGCCCATTCTCCGCCCCATGGCTGACTAATTTTTTTTATTTATACAGAGGCCGAGGCCGCCTCGGCCTCT
GAGCTATTCCAGAAGTAGTGAGGAGGCTTTTTTGGAGGCCTAGGCTTTTGCAAAAAGCTTGATTGGGATCCACCGGTCGCCAC
CATGGTGAGCAAGGGCGAGGAGCTGTTCACCGGGGTGGTGCCCATCCTGGTCGAGCTGGACGGCGACGTAAACGGCCACAA
GTTCAGCGTGTCCGGCGAGGGCGAGGGCGATGCCACCTACGGCAAGCTGACCCTGAAGTTCATCTGCACCACCGGCAAGCTG
CCCGTGCCCTGGCCCACCCTCGTGACCACCCTGACCTACGGCGTGCAGTGCTTCAGCCGCTACCCCGACCACATGAAGCAGC
ACGACTTCTTCAAGTCCGCCATGCCCGAAGGCTACGTCCAGGAGCGCACCATCTTCTTCAAGGACGACGGCAACTACAAGACC
CGCGCCGAGGTGAAGTTCGAGGGCGACACCCTGGTGAACCGCATCGAGCTGAAGGGCATCGACTTCAAGGAGGACGGCAAC
ATCCTGGGGCACAAGCTGGAGTACAACTACAACAGCCACAACGTCTATATCATGGCCGACAAGCAGAAGAACGGCATCAAGGT
GAACTTCAAGATCCGCCACAACATCGAGGACGGCAGCGTGCAGCTCGCCGACCACTACCAGCAGAACACCCCCATCGGCGAC
GGCCCCGTGCTGCTGCCCGACAACCACTACCTGAGCACCCAGTCCGCCCTGAGCAAAGACCCCAACGAGAAGCGCGATCACA
TGGTCCTGCTGGAGTTCGTGACCGCCGCCGGGATCACTCTCGGCATGGACGAGCTGTACAAGTAAAGCGGCCGCTTCGAGCA
GACATGATAAGATACATTGATGAGTTTGGACAAACCACAACTAGAATGCAGTGAAAAAAATGCTTTATTTGTGAAATTTGTGATG
CTATTGCTTTATTTGTAACCATTATAAGCTGCAATAAACAAGTTAACAACAACAATTGCATTCATTTTATGTTTCAGGTTCAGGGG

GAGGTGTGGGAGGTTTTTTAAAGCAAGTAAAACCTCTACAAATGTGGTAAAATCGATAAGGATCCGGGCTGGCGTAATAGCGAA
GAGGCCCGCACCGATCGCCCTTCCCAACAGTTGCGGTGGAGAAGAGCATGCGTGAGGCTCCGGTGCCCGTCAGTGGGCAGA
GCGCACATCGCCCACAGTCCCCGAGAAGTTGGGGGGGAGGGGTCGGCAATTGAACCGGTGCCTAGAGAAGGTGGCGCGGGGT
AAACTGGGAAAGTGATGTCGTGTACTGGCTCCGCCCTTTTCCCGAGGGTGGGGGAGAACCGTATATAAGTGCAGTAGTCGCTG
TGAACGTTCTTTTTCGCAACGGGTTTGCCGCCAGAACACAGGTAAGTGCCGTGTGTGGTTCCCGCGGGCCTGGCCTCTTTACG
GGTTATGGCCCTTGCGTGCCTTGAATTACTTCCACCTGGCTGCAGTACGTGATTCTTGATCCCGAGCTTCGGGTTGGAAGTGG
GTGGGAGAGTTCGAGGCCTTGCGCTTAAGGAGCCCCTTCGCCTCGTGCTTGAGTTGAGGCCTGGCCTGGGCGCTGGGGCCG
CCGCGTGCGAATCTGGTGGCACCTTCGCGCCTGTCTCGCTGCTTTCGATAAGTCTCTAGCCATTTAAAATTTTTGATGACCTGC
TGCGACGCTTTTTTTCTGGCAAGATAGTCTTGTAAATGCGGGCCAAGATCTGCACACTGGTATTTCGGTTTTTGGGGCCGCGGG
CGGCGACGGGGCCCGTGCGTCCCAGCGCACATGTTCGGCGAGGCGGGGCCTGCGAGCGCGGCCACCGAGAATCGGACGGG
GGTAGTCTCAAGCTGGCCGGCCTGCTCTGGTGCCTGGCCTCGCGCCGCCGTGTATCGCCCCGCCCTGGGCGGCAAGGCTGG
CCCGGTCGGCACCAGTTGCGTGAGCGGAAAGATGGCCGCTTCCCGGCCCTGCTGCAGGGAGCTCAAAATGGAGGACGCGGC
GCTCGGGAGAGCGGGCGGGTGAGTCACCCACACAAAGGAAAAGGGCCTTTCCGTCCTCAGCCGTCGCTTCATGTGACTCCAC
GGAGTACCGGGCGCCGTCCAGGCACCTCGATTAGTTCTCGAGCTTTTGGAGTACGTCGTCTTTAGGTTGGGGGGAGGGGTTTT
ATGCGATGGAGTTTCCCCACACTGAGTGGGTGGAGACTGAAGTTAGGCCAGCTTGGCACTTGATGTAATTCTCCTTGGAATTTG
CCCTTTTTGAGTTTGGATCTTGGTTCATTCTCAAGCCTCAGACAGTGGTTCAAAGTTTTTTTCTTCCATTTCAGGTGTCGTGAGGA
ATTCTCTAGAGCTTGATCAAACAAGTTTGTACAAAAAAGCAGGCTTCCGGAACCACCATGGCACCAAAGCGCAAGTCAGGGGTC
AGCAAATGTGAAACCAAGTGCACCAAGGCATGCCCCCGCCCTGCACCCGTCCCAAAGCTCTTGATCAAGGGCGGCATGGAAG
TCCTCGATCTGGTCACCGGCCCCGATTCCGTCACCGAGATCGAGGCATTCCTGAATCCACGCATGGGCCAACCCCCAACACCC
GAGTCACTGACCGAAGGCGGCCAGTATTACGGCTGGAGCCAGGGCATCAACCTCGCCACCAGCGACACCGAAGACAGTCCCG
GAAACAACACCTTGCCAACCTGGTCCATGGCCAAACTGCAACTGCCAATGCTGAACGAAGATCTGACATGCGATACATTGCAAA
TGTGGGAAGCCGTCAGCGTCAAGACAGAAGTCGTCGGGAGCGGGAGCCTGCTCGATGTCCACGGCTTCAACAAGCCAACCGA
CACCGTGAACACCAAGGGCATCAGTACCCCGGTTGAGGGGTCACAGTACCACGTCTTCGCCGTCGGGGGCGAGCCCCTGGAT
CTGCAAGGCTTGGTCACCGACGCACGCACCAAGTTCAAAGAGGAGGGCGTGGTCACCATCAAGACCATTACCAAGAAGGACAT
GGTCAACAAGGATCAGGTGCTCAACCCCATCTCAAAAGCAAAGCTCGACAAGGATGGCATGTACCCCGTCGAGATTTGGCACC
CCGACCCCGCCAAGAACGAAAACACCCGCTACTTCGGGAACTATACCGGCGGGACCACCACCCCACCGGTGCTCCAATTCAC
CAATACACTCACCACCGTCCTGCTGGACGAGAACGGCGTCGGCCCACTGTGCAAGGGCGAAGGGTTGTATCTGAGTTGCGTG
GACATCATGGGGTGGCGCGTCACCCGCAACTACGACGTCCACCAGTGGCGCGGCCTGCCACGCTACTTCAAGATTACACTCC
GCAAGCGCTGGGTCAAGAACCCATACCCAATGGCAAGTCTGATCTCGAGTCTGTTCAACAATATGTTGCCACAAGTCCAGGGG
CAGCCAATGGAGGGCGAAAACACACAAGTGGAAGAAGTCCGCGTCTACGACGGCACCGAGCCCGTGCCCGGCGATCCCGAC
ATGACCAGATACGTCGATAGGTTCGGCAAGACCAAAACCGTGTTCCCAGGAAACTGAGCCTAGGACCCAGCTTTCTTGTACAAA
GTGGTTCGATCTAGAATGGCTAGTGGATCCCCCGGGCTGCAGGAATTCGATATCAAGCTTATCGATAATCAACCTCTGGATTAC
AAAATTTGTGAAAGATTGACTGGTATTCTTAACTATGTTGCTCCTTTTACGCTATGTGGATACGCTGCTTTAATGCCTTTGTATCA
TGCTATTGCTTCCCGTATGGCTTTCATTTTCTCCTCCTTGTATAAATCCTGGTTGCTGTCTCTTTATGAGGAGTTGTGGCCCGTTG
TCAGGCAACGTGGCGTGGTGTGCACTGTGTTTGCTGACGCAACCCCCACTGGTTGGGGCATTGCCACCACCTGTCAGCTCCTT
TCCGGGACTTTCGCTTTCCCCCTCCCTATTGCCACGGCGGAACTCATCGCCGCCTGCCTTGCCCGCTGCTGGACAGGGGCTC
GGCTGTTGGGCACTGACAATTCCGTGGTGTTGTCGGGGAAATCATCGTCCTTTCCTTGGCTGCTCGCCTGTGTTGCCACCTGG
ATTCTGCGCGGGACGTCCTTCTGCTACGTCCCTTCGGCCCTCAATCCAGCGGACCTTCCTTCCCGCGGCCTGCTGCCGGCTCT
GCGGCCTCTTCCGCGTCTTCGCCTTCGCCCTCAGACGAGTCGGATCTCCCTTTGGGCCGCCTCCCCGCATCGATACCGTCGG
CCCACTGCTCCCTAAACCTGAGCTAGCATTATCCCTAATACCTGCCACCCCACTCTTAATCAGTGGTGGAAGAACGGTCTCAGA
ACTGTTTGTTTCAATTGGCCATTTAAGTTTAGTAGTAAAAGACTGGTTAATGATAACAATGCATCGTAAAACCTTCAGAAGGAAAG
GAGAATGTTTTGTGGACCACTTTGGTTTTCTTTTTTGCGTGTGGCAGTTTTAAGTTATTAGTTTTTAAAATCAGTACTTTTTAATGG
AAACAACTTGACCAAAAATTTGTCACAGAATTTTGAGACCCATTAAAAAAGTTAAATGAGAAACCTGTGTGTTCCTTTGGTCAACA
CCGAGACATTTAGGTGAAAGACATCTAATTCTGGTTTTACGAATCTGGAAACTTCTTGAAAATGTAATTCTTGAGTTAACACTTCT
GGGTGGAGAATAGGGTTGTTTTCCCCCCACATAATTGGAAGGGGAAGGAATATCATTTAAAGCTATGGGAGGGTTTCTTTGATT
ACAACACTGGAGAGAAATGCAGCATGTTGCTGATTGCCTGTCACTAAAACAGGCCAAAAACTGAGTCCTTGGGTTGCATAGAAA
GCTTCATGTTGCTAAACCAATGTTAAGTGAATCTTTGGAAACAAAATGTTTCCAAATTACTGGGATGTGCATGTTGAAACGTGGG
TTAATTAACTAGCCATGACCAAAATCCCTTAACGTGAGTTTTCGTTCCACTGAGCGTCAGACCCCGTAGAAAAGATCAAAGGATC
TTCTTGAGATCCTTTTTTTTCTGCGCGTAATCTGCTGCTTGCAAACAAAAAAACCACCGCTACCAGCGGTGGTTTGTTTGCCGGAT
CAAGAGCTACCAACTCTTTTTCCGAAGGTAACTGGCTTCAGCAGAGCGCAGATACCAAATACTGTTCTTCTAGTGTAGCCGTAG
TTAGGCCACCACTTCAAGAACTCTGTAGCACCGCCTACATACCTCGCTCTGCTAATCCTGTTACCAGTGGCTGCTGCCAGTGGC
GATAAGTCGTGTCTTACCGGGTTGGACTCAAGACGATAGTTACCGGATAAGGCGCAGCGGTCGGGCTGAACGGGGGGTTCGT
GCACACAGCCCAGCTTGGAGCGAACGACCTACACCGAACTGAGATACCTACAGCGTGAGCTATGAGAAAGCGCCACGCTTCC
CGAAGGGAGAAAGGCGGACAGGTATCCGGTAAGCGGCAGGGTCGGAACAGGAGAGCGCACGAGGGAGCTTCCAGGGGGAA
ACGCCTGGTATCTTTATAGTCCTGTCGGGTTTCGCCACCTCTGACTTGAGCGTCGATTTTTGTGATGCTCGTCAGGGGGGCGGA
GCCTATGGAAAAACGCCAGCAACGCGGCCTTTTTACGGTTCCTGGCCTTTTGCTGGCCTTTTGCTCACATGTTCTTAATTAAATT
TTTCAAAAGTAGTTGACAATTAATCATCGGCATAGTATATCGGCATAGTATAATACGACTCACTATAGGAGGGCCATCATGGCCA
AGTTGACCAGTGCTGTCCCAGTGCTCACAGCCAGGGATGTGGCTGGAGCTGTTGAGTTCTGGACTGACAGGTTGGGGTTCTCC
AGAGATTTTGTGGAGGATGACTTTGCAGGTGTGGTCAGAGATGATGTCACCCTGTTCATCTCAGCAGTCCAGGACCAGGTGGT
GCCTGACAACACCCTGGCTTGGGTGTGGGTGAGAGGACTGGATGAGCTGTATGCTGAGTGGAGTGAGGTGGTCTCCACCAAC
TTCAGGGATGCCAGTGGCCCTGCCATGACAGAGATTGGAGAGCAGCCCTGGGGGAGAGAGTTTGCCCTGAGAGACCCAGCAG

GCAACTGTGTGCACTTTGTGGCAGAGGAGCAGGACTGAGGATAAGAATTGTAACAAAAAACCCCGCCCCGGCGGGGTTTTTTG
TTAATTAA

ZsGreen Reporter

Reporter plasmid for MuPyV pseudovirus used in combination with pwP (RA, LNV, or SA), ph2p (addgene #22520) and ph3p (addgene # 22521). This plasmid was assembled from Luc-Zsgreen (addgene #39196) and pwP (addgene #22519).

Figure A2.4: ZsGreen Reporter

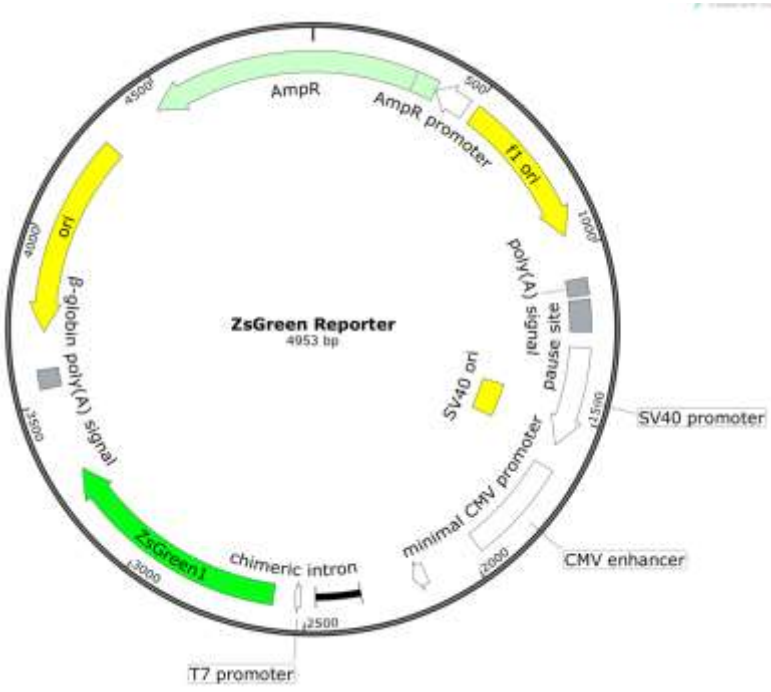

Sequence:

ATGGCAGCACTGCATAATTCTCTTACTGTCATGCCATCCGTAAGATGCTTTTCTGTGACTGGTGAGTACTCAACCAAGTCATTCT
GAGAATAGTGTATGCGGCGACCGAGTTGCTCTTGCCCGGCGTCAATACGGGATAATACCGCGCCACATAGCAGAACTTTAAAA
GTGCTCATCATTGGAAAACGTTCTTCGGGGCGAAAACTCTCAAGGATCTTACCGCTGTTGAGATCCAGTTCGATGTAACCCACT
CGTGCACCCAACTGATCTTCAGCATCTTTTACTTTCACCAGCGTTTCTGGGTGAGCAAAAACAGGAAGGCAAAATGCCGCAAAA
AAGGGAATAAGGGCGACACGGAAATGTTGAATACTCATACTCTTCCTTTTTCAATATTATTGAAGCATTTATCAGGGTTATTGTCT
CATGAGCGGATACATATTTGAATGTATTTAGAAAAATAAACAAATAGGGGTTCCGCGCACATTTCCCCGAAAAGTGCCACCTGAC
GCGCCCTGTAGCGGCGCATTAAGCGCGGCGGGTGTGGTGGTTACGCGCAGCGTGACCGCTACACTTGCCAGCGCCCTAGCG
CCCGCTCCTTTCGCTTTCTTCCCTTCCTTTCTCGCCACGTTCGCCGGCTTTCCCCGTCAAGCTCTAAATCGGGGGCTCCCTTTA
GGGTTCCGATTTAGTGCTTTACGGCACCTCGACCCCAAAAAACTTGATTAGGGTGATGGTTCACGTAGTGGGCCATCGCCCTGA
TAGACGGTTTTTCGCCCTTTGACGTTGGAGTCCACGTTCTTTAATAGTGGACTCTTGTTCCAAACTGGAACAACACTCAACCCTA
TCTCGGTCTATTCTTTTGATTTATAAGGGATTTTGCCGATTTCGGCCTATTGGTTAAAAAATGAGCTGATTTAACAAAAATTTAAC
GCGAATTTTAACAAAATATTAACGTTTACAATTTCCCATTCGCCATTCAGGCTGCGCAACTGTTGGGAAGGGCGATCGGTGCGG
GCCTCTTCGCTATTACGCCAGCCCAAGCTACCATGATAAGTAAGTAATATTAAGGTACGGGAGGTACTTGGAGCGGCCGCAATA
AAATATCTTTATTTTCATTACATCTGTGTGTTGGTTTTTTGTGTGAATCGATAGTACTAACATACGCTCTCCATCAAAACAAAACGA
AACAAAACAAACTAGCAAAATAGGCTGTCCCCAGTGCAAGTGCAGGTGCCAGAACATTTCTCTATCGATATGAGGCGGAAAGAA
CCAGCTGTGGAATGTGTGTCAGTTAGGGTGTGGAAAGTCCCCAGGCTCCCCAGCAGGCAGAAGTATGCAAAGCATGCATCTCA
ATTAGTCAGCAACCAGGTGTGGAAAGTCCCCAGGCTCCCCAGCAGGCAGAAGTATGCAAAGCATGCATCTCAATTAGTCAGCA

ACCATAGTCCCGCCCCTAACTCCGCCCATCCCGCCCCTAACTCCGCCCAGTTCCGCCCATTCTCCGCCCCATGGCTGACTAAT
TTTTTTTATTTATGCAGAGGCCGAGGCCGCCTCGGCCTCTGAGCTATTCCAGAAGTAGTGAGGAGGCTTTTTTGGAGGCCTAGC
TAGTTATTAATAGTAATCAATTACGGGGTCATTAGTTCATAGCCCATATATGGAGTTCCGCGTTACATAACTTACGGTAAATGGC
CCGCCTGGCTGACCGCCCAACGACCCCCGCCCATTGACGTCAATAATGACGTATGTTCCCATAGTAACGCCAATAGGGACTTT
CCATTGACGTCAATGGGTGGAGTATTTACGGTAAACTGCCCACTTGGCAGTACATCAAGTGTATCATATGCCAAGTCCGCCCCC
TATTGACGTCAATGACGGTAAATGGCCCGCCTGGCATTATGCCCAGTACATGACCTTACGGGACTTTCCTACTTGGCAGTACAT
CTACGTATTAGTCATCGCTATTACCATGGTGATGCGGTTTTGGCAGTACACCAATGGGCGTGGATAGCGGTTTGACTCACGGGG
ATTTCCAAGTCTCCACCCCATTGACGTCAATGGGAGTTTGTTTTGGCACCAAAATCAACGGGACTTTCCAAAATGTCGTAACAAC
TGCGATCGCCCGCCCCGTTGACGCAAATGGGCGGTAGGCGTGTACGGTGGGAGGTCTATATAAGCAGAGCTCGTTTAGTGAA
CCGTCAGATCACTAGAAGCTTTATTGCGGTAGTTTATCACAGTTAAATTGCTAACGCAGTCAGTGCTTCTGACACAACAGTCTCG
AACTTAAGCTGCAGTGACTCTCTTAAGGTAGCCTTGCAGAAGTTGGTCGTGAGGCACTGGGCAGGTAAGTATCAAGGTTACAAG
ACAGGTTTAAGGAGACCAATAGAAACTGGGCTTGTCGAGACAGAGAAGACTCTTGCGTTTCTGATAGGCACCTATTGGTCTTAC
TGACATCCACTTTGCCTTTCTCTCCACAGGTGTCCACTCCCAGTTCAATTACAGCTCTTAAGGCTAGAGTACTTAATACGACTCA
CTATAGGCTAGCCTCGAGAATTCTGCAGTCGACGGTACCGCGGGCCCGGGATCCACCGGTCGCCACCATGGCCCAGTCCAAG
CACGGCCTGACCAAGGAGATGACCATGAAGTACCGCATGGAGGGCTGCGTGGACGGCCACAAGTTCGTGATCACCGGCGAG
GGCATCGGCTACCCCTTCAAGGGCAAGCAGGCCATCAACCTGTGCGTGGTGGAGGGCGGCCCCTTGCCCTTCGCCGAGGAC
ATCTTGTCCGCCGCCTTCATGTACGGCAACCGCGTGTTCACCGAGTACCCCCAGGACATCGTCGACTACTTCAAGAACTCCTG
CCCCGCCGGCTACACCTGGGACCGCTCCTTCCTGTTCGAGGACGGCGCCGTGTGCATCTGCAACGCCGACATCACCGTGAGC
GTGGAGGAGAACTGCATGTACCACGAGTCCAAGTTCTACGGCGTGAACTTCCCCGCCGACGGCCCCGTGATGAAGAAGATGA
CCGACAACTGGGAGCCCTCCTGCGAGAAGATCATCCCCGTGCCCAAGCAGGGCATCTTGAAGGGCGACGTGAGCATGTACCT
GCTGCTGAAGGACGGTGGCCGCTTGCGCTGCCAGTTCGACACCGTGTACAAGGCCAAGTCCGTGCCCCGCAAGATGCCCGAC
TGGCACTTCATCCAGCACAAGCTGACCCGCGAGGACCGCAGCGACGCCAAGAACCAGAAGTGGCACCTGACCGAGCACGCCA
TCGCCTCCGGCTCCGCCTTGCCCTGAGCGGCCGCGACTCTAGATCATAATCAGCCATACCACATTTGTAGAGGTTTTACTTGCT
TTAAAAAACCTCCCACACCTCCCCCTGAACCTGAAACATAAAATGAATGCAATTCACTCCTCAGGTGCAGGCTGCCTATCAGAA
GGTGGTGGCTGGTGTGGCCAATGCCCTGGCTCACAAATACCACTGAGATCTTTTTCCCTCTGCCAAAAATTATGGGGACATCAT
GAAGCCCCTTGAGCATCTGACTTCTGGCTAATAAAGGAAATTTATTTTCATTGCAATAGTGTGTTGGAATTTTTTGTGTCTCTCAC
TCGGAAGGACATATGGGAGGGCAAATCATTTAAAACATCAGAATGAGTATTTGGTTTAGAGTTTGGCAACATATGCCATATGCTG
GCTGCCATGAACAAAGGGGCGTTTTTCCATAGGCTCCGCCCCCCTGACGAGCATCACAAAAATCGACGCTCAAGTCAGAGGTG
GCGAAACCCGACAGGACTATAAAGATACCAGGCGTTTCCCCCTGGAAGCTCCCTCGTGCGCTCTCCTGTTCCGACCCTGCCGC
TTACCGGATACCTGTCCGCCTTTCTCCCTTCGGGAAGCGTGGCGCTTTCTCATAGCTCACGCTGTAGGTATCTCAGTTCGGTGT
AGGTCGTTCGCTCCAAGCTGGGCTGTGTGCACGAACCCCCCGTTCAGCCCGACCGCTGCGCCTTATCCGGTAACTATCGTCTT
GAGTCCAACCCGGTAAGACACGACTTATCGCCACTGGCAGCAGCCACTGGTAACAGGATTAGCAGAGCGAGGTATGTAGGCG
GTGCTACAGAGTTCTTGAAGTGGTGGCCTAACTACGGCTACACTAGAAGGACAGTATTTGGTATCTGCGCTCTGCTGAAGCCAG
TTACCTTCGGAAAAAGAGTTGGTAGCTCTTGATCCGGCAAACAAACCACCGCTGGTAGCGGTGGTTTTTTTGTTTGCAAGCAGC
AGATTACGCGCAGAAAAAAAGGATCTCAAGAAGATCCTTTGATCTTTTCTACGGGGTCTGACGCTCAGTGGAACGAAAACTCAC
GTTAAGGGATTTTGGTCATGAGATTATCAAAAAGGATCTTCACCTAGATCCTTTTAAATTAAAAATGAAGTTTTAAATCAATCTAAA
GTATATATGAGTAAACTTGGTCTGACAGTTACCAATGCTTAATCAGTGAGGCACCTATCTCAGCGATCTGTCTATTTCGTTCATC
CATAGTTGCCTGACTCCCCGTCGTGTAGATAACTACGATACGGGAGGGCTTACCATCTGGCCCCAGTGCTGCAATGATACCGC
GAGACCCACGCTCACCGGCTCCAGATTTATCAGCAATAAACCAGCCAGCCGGAAGGGCCGAGCGCAGAAGTGGTCCTGCAAC
TTTATCCGCCTCCATCCAGTCTATTAATTGTTGCCGGGAAGCTAGAGTAAGTAGTTCGCCAGTTAATAGTTTGCGCAACGTTGTT
GCCATTGCTACAGGCATCGTGGTGTCACGCTCGTCGTTTGGTATGGCTTCATTCAGCTCCGGTTCCCAACGATCAAGGCGAGTT
ACATGATCCCCCATGTTGTGCAAAAAAGCGGTTAGCTCCTTCGGTCCTCCGATCGTTGTCAGAAGTAAGTTGGCCGCAGTGTTA
TCACTCATGGTT

VP1-GST FL pwP

Plasmid for mouse polyomavirus (strain RA) VP1 pentamer purification from 293TT cells. The VP1 is full length with a glutathione transferase tag attached by a thrombin cleavage site. The plasmid was assembled from pwP (addgene #22519) and VP1 in a pGEX backbone.

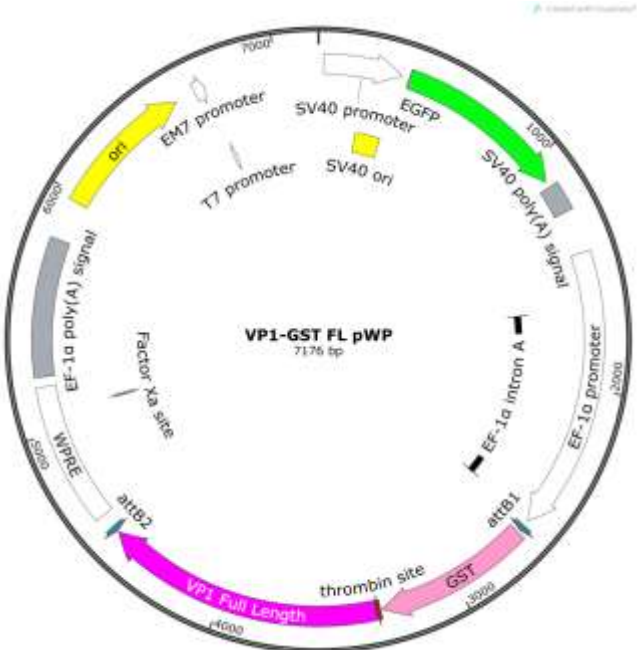

Figure A2.5: VP1-GST FL pwP

Sequence:

ACTTGGTTAGGTACCTGTGGAATGTGTGTCAGTTAGGGTGTGGAAAGTCCCCAGGCTCCCCAGCAGGCAGAAGTATGCAAAGC
ATGCATCTCAATTAGTCAGCAACCAGGTGTGGAAAGTCCCCAGGCTCCCCAGCAGGCAGAAGTATGCAAAGCATGCATCTCAA
TTAGTCAGCAACCATAGTCCCGCCCCTAACTCCGCCCATCCCGCCCCTAACTCCGCCCAGTTCCGCCCATTCTCCGCCCCATG
GCTGACTAATTTTTTTTATTTATACAGAGGCCGAGGCCGCCTCGGCCTCTGAGCTATTCCAGAAGTAGTGAGGAGGCTTTTTTG
GAGGCCTAGGCTTTTGCAAAAAGCTTGATTGGGATCCACCGGTCGCCACCATGGTGAGCAAGGGCGAGGAGCTGTTCACCGG
GGTGGTGCCCATCCTGGTCGAGCTGGACGGCGACGTAAACGGCCACAAGTTCAGCGTGTCCGGCGAGGGCGAGGGCGATGC
CACCTACGGCAAGCTGACCCTGAAGTTCATCTGCACCACCGGCAAGCTGCCCGTGCCCTGGCCCACCCTCGTGACCACCCTG
ACCTACGGCGTGCAGTGCTTCAGCCGCTACCCCGACCACATGAAGCAGCACGACTTCTTCAAGTCCGCCATGCCCGAAGGCTA
CGTCCAGGAGCGCACCATCTTCTTCAAGGACGACGGCAACTACAAGACCCGCGCCGAGGTGAAGTTCGAGGGCGACACCCTG
GTGAACCGCATCGAGCTGAAGGGCATCGACTTCAAGGAGGACGGCAACATCCTGGGGCACAAGCTGGAGTACAACTACAACA
GCCACAACGTCTATATCATGGCCGACAAGCAGAAGAACGGCATCAAGGTGAACTTCAAGATCCGCCACAACATCGAGGACGGC
AGCGTGCAGCTCGCCGACCACTACCAGCAGAACACCCCCATCGGCGACGGCCCCGTGCTGCTGCCCGACAACCACTACCTGA
GCACCCAGTCCGCCCTGAGCAAAGACCCCAACGAGAAGCGCGATCACATGGTCCTGCTGGAGTTCGTGACCGCCGCCGGGAT
CACTCTCGGCATGGACGAGCTGTACAAGTAAAGCGGCCGCTTCGAGCAGACATGATAAGATACATTGATGAGTTTGGACAAAC
CACAACTAGAATGCAGTGAAAAAAATGCTTTATTTGTGAAATTTGTGATGCTATTGCTTTATTTGTAACCATTATAAGCTGCAATAA
ACAAGTTAACAACAACAATTGCATTCATTTTATGTTTCAGGTTCAGGGGGAGGTGTGGGAGGTTTTTTAAAGCAAGTAAAACCTC
TACAAATGTGGTAAAATCGATAAGGATCCGGGCTGGCGTAATAGCGAAGAGGCCCGCACCGATCGCCCTTCCCAACAGTTGCG
GTGGAGAAGAGCATGCGTGAGGCTCCGGTGCCCGTCAGTGGGCAGAGCGCACATCGCCCACAGTCCCCGAGAAGTTGGGGG
GAGGGGTCGGCAATTGAACCGGTGCCTAGAGAAGGTGGCGCGGGGTAAACTGGGAAAGTGATGTCGTGTACTGGCTCCGCCC
TTTTCCCGAGGGTGGGGGAGAACCGTATATAAGTGCAGTAGTCGCTGTGAACGTTCTTTTTCGCAACGGGTTTGCCGCCAGAA
CACAGGTAAGTGCCGTGTGTGGTTCCCGCGGGCCTGGCCTCTTTACGGGTTATGGCCCTTGCGTGCCTTGAATTACTTCCACC
TGGCTGCAGTACGTGATTCTTGATCCCGAGCTTCGGGTTGGAAGTGGGTGGGAGAGTTCGAGGCCTTGCGCTTAAGGAGCCC
CTTCGCCTCGTGCTTGAGTTGAGGCCTGGCCTGGGCGCTGGGGCCGCCGCGTGCGAATCTGGTGGCACCTTCGCGCCTGTCT
CGCTGCTTTCGATAAGTCTCTAGCCATTTAAAATTTTTGATGACCTGCTGCGACGCTTTTTTTCTGGCAAGATAGTCTTGTAAATG
CGGGCCAAGATCTGCACACTGGTATTTCGGTTTTTGGGGCCGCGGGCGGCGACGGGGCCCGTGCGTCCCAGCGCACATGTTC
GGCGAGGCGGGGCCTGCGAGCGCGGCCACCGAGAATCGGACGGGGGTAGTCTCAAGCTGGCCGGCCTGCTCTGGTGCCTG
GCCTCGCGCCGCCGTGTATCGCCCCGCCCTGGGCGGCAAGGCTGGCCCGGTCGGCACCAGTTGCGTGAGCGGAAAGATGGC
CGCTTCCCGGCCCTGCTGCAGGGAGCTCAAAATGGAGGACGCGGCGCTCGGGAGAGCGGGCGGGTGAGTCACCCACACAAA
GGAAAAGGGCCTTTCCGTCCTCAGCCGTCGCTTCATGTGACTCCACGGAGTACCGGGCGCCGTCCAGGCACCTCGATTAGTTC
TCGAGCTTTTGGAGTACGTCGTCTTTAGGTTGGGGGGAGGGGTTTTATGCGATGGAGTTTCCCCACACTGAGTGGGTGGAGAC
TGAAGTTAGGCCAGCTTGGCACTTGATGTAATTCTCCTTGGAATTTGCCCTTTTTGAGTTTGGATCTTGGTTCATTCTCAAGCCT
CAGACAGTGGTTCAAAGTTTTTTTCTTCCATTTCAGGTGTCGTGAGGAATTCTCTAGAGCTTGATCAAACAAGTTTGTACAAAAAA
GCAGGCTTCCGGAACCACCATGTCCCCTATACTAGGTTATTGGAAAATTAAGGGCCTTGTGCAACCCACTCGACTTCTTTTGGA

ATATCTTGAAGAAAAATATGAAGAGCATTTGTATGAGCGCGATGAAGGTGATAAATGGCGAAACAAAAAGTTTGAATTGGGTTTG
GAGTTTCCCAATCTTCCTTATTATATTGATGGTGATGTTAAATTAACACAGTCTATGGCCATCATACGTTATATAGCTGACAAGCA
CAACATGTTGGGTGGTTGTCCAAAAGAGCGTGCAGAGATTTCAATGCTTGAAGGAGCGGTTTTGGATATTAGATACGGTGTTTC
GAGAATTGCATATAGTAAAGACTTTGAAACTCTCAAAGTTGATTTTCTTAGCAAGCTACCTGAAATGCTGAAAATGTTCGAAGATC
GTTTATGTCATAAAACATATTTAAATGGTGATCATGTAACCCATCCTGACTTCATGTTGTATGACGCTCTTGATGTTGTTTTATACA
TGGACCCAATGTGCCTGGATGCGTTCCCAAAATTAGTTTGTTTTAAAAAACGTATTGAAGCTATCCCACAAATTGATAAGTACTT
GAAATCCAGCAAGTATATAGCATGGCCTTTGCAGGGCTGGCAAGCCACGTTTGGTGGTGGCGACCATCCTCCAAAATCGGATC
TGGTTCCGCGTGGATCCGGAGGAATGGCCCCCAAAAGAAAAAGCGGCGTCTCTAAATGCGAGACAAAATGTACAAAGGCCTGT
CCAAGACCCGCACCCGTTCCCAAACTGCTTATTAAAGGGGGTATGGAGGTGCTGGACCTTGTGACAGGGCCAGACAGTGTGAC
AGAAATAGAAGCTTTTCTGAACCCCAGAATGGGGCAGCCACCCACCCCTGAAAGCCTAACAGAGGGAGGGCAATACTATGGTT
GGAGCAGAGGGATTAATTTGGCTACATCAGATACAGAGGATTCCCCAGGAAATAATACACTTCCCACATGGAGTATGGCAAAGC
TCCAGCTTCCCATGCTCAATGAGGACCTCACCTGTGACACCCTACAAATGTGGGAGGCAGTCTCAGTGAAAACCGAGGTGGTG
GGCTCTGGCTCACTGTTAGATGTGCATGGGTTCAACAAACCCACAGATACAGTAAACACAAAAGGAATTTCCACTCCAGTGGAA
GGCAGCCAATATCATGTGTTTGCTGTGGGCGGGGAACCGCTTGACCTCCAGGGACTTGTGACAGATGCCAGAACAAAATACAA
GGAAGAAGGGGTAGTAACAATCAAAACAATCACAAAGAAGGACATGGTCAACAAAGACCAAGTCCTGAATCCAATTAGCAAGGC
CAAGCTGGATAAGGACGGAATGTATCCAGTTGAAATCTGGCATCCAGATCCAGCAAAAAATGAGAACACAAGGTACTTTGGCAA
TTACACTGGAGGCACAACAACTCCACCCGTCCTGCAGTTCACAAACACCCTGACAACTGTGCTCCTAGATGAAAATGGAGTTGG
GCCCCTCTGTAAAGGAGAGGGCCTATACCTCTCCTGTGTAGATATAATGGGCTGGAGAGTTACAAGAAACTATGATGTCCATCA
CTGGAGAGGGCTTCCCAGATATTTCAAAATCACCCTGAGAAAAAGATGGGTCAAAAATCCCTATCCCATGGCCTCCCTCATAAG
TTCCCTTTTCAACAACATGCTCCCCCAAGTGCAGGGCCAACCCATGGAAGGGGAGAACACCCAGGTAGAGGAGGTTAGAGTGT
ATGATGGGACTGAACCTGTACCGGGGGACCCTGATATGACGCGCTATGTTGACCGCTTTGGAAAAACAAAGACTGTATTTCCTG
GAAATTAACCTAGGACCCAGCTTTCTTGTACAAAGTGGTTCGATCTAGAATGGCTAGTGGATCCCCCGGGCTGCAGGAATTCGA
TATCAAGCTTATCGATAATCAACCTCTGGATTACAAAATTTGTGAAAGATTGACTGGTATTCTTAACTATGTTGCTCCTTTTACGCT
ATGTGGATACGCTGCTTTAATGCCTTTGTATCATGCTATTGCTTCCCGTATGGCTTTCATTTTCTCCTCCTTGTATAAATCCTGGT
TGCTGTCTCTTTATGAGGAGTTGTGGCCCGTTGTCAGGCAACGTGGCGTGGTGTGCACTGTGTTTGCTGACGCAACCCCCACT
GGTTGGGGCATTGCCACCACCTGTCAGCTCCTTTCCGGGACTTTCGCTTTCCCCCTCCCTATTGCCACGGCGGAACTCATCGC
CGCCTGCCTTGCCCGCTGCTGGACAGGGGCTCGGCTGTTGGGCACTGACAATTCCGTGGTGTTGTCGGGGAAATCATCGTCC
TTTCCTTGGCTGCTCGCCTGTGTTGCCACCTGGATTCTGCGCGGGACGTCCTTCTGCTACGTCCCTTCGGCCCTCAATCCAGC
GGACCTTCCTTCCCGCGGCCTGCTGCCGGCTCTGCGGCCTCTTCCGCGTCTTCGCCTTCGCCCTCAGACGAGTCGGATCTCC
CTTTGGGCCGCCTCCCCGCATCGATACCGTCGGCCCACTGCTCCCTAAACCTGAGCTAGCATTATCCCTAATACCTGCCACCC
CACTCTTAATCAGTGGTGGAAGAACGGTCTCAGAACTGTTTGTTTCAATTGGCCATTTAAGTTTAGTAGTAAAAGACTGGTTAAT
GATAACAATGCATCGTAAAACCTTCAGAAGGAAAGGAGAATGTTTTGTGGACCACTTTGGTTTTCTTTTTTGCGTGTGGCAGTTT
TAAGTTATTAGTTTTTAAAATCAGTACTTTTTAATGGAAACAACTTGACCAAAAATTTGTCACAGAATTTTGAGACCCATTAAAAAA
GTTAAATGAGAAACCTGTGTGTTCCTTTGGTCAACACCGAGACATTTAGGTGAAAGACATCTAATTCTGGTTTTACGAATCTGGA
AACTTCTTGAAAATGTAATTCTTGAGTTAACACTTCTGGGTGGAGAATAGGGTTGTTTTCCCCCCACATAATTGGAAGGGGAAGG
AATATCATTTAAAGCTATGGGAGGGTTTCTTTGATTACAACACTGGAGAGAAATGCAGCATGTTGCTGATTGCCTGTCACTAAAA
CAGGCCAAAAACTGAGTCCTTGGGTTGCATAGAAAGCTTCATGTTGCTAAACCAATGTTAAGTGAATCTTTGGAAACAAAATGTT
TCCAAATTACTGGGATGTGCATGTTGAAACGTGGGTTAATTAACTAGCCATGACCAAAATCCCTTAACGTGAGTTTTCGTTCCAC
TGAGCGTCAGACCCCGTAGAAAAGATCAAAGGATCTTCTTGAGATCCTTTTTTTCTGCGCGTAATCTGCTGCTTGCAAACAAAAA
AACCACCGCTACCAGCGGTGGTTTGTTTGCCGGATCAAGAGCTACCAACTCTTTTTCCGAAGGTAACTGGCTTCAGCAGAGCG
CAGATACCAAATACTGTTCTTCTAGTGTAGCCGTAGTTAGGCCACCACTTCAAGAACTCTGTAGCACCGCCTACATACCTCGCT
CTGCTAATCCTGTTACCAGTGGCTGCTGCCAGTGGCGATAAGTCGTGTCTTACCGGGTTGGACTCAAGACGATAGTTACCGGAT
AAGGCGCAGCGGTCGGGCTGAACGGGGGGTTCGTGCACACAGCCCAGCTTGGAGCGAACGACCTACACCGAACTGAGATAC
CTACAGCGTGAGCTATGAGAAAGCGCCACGCTTCCCGAAGGGAGAAAGGCGGACAGGTATCCGGTAAGCGGCAGGGTCGGA
ACAGGAGAGCGCACGAGGGAGCTTCCAGGGGGAAACGCCTGGTATCTTTATAGTCCTGTCGGGTTTCGCCACCTCTGACTTGA
GCGTCGATTTTTGTGATGCTCGTCAGGGGGGCGGAGCCTATGGAAAAACGCCAGCAACGCGGCCTTTTTACGGTTCCTGGCCT
TTTGCTGGCCTTTTGCTCACATGTTCTTAATTAAATTTTTCAAAAGTAGTTGACAATTAATCATCGGCATAGTATATCGGCATAGTA
TAATACGACTCACTATAGGAGGGCCATCATGGCCAAGTTGACCAGTGCTGTCCCAGTGCTCACAGCCAGGGATGTGGCTGGAG
CTGTTGAGTTCTGGACTGACAGGTTGGGGTTCTCCAGAGATTTTGTGGAGGATGACTTTGCAGGTGTGGTCAGAGATGATGTCA
CCCTGTTCATCTCAGCAGTCCAGGACCAGGTGGTGCCTGACAACACCCTGGCTTGGGTGTGGGTGAGAGGACTGGATGAGCT
GTATGCTGAGTGGAGTGAGGTGGTCTCCACCAACTTCAGGGATGCCAGTGGCCCTGCCATGACAGAGATTGGAGAGCAGCCC
TGGGGGAGAGAGTTTGCCCTGAGAGACCCAGCAGGCAACTGTGTGCACTTTGTGGCAGAGGAGCAGGACTGAGGATAAGAAT
TGTAACAAAAAACCCCGCCCCGGCGGGGTTTTTTGTTAATTAACCCTGCAGGGCCTGAAATAACCTCTGAAAGAGGA

VP1-GST C30 Deletion pwP

Plasmid for mouse polyomavirus (strain RA) VP1 with a 30 amino acid deletion at the C-terminus to abrograte pentamer-pentamer interactions. This plasmid is for purification of VP1-GST from 293TT cells. The VP1 contains a glutathione transferase tag attached by a thrombin cleavage site at the N-terminus. The plasmid was assembled from pwP (addgene #22519) and VP1-GST FL pwP.

Figure A2.6: VP1-GST C30 Deletion pwP

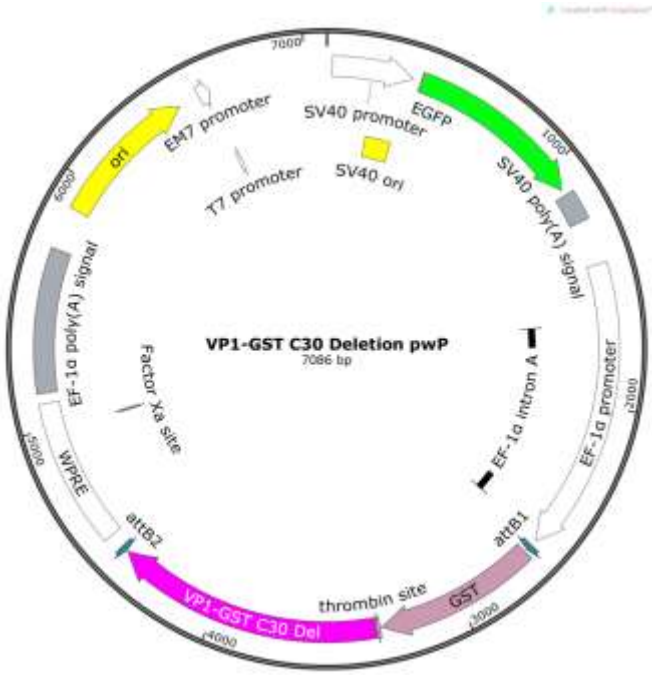

Sequence:

ACTTGGTTAGGTACCTGTGGAATGTGTGTCAGTTAGGGTGTGGAAAGTCCCCAGGCTCCCCAGCAGGCAGAAGTATGCAAAGC
ATGCATCTCAATTAGTCAGCAACCAGGTGTGGAAAGTCCCCAGGCTCCCCAGCAGGCAGAAGTATGCAAAGCATGCATCTCAA
TTAGTCAGCAACCATAGTCCCGCCCCTAACTCCGCCCATCCCGCCCCTAACTCCGCCCAGTTCCGCCCATTCTCCGCCCCATG
GCTGACTAATTTTTTTTATTTATACAGAGGCCGAGGCCGCCTCGGCCTCTGAGCTATTCCAGAAGTAGTGAGGAGGCTTTTTTG
GAGGCCTAGGCTTTTGCAAAAAGCTTGATTGGGATCCACCGGTCGCCACCATGGTGAGCAAGGGCGAGGAGCTGTTCACCGG
GGTGGTGCCCATCCTGGTCGAGCTGGACGGCGACGTAAACGGCCACAAGTTCAGCGTGTCCGGCGAGGGCGAGGGCGATGC
CACCTACGGCAAGCTGACCCTGAAGTTCATCTGCACCACCGGCAAGCTGCCCGTGCCCTGGCCCACCCTCGTGACCACCCTG
ACCTACGGCGTGCAGTGCTTCAGCCGCTACCCCGACCACATGAAGCAGCACGACTTCTTCAAGTCCGCCATGCCCGAAGGCTA
CGTCCAGGAGCGCACCATCTTCTTCAAGGACGACGGCAACTACAAGACCCGCGCCGAGGTGAAGTTCGAGGGCGACACCCTG
GTGAACCGCATCGAGCTGAAGGGCATCGACTTCAAGGAGGACGGCAACATCCTGGGGCACAAGCTGGAGTACAACTACAACA
GCCACAACGTCTATATCATGGCCGACAAGCAGAAGAACGGCATCAAGGTGAACTTCAAGATCCGCCACAACATCGAGGACGGC
AGCGTGCAGCTCGCCGACCACTACCAGCAGAACACCCCCATCGGCGACGGCCCCGTGCTGCTGCCCGACAACCACTACCTGA
GCACCCAGTCCGCCCTGAGCAAAGACCCCAACGAGAAGCGCGATCACATGGTCCTGCTGGAGTTCGTGACCGCCGCCGGGAT
CACTCTCGGCATGGACGAGCTGTACAAGTAAAGCGGCCGCTTCGAGCAGACATGATAAGATACATTGATGAGTTTGGACAAAC
CACAACTAGAATGCAGTGAAAAAAATGCTTTATTTGTGAAATTTGTGATGCTATTGCTTTATTTGTAACCATTATAAGCTGCAATAA
ACAAGTTAACAACAACAATTGCATTCATTTTATGTTTCAGGTTCAGGGGGAGGTGTGGGAGGTTTTTTAAAGCAAGTAAAACCTC
TACAAATGTGGTAAAATCGATAAGGATCCGGGCTGGCGTAATAGCGAAGAGGCCCGCACCGATCGCCCTTCCCAACAGTTGCG

GTGGAGAAGAGCATGCGTGAGGCTCCGGTGCCCGTCAGTGGGCAGAGCGCACATCGCCCACAGTCCCCGAGAAGTTGGGGG
GAGGGGTCGGCAATTGAACCGGTGCCTAGAGAAGGTGGCGCGGGGTAAACTGGGAAAGTGATGTCGTGTACTGGCTCCGCCC
TTTTCCCGAGGGTGGGGGAGAACCGTATATAAGTGCAGTAGTCGCTGTGAACGTTCTTTTTCGCAACGGGTTTGCCGCCAGAA
CACAGGTAAGTGCCGTGTGTGGTTCCCGCGGGCCTGGCCTCTTTACGGGTTATGGCCCTTGCGTGCCTTGAATTACTTCCACC
TGGCTGCAGTACGTGATTCTTGATCCCGAGCTTCGGGTTGGAAGTGGGTGGGAGAGTTCGAGGCCTTGCGCTTAAGGAGCCC
CTTCGCCTCGTGCTTGAGTTGAGGCCTGGCCTGGGCGCTGGGGCCGCCGCGTGCGAATCTGGTGGCACCTTCGCGCCTGTCT
CGCTGCTTTCGATAAGTCTCTAGCCATTTAAAATTTTTGATGACCTGCTGCGACGCTTTTTTTCTGGCAAGATAGTCTTGTAAATG
CGGGCCAAGATCTGCACACTGGTATTTCGGTTTTTGGGGCCGCGGGCGGCGACGGGGCCCGTGCGTCCCAGCGCACATGTTC
GGCGAGGCGGGGCCTGCGAGCGCGGCCACCGAGAATCGGACGGGGGTAGTCTCAAGCTGGCCGGCCTGCTCTGGTGCCTG
GCCTCGCGCCGCCGTGTATCGCCCCGCCCTGGGCGGCAAGGCTGGCCCGGTCGGCACCAGTTGCGTGAGCGGAAAGATGGC
CGCTTCCCGGCCCTGCTGCAGGGAGCTCAAAATGGAGGACGCGGCGCTCGGGAGAGCGGGCGGGTGAGTCACCCACACAAA
GGAAAAGGGCCTTTCCGTCCTCAGCCGTCGCTTCATGTGACTCCACGGAGTACCGGGCGCCGTCCAGGCACCTCGATTAGTTC
TCGAGCTTTTGGAGTACGTCGTCTTTAGGTTGGGGGGAGGGGTTTTATGCGATGGAGTTTCCCCACACTGAGTGGGTGGAGAC
TGAAGTTAGGCCAGCTTGGCACTTGATGTAATTCTCCTTGGAATTTGCCCTTTTTGAGTTTGGATCTTGGTTCATTCTCAAGCCT
CAGACAGTGGTTCAAAGTTTTTTTCTTCCATTTCAGGTGTCGTGAGGAATTCTCTAGAGCTTGATCAAACAAGTTTGTACAAAAAA
GCAGGCTTCCGGAACCACCATGTCCCCTATACTAGGTTATTGGAAAATTAAGGGCCTTGTGCAACCCACTCGACTTCTTTTGGA
ATATCTTGAAGAAAAATATGAAGAGCATTTGTATGAGCGCGATGAAGGTGATAAATGGCGAAACAAAAAGTTTGAATTGGGTTTG
GAGTTTCCCAATCTTCCTTATTATATTGATGGTGATGTTAAATTAACACAGTCTATGGCCATCATACGTTATATAGCTGACAAGCA
CAACATGTTGGGTGGTTGTCCAAAAGAGCGTGCAGAGATTTCAATGCTTGAAGGAGCGGTTTTGGATATTAGATACGGTGTTTC
GAGAATTGCATATAGTAAAGACTTTGAAACTCTCAAAGTTGATTTTCTTAGCAAGCTACCTGAAATGCTGAAAATGTTCGAAGATC
GTTTATGTCATAAAACATATTTAAATGGTGATCATGTAACCCATCCTGACTTCATGTTGTATGACGCTCTTGATGTTGTTTTATACA
TGGACCCAATGTGCCTGGATGCGTTCCCAAAATTAGTTTGTTTTAAAAAACGTATTGAAGCTATCCCACAAATTGATAAGTACTT
GAAATCCAGCAAGTATATAGCATGGCCTTTGCAGGGCTGGCAAGCCACGTTTGGTGGTGGCGACCATCCTCCAAAATCGGATC
TGGTTCCGCGTGGATCCGGAGGAATGGCCCCCAAAAGAAAAAGCGGCGTCTCTAAATGCGAGACAAAATGTACAAAGGCCTGT
CCAAGACCCGCACCCGTTCCCAAACTGCTTATTAAAGGGGGTATGGAGGTGCTGGACCTTGTGACAGGGCCAGACAGTGTGAC
AGAAATAGAAGCTTTTCTGAACCCCAGAATGGGGCAGCCACCCACCCCTGAAAGCCTAACAGAGGGAGGGCAATACTATGGTT
GGAGCAGAGGGATTAATTTGGCTACATCAGATACAGAGGATTCCCCAGGAAATAATACACTTCCCACATGGAGTATGGCAAAGC
TCCAGCTTCCCATGCTCAATGAGGACCTCACCTGTGACACCCTACAAATGTGGGAGGCAGTCTCAGTGAAAACCGAGGTGGTG
GGCTCTGGCTCACTGTTAGATGTGCATGGGTTCAACAAACCCACAGATACAGTAAACACAAAAGGAATTTCCACTCCAGTGGAA
GGCAGCCAATATCATGTGTTTGCTGTGGGCGGGGAACCGCTTGACCTCCAGGGACTTGTGACAGATGCCAGAACAAAATACAA
GGAAGAAGGGGTAGTAACAATCAAAACAATCACAAAGAAGGACATGGTCAACAAAGACCAAGTCCTGAATCCAATTAGCAAGGC
CAAGCTGGATAAGGACGGAATGTATCCAGTTGAAATCTGGCATCCAGATCCAGCAAAAAATGAGAACACAAGGTACTTTGGCAA
TTACACTGGAGGCACAACAACTCCACCCGTCCTGCAGTTCACAAACACCCTGACAACTGTGCTCCTAGATGAAAATGGAGTTGG
GCCCCTCTGTAAAGGAGAGGGCCTATACCTCTCCTGTGTAGATATAATGGGCTGGAGAGTTACAAGAAACTATGATGTCCATCA
CTGGAGAGGGCTTCCCAGATATTTCAAAATCACCCTGAGAAAAAGATGGGTCAAAAATCCCTATCCCATGGCCTCCCTCATAAG
TTCCCTTTTCAACAACATGCTCCCCCAAGTGCAGGGCCAACCCATGGAAGGGGAGAACACCCAGGTAGAGGAGGTTAGAGTGT
ATGATGGGACTGAACCTGTACCGGGGGACCCTGATATGACGCGCTATGTTGACCGCTTTGGAAAAACAAAGACTGTATTTCCTG
GAAATTAACCTAGGACCCAGCTTTCTTGTACAAAGTGGTTCGATCTAGAATGGCTAGTGGATCCCCCGGGCTGCAGGAATTCGA
TATCAAGCTTATCGATAATCAACCTCTGGATTACAAAATTTGTGAAAGATTGACTGGTATTCTTAACTATGTTGCTCCTTTTACGCT
ATGTGGATACGCTGCTTTAATGCCTTTGTATCATGCTATTGCTTCCCGTATGGCTTTCATTTTCTCCTCCTTGTATAAATCCTGGT
TGCTGTCTCTTTATGAGGAGTTGTGGCCCGTTGTCAGGCAACGTGGCGTGGTGTGCACTGTGTTTGCTGACGCAACCCCCACT
GGTTGGGGCATTGCCACCACCTGTCAGCTCCTTTCCGGGACTTTCGCTTTCCCCCTCCCTATTGCCACGGCGGAACTCATCGC
CGCCTGCCTTGCCCGCTGCTGGACAGGGGCTCGGCTGTTGGGCACTGACAATTCCGTGGTGTTGTCGGGGAAATCATCGTCC
TTTCCTTGGCTGCTCGCCTGTGTTGCCACCTGGATTCTGCGCGGGACGTCCTTCTGCTACGTCCCTTCGGCCCTCAATCCAGC
GGACCTTCCTTCCCGCGGCCTGCTGCCGGCTCTGCGGCCTCTTCCGCGTCTTCGCCTTCGCCCTCAGACGAGTCGGATCTCC
CTTTGGGCCGCCTCCCCGCATCGATACCGTCGGCCCACTGCTCCCTAAACCTGAGCTAGCATTATCCCTAATACCTGCCACCC
CACTCTTAATCAGTGGTGGAAGAACGGTCTCAGAACTGTTTGTTTCAATTGGCCATTTAAGTTTAGTAGTAAAAGACTGGTTAAT
GATAACAATGCATCGTAAAACCTTCAGAAGGAAAGGAGAATGTTTTGTGGACCACTTTGGTTTTCTTTTTTGCGTGTGGCAGTTT
TAAGTTATTAGTTTTTAAAATCAGTACTTTTTAATGGAAACAACTTGACCAAAAATTTGTCACAGAATTTTGAGACCCATTAAAAAA
GTTAAATGAGAAACCTGTGTGTTCCTTTGGTCAACACCGAGACATTTAGGTGAAAGACATCTAATTCTGGTTTTACGAATCTGGA
AACTTCTTGAAAATGTAATTCTTGAGTTAACACTTCTGGGTGGAGAATAGGGTTGTTTTCCCCCCACATAATTGGAAGGGGAAGG
AATATCATTTAAAGCTATGGGAGGGTTTCTTTGATTACAACACTGGAGAGAAATGCAGCATGTTGCTGATTGCCTGTCACTAAAA
CAGGCCAAAAACTGAGTCCTTGGGTTGCATAGAAAGCTTCATGTTGCTAAACCAATGTTAAGTGAATCTTTGGAAACAAAATGTT
TCCAAATTACTGGGATGTGCATGTTGAAACGTGGGTTAATTAACTAGCCATGACCAAAATCCCTTAACGTGAGTTTTCGTTCCAC
TGAGCGTCAGACCCCGTAGAAAAGATCAAAGGATCTTCTTGAGATCCTTTTTTTCTGCGCGTAATCTGCTGCTTGCAAACAAAAA
AACCACCGCTACCAGCGGTGGTTTGTTTGCCGGATCAAGAGCTACCAACTCTTTTTCCGAAGGTAACTGGCTTCAGCAGAGCG
CAGATACCAAATACTGTTCTTCTAGTGTAGCCGTAGTTAGGCCACCACTTCAAGAACTCTGTAGCACCGCCTACATACCTCGCT
CTGCTAATCCTGTTACCAGTGGCTGCTGCCAGTGGCGATAAGTCGTGTCTTACCGGGTTGGACTCAAGACGATAGTTACCGGAT
AAGGCGCAGCGGTCGGGCTGAACGGGGGGTTCGTGCACACAGCCCAGCTTGGAGCGAACGACCTACACCGAACTGAGATAC
CTACAGCGTGAGCTATGAGAAAGCGCCACGCTTCCCGAAGGGAGAAAGGCGGACAGGTATCCGGTAAGCGGCAGGGTCGGA
ACAGGAGAGCGCACGAGGGAGCTTCCAGGGGGAAACGCCTGGTATCTTTATAGTCCTGTCGGGTTTCGCCACCTCTGACTTGA

GCGTCGATTTTTGTGATGCTCGTCAGGGGGGCGGAGCCTATGGAAAAACGCCAGCAACGCGGCCTTTTTACGGTTCCTGGCCT
TTTGCTGGCCTTTTGCTCACATGTTCTTAATTAAATTTTTCAAAAGTAGTTGACAATTAATCATCGGCATAGTATATCGGCATAGTA
TAATACGACTCACTATAGGAGGGCCATCATGGCCAAGTTGACCAGTGCTGTCCCAGTGCTCACAGCCAGGGATGTGGCTGGAG
CTGTTGAGTTCTGGACTGACAGGTTGGGGTTCTCCAGAGATTTTGTGGAGGATGACTTTGCAGGTGTGGTCAGAGATGATGTCA
CCCTGTTCATCTCAGCAGTCCAGGACCAGGTGGTGCCTGACAACACCCTGGCTTGGGTGTGGGTGAGAGGACTGGATGAGCT
GTATGCTGAGTGGAGTGAGGTGGTCTCCACCAACTTCAGGGATGCCAGTGGCCCTGCCATGACAGAGATTGGAGAGCAGCCC
TGGGGGAGAGAGTTTGCCCTGAGAGACCCAGCAGGCAACTGTGTGCACTTTGTGGCAGAGGAGCAGGACTGAGGATAAGAAT
TGTAACAAAAAACCCCGCCCCGGCGGGGTTTTTTGTTAATTAACCCTGCAGGGCCTGAAATAACCTCTGAAAGAGGA

VP1-LCTPSR pGEX

VP1-GST with point mutations on N-Terminus adding the LCTPSR motif. The central cysteine of this motif can be modified by the Formylglycine Generating Enzyme (FGE) enzyme to create a reactive formylglycine (fGly). The fGly can then be chemically modified though a covalent linkage. This plasmid was generated for use in atomic force microscopy (AFM) experiments to covalently link VP1 pentamers to the AFM tip.

Figure A2.7: VP1-LCTPSR pGEX

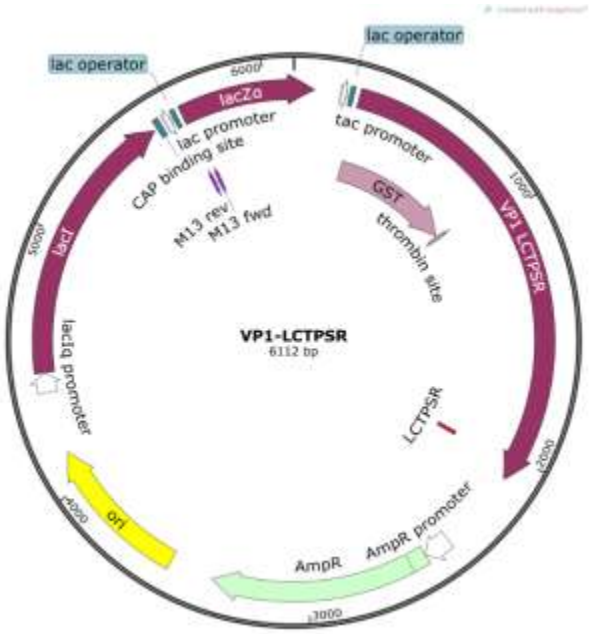

ACGTTATCGACTGCACGGTGCACCAATGCTTCTGGCGTCAGGCAGCCATCGGAAGCTGTGGTATGGCTGTGCAGGTCGTAAAT
CACTGCATAATTCGTGTCGCTCAAGGCGCACTCCCGTTCTGGATAATGTTTTTTGCGCCGACATCATAACGGTTCTGGCAAATAT
TCTGAAATGAGCTGTTGACAATTAATCATCGGCTCGTATAATGTGTGGAATTGTGAGCGGATAACAATTTCACACAGGAAACAGT
ATTCATGTCCCCTATACTAGGTTATTGGAAAATTAAGGGCCTTGTGCAACCCACTCGACTTCTTTTGGAATATCTTGAAGAAAAAT
ATGAAGAGCATTTGTATGAGCGCGATGAAGGTGATAAATGGCGAAACAAAAAGTTTGAATTGGGTTTGGAGTTTCCCAATCTTC
CTTATTATATTGATGGTGATGTTAAATTAACACAGTCTATGGCCATCATACGTTATATAGCTGACAAGCACAACATGTTGGGTGGT
TGTCCAAAAGAGCGTGCAGAGATTTCAATGCTTGAAGGAGCGGTTTTGGATATTAGATACGGTGTTTCGAGAATTGCATATAGTA
AAGACTTTGAAACTCTCAAAGTTGATTTTCTTAGCAAGCTACCTGAAATGCTGAAAATGTTCGAAGATCGTTTATGTCATAAAACA
TATTTAAATGGTGATCATGTAACCCATCCTGACTTCATGTTGTATGACGCTCTTGATGTTGTTTTATACATGGACCCAATGTGCCT
GGATGCGTTCCCAAAATTAGTTTGTTTTAAAAAACGTATTGAAGCTATCCCACAAATTGATAAGTACTTGAAATCCAGCAAGTATA
TAGCATGGCCTTTGCAGGGCTGGCAAGCCACGTTTGGTGGTGGCGACCATCCTCCAAAATCGGATctggttccgcgtggatccGGAGGA
atggcccccaaaagaaaaagcggcgtctctaaatgcgagacaaaatgtacaaaggcctgtccaagacccgcacccgttcccaaactgcttattaaaggggtatggaggtgctggacc
ttgtgacagggccagacagtgtgacagaaatagaagcttttctgaaccccagaatggggcagccacccacccctgaaagcctaacagagggagggcaatactatggttggagcagag

ggattaatttggctacatcagatacagaggattccccaggaaataatacacttcccacatggagtatggcaaagctccagcttcccatgctcaatgaggacctcacctgtgacaccctacaa
atgtgggaggcagtctcagtgaaaaccgaggtggtgggctctggctcactgttagatgtgcatgggttcaacaaacccacagatacagtaaacacaaaaggaatttccactccagtggaa
ggcagccaatatcatgtgtttgctgtgggcggggaaccgcttgacctccagggacttgtgacagatgccagaacaaaatacaaggaagaaggggtagtaacaatcaaaacaatcacaa
agaaggacatggtcaacaaagaccaagtcctgaatccaattagcaaggccaagctggataaggacggaatgtatccagttgaaatctggcatccagatccagcaaaaaatgagaaca
caaggtactttggcaattacactggaggcacaacaactccacccgtcctgcagttcacaaacaccctgacaactgtgctcctagatgaaaatggagttgggcccctctgtaaaggagagg
gcctatacctctcctgtgtagatataatgggctggagagttacaagaaactatgatgtccatcactggagagggcttcccagatatttcaaaatcaccctgagaaaaagatgggtcaaaaat
ccctatcccatggcctccctcataagttccctttcaacaacatgctccccaagtgcagggccaacccatggaaggggagaacacccaggtagaggaggttagagtgtatgatgggact
gaacctgtactgtgcaccctagtaggacgcgctatgttgaccgctttggaaaaacaaagactgtatttcctggaaattaaCTCGAGCGGCCGCATCGTGACTGACTGA
CGATCTGCCTCGCGCGTTTCGGTGATGACGGTGAAAACCTCTGACACATGCAGCTCCCGGAGACGGTCACAGCTTGTCTGTAA
GCGGATGCCGGGAGCAGACAAGCCCGTCAGGGCGCGTCAGCGGGTGTTGGCGGGTGTCGGGGCGCAGCCATGACCCAGTC
ACGTAGCGATAGCGGAGTGTATAATTCTTGAAGACGAAAGGGCCTCGTGATACGCCTATTTTTATAGGTTAATGTCATGATAATA
ATGGTTTCTTAGACGTCAGGTGGCACTTTTCGGGGAAATGTGCGCGGAACCCCTATTTGTTTATTTTTCTAAATACATTCAAATAT
GTATCCGCTCATGAGACAATAACCCTGATAAATGCTTCAATAATATTGAAAAAGGAAGAGTATGAGTATTCAACATTTCCGTGTC
GCCCTTATTCCCTTTTTTGCGGCATTTTGCCTTCCTGTTTTTGCTCACCCAGAAACGCTGGTGAAAGTAAAAGATGCTGAAGATC
AGTTGGGTGCACGAGTGGGTTACATCGAACTGGATCTCAACAGCGGTAAGATCCTTGAGAGTTTTCGCCCCGAAGAACGTTTTC
CAATGATGAGCACTTTTAAAGTTCTGCTATGTGGCGCGGTATTATCCCGTGTTGACGCCGGGCAAGAGCAACTCGGTCGCCGC
ATACACTATTCTCAGAATGACTTGGTTGAGTACTCACCAGTCACAGAAAAGCATCTTACGGATGGCATGACAGTAAGAGAATTAT
GCAGTGCTGCCATAACCATGAGTGATAACACTGCGGCCAACTTACTTCTGACAACGATCGGAGGACCGAAGGAGCTAACCGCT
TTTTTGCACAACATGGGGGATCATGTAACTCGCCTTGATCGTTGGGAACCGGAGCTGAATGAAGCCATACCAAACGACGAGCG
TGACACCACGATGCCTGCAGCAATGGCAACAACGTTGCGCAAACTATTAACTGGCGAACTACTTACTCTAGCTTCCCGGCAACA
ATTAATAGACTGGATGGAGGCGGATAAAGTTGCAGGACCACTTCTGCGCTCGGCCCTTCCGGCTGGCTGGTTTATTGCTGATAA
ATCTGGAGCCGGTGAGCGTGGGTCTCGCGGTATCATTGCAGCACTGGGGCCAGATGGTAAGCCCTCCCGTATCGTAGTTATCT
ACACGACGGGGAGTCAGGCAACTATGGATGAACGAAATAGACAGATCGCTGAGATAGGTGCCTCACTGATTAAGCATTGGTAA
CTGTCAGACCAAGTTTACTCATATATACTTTAGATTGATTTAAAACTTCATTTTTAATTTAAAAGGATCTAGGTGAAGATCCTTTTT
GATAATCTCATGACCAAAATCCCTTAACGTGAGTTTTCGTTCCACTGAGCGTCAGACCCCGTAGAAAAGATCAAAGGATCTTCTT
GAGATCCTTTTTTTCTGCGCGTAATCTGCTGCTTGCAAACAAAAAAACCACCGCTACCAGCGGTGGTTTGTTTGCCGGATCAAG
AGCTACCAACTCTTTTTCCGAAGGTAACTGGCTTCAGCAGAGCGCAGATACCAAATACTGTCCTTCTAGTGTAGCCGTAGTTAG
GCCACCACTTCAAGAACTCTGTAGCACCGCCTACATACCTCGCTCTGCTAATCCTGTTACCAGTGGCTGCTGCCAGTGGCGATA
AGTCGTGTCTTACCGGGTTGGACTCAAGACGATAGTTACCGGATAAGGCGCAGCGGTCGGGCTGAACGGGGGGTTCGTGCAC
ACAGCCCAGCTTGGAGCGAACGACCTACACCGAACTGAGATACCTACAGCGTGAGCTATGAGAAAGCGCCACGCTTCCCGAA
GGGAGAAAGGCGGACAGGTATCCGGTAAGCGGCAGGGTCGGAACAGGAGAGCGCACGAGGGAGCTTCCAGGGGGAAACGC
CTGGTATCTTTATAGTCCTGTCGGGTTTCGCCACCTCTGACTTGAGCGTCGATTTTTGTGATGCTCGTCAGGGGGGCGGAGCCT
ATGGAAAAACGCCAGCAACGCGGCCTTTTTACGGTTCCTGGCCTTTTGCTGGCCTTTTGCTCACATGTTCTTTCCTGCGTTATCC
CCTGATTCTGTGGATAACCGTATTACCGCCTTTGAGTGAGCTGATACCGCTCGCCGCAGCCGAACGACCGAGCGCAGCGAGTC
AGTGAGCGAGGAAGCGGAAGAGCGCCTGATGCGGTATTTTCTCCTTACGCATCTGTGCGGTATTTCACACCGCATAAATTCCG
ACACCATCGAATGGTGCAAAACCTTTCGCGGTATGGCATGATAGCGCCCGGAAGAGAGTCAATTCAGGGTGGTGAATGTGAAA
CCAGTAACGTTATACGATGTCGCAGAGTATGCCGGTGTCTCTTATCAGACCGTTTCCCGCGTGGTGAACCAGGCCAGCCACGT
TTCTGCGAAAACGCGGGAAAAAGTGGAAGCGGCGATGGCGGAGCTGAATTACATTCCCAACCGCGTGGCACAACAACTGGCG
GGCAAACAGTCGTTGCTGATTGGCGTTGCCACCTCCAGTCTGGCCCTGCACGCGCCGTCGCAAATTGTCGCGGCGATTAAATC
TCGCGCCGATCAACTGGGTGCCAGCGTGGTGGTGTCGATGGTAGAACGAAGCGGCGTCGAAGCCTGTAAAGCGGCGGTGCA
CAATCTTCTCGCGCAACGCGTCAGTGGGCTGATCATTAACTATCCGCTGGATGACCAGGATGCCATTGCTGTGGAAGCTGCCT
GCACTAATGTTCCGGCGTTATTTCTTGATGTCTCTGACCAGACACCCATCAACAGTATTATTTTCTCCCATGAAGACGGTACGCG
ACTGGGCGTGGAGCATCTGGTCGCATTGGGTCACCAGCAAATCGCGCTGTTAGCGGGCCCATTAAGTTCTGTCTCGGCGCGTC
TGCGTCTGGCTGGCTGGCATAAATATCTCACTCGCAATCAAATTCAGCCGATAGCGGAACGGGAAGGCGACTGGAGTGCCATG
TCCGGTTTTCAACAAACCATGCAAATGCTGAATGAGGGCATCGTTCCCACTGCGATGCTGGTTGCCAACGATCAGATGGCGCT
GGGCGCAATGCGCGCCATTACCGAGTCCGGGCTGCGCGTTGGTGCGGATATCTCGGTAGTGGGATACGACGATACCGAAGAC
AGCTCATGTTATATCCCGCCGTTAACCACCATCAAACAGGATTTTCGCCTGCTGGGGCAAACCAGCGTGGACCGCTTGCTGCA
ACTCTCTCAGGGCCAGGCGGTGAAGGGCAATCAGCTGTTGCCCGTCTCACTGGTGAAAAGAAAAACCACCCTGGCGCCCAATA
CGCAAACCGCCTCTCCCCGCGCGTTGGCCGATTCATTAATGCAGCTGGCACGACAGGTTTCCCGACTGGAAAGCGGGCAGTG
AGCGCAACGCAATTAATGTGAGTTAGCTCACTCATTAGGCACCCCAGGCTTTACACTTTATGCTTCCGGCTCGTATGTTGTGTG
GAATTGTGAGCGGATAACAATTTCACACAGGAAACAGCTATGACCATGATTACGGATTCACTGGCCGTCGTTTTACAACGTCGT
GACTGGGAAAACCCTGGCGTTACCCAACTTAATCGCCTTGCAGCACATCCCCCTTTCGCCAGCTGGCGTAATAGCGAAGAGGC
CCGCACCGATCGCCCTTCCCAACAGTTGCGCAGCCTGAATGGCGAATGGCGCTTTGCCTGGTTTCCGGCACCAGAAGCGGTG
CCGGAAAGCTGGCTGGAGTGCGATCTTCCTGAGGCCGATACTGTCGTCGTCCCCTCAAACTGGCAGATGCACGGTTACGATGC
GCCCATCTACACCAACGTAACCTATCCCATTACGGTCAATCCGCCGTTTGTTCCCACGGAGAATCCGACGGGTTGTTACTCGCT
CACATTTAATGTTGATGAAAGCTGGCTACAGGAAGGCCAGACGCGAATTATTTTTGATGGCGTTGGAATT

Appendix III: Primers

Table A3.1 Mutagenesis and Gibson Assembly Primers	
Primer Name	**Sequence**
t557a	5'-cgcacgcaccaagtacaaagaggagggcg-3'
t557a antisense	5'-cgccctcctctttgtacttggtgcgtgcg-3'
c890t_a891g	5'-ccgcaactacgacgtgcaccattggcgcgg-3'
c890t_a891g antisense	5'-ccgcgccaatggtgcacgtcgtagttgcgg-3'
g412a_t414c	5'-gcgggagcctgctcaacgtccacggcttcaa-3'
g412a_t414c antisense	5'-ttgaagccgtggacgttgagcaggctcccgc-3'
g25a_c26g_antisense	gcgaggttgatgccctggctccagccgtaa
g25a_c26g	ttacggctggagccAGggcatcaacctcgc
t24g_antisense	gccgcgccactggtggacgtcgtagtt
t24g	aactacgacgtccaccaGtggcgcggc
ZsGreen Backbone R	ATATCGATAGAGAAATGTTCTGG
ZsGreen Backbone F	GGCGTTTTTCCATAGGCTC
ZsGreen Fragment F	aacatttctctatcgatatGAGGCGGAAAGAACCAGC
ZsGreen Fragment R	cctatggaaaaacgccCCTTTGTTCATGGCAGCC
Tomato Backbone R	GGGTTAAAAAATGAGCTGATTTAAC
Tomato Backbone F	AGACCCCGTAGAAAAGATC
Tomato Res Fragment F	cagctcatttttttaacccCACCCGCCGCGCTTAATG
Tomato Res Fragment R	atcttttctacggggtctGGTGGAATCGAAATCTCGTGATG
VP1_Cdelta_30 F	GCTTCCGGAACCACCATGTCCCCTATACTAGGTTATTG
VP1_Cdelta_30 R	AAGCTGGGTAGGTTACACTCTAACCTCCTCTAG
pwP ZEO Fwd	CCTAGGACCCAGCTTTCTTG
pwP ZEO Rev	GGTGGTTCCGGAAGCCTG
VP1-GST F	GCTTCCGGAAACCACCATGTCCCCTATACTAGGTTATTG
VP1-GST R	AAGCTGGGTCCTAGGTTAATTTCCAGGAAATACAGTC
c23g_a29c F	CCACCAGCGACAGCGAAGCCAGTCCCGGAAA
c23g_a29c R	TTTCCGGGACTGGCTTCGTCGCTGGTGG
a22c_c23a_c24g_g25a_a26t F	GTGTTGTTTCCGGGACTGTCTATCTGGTCGCTGGTGGCGAGGTTGGAT
a22c_c23a_c24g_g25a_a26t R	ATCAACCTCGCCACCAGCGACCAGATAGACAGTCCCGGAAACAACAC

Table A3.2 Sequencing and qPCR Primers

Primer Name	Sequence
Zs Green 1F	CCGGCGTCAATACGGGATAA
Zs Green 1R	TCCTTGAGAGTTTTCGCCCC
Zs Green 2F	GCCCCTTGAGCATCTGACTT
Zs Green 2R	CAGCAGGGGGCTGTTTCATA
Zs Green 3F	TGAAGCCCCTTGAGCATCTG
Zs Green 3R	GCCACCTTTGTTCATGGCAG
pCMV-tdTomato 1F	GCCCACTACGTGAACCATCA
pCMV-tdTomato 1R	TTCCCTTCCTTTCTCGCCAC
pCMV-tdTomato 2F	CGGTGTTGGGTCGTTTGTTC
pCMV-tdTomato 2R	GGGTATCGACAGAGTGCCAG
pCMV-tdTomato 3F	CGCCTACATACCTCGCTCTG
pCMV-tdTomato 3R	GTGTAGGTCGTTCGCTCCAA
N-Myc 1F	CTGGGAACTGGGTTGGAGCC
N-Myc 1R	CAACCTCCAACTCTCCCGCAG
N-Myc 2F	CGCTAGCCAGGCGTAAG
N-Myc 2R	TTTAATATGGGGGAGTGCTTCCT
N-Myc 3F	GAGCGCTAGCCAGGCGTAA
N-Myc 3R	GGGAGTGCTTCCTTCCCGT
N-Myc 4F	GGGTTGGAGCCGAACGA
N-Myc 4R	GCATGGGTTCGCCTCTCTTTTA
C-JUN 1A F	GCACCTCCGCGCCAAGAACT
C-JUN 1A R	AAGCCCTCCTGCTCGTCGGT
C-JUN 2A F	GCCGGAGATGCCGGGAGAGA
C-JUN 2A R	AGGCGGCAATGCGGTTCCTC
C-JUN 3A F	AGGAACCGCATTGCCGCCTC
C-JUN 3A R	TGTTGGCCGTGGATGCCAGC
MPyV Early 1 F	TCCAACAGATACACCCGCAC
MPyV Early 1 R	GGGGATATGCTGTCATCGGG
MPyV Early 2 F	AGTCTGGCATCCAGGAGACT

MPyV Early 2 F	GACACTGGTACCAAGCGACA
MpyV Near Ori 1 F	AGTGACTAACTGACCGCAGC
MpyV Near Ori 1 R	CCTGGGTGGAGAGGCTTTTT
MpyV Near Ori 2 F	CTGCTACTGCACCCAGACAA
MpyV Near Ori 2 R	CCATCCGCATGTAGCCTTCT
MpyV Collision F	CATAGCGCGTCATATCAGGGT
MPyV Collision R	ATGGAAGGGGAGAACACCCA
pwP Primer Foward	CCCGTCCCAAAGCTCTTGAT
pwP Primer Rev	TCTTGCCGAACCTATCGACG